

Towards emission-free sea dike revetments

Making sustainable design choices by employing probabilistic safety assessment and integrating the environmental cost indicator in the parametric design process of sea dike revetments

K. J. van Donselaar

November, 2023



Towards emission-free sea dike revetments

Making sustainable design choices by
employing probabilistic safety assessment and
integrating the environmental cost indicator in
the parametric design process of sea dike
revetments

by

K. J. van Donselaar

To obtain the degree of Master of Science
at the Delft University of Technology,
to be defended publicly on November 22, 2023

Student number: 5183723
Project duration: February 13, 2023 – November 22, 2023
Thesis committee: Ass. Prof. Dr. Ir. C. Mai Van, TU Delft, Chair
Ass. Prof. Dr. Ir. A. Antonini, TU Delft
Ir. M. Aldershof, -
Ing. L. Kwakman, Arcadis

An electronic version of this thesis is available at <http://repository.tudelft.nl/>.
Cover: Artist impression cross-section Lauwersmeerdijk (Waterschap Noorderzijlvest, 2023)

Abstract

Large parts of the Netherlands lay below mean sea level. An extensive network of flood protection measures is in place to prevent flooding. Periodic safety assessment and reinforcement are required to guarantee a resilient system. Currently, in the Netherlands, an extensive sea dike reinforcement program is underway to meet the safety standards mandated by the Dutch government. A dike reinforcement project encompasses several components, often interacting with each other. This study focuses on the outer dike revetment. Traditionally, the revetment design is optimised for financial costs. This study aims to optimise the dike revetment design for the lowest Environmental Cost Indicator (ECI). This quantifies the carbon dioxide equivalent emissions generated throughout the entire life cycle of a construction project or its constituent parts. This is pertinent in the current context as the Dutch Government harbors ambitions of achieving a fully circular economy by 2050, with an interim goal of a 50% circular economy by 2030. This ambition is to be implemented by companies within their organization. The revetment is optimised as a whole by assessing the entire outer revetment and applying different types of revetment based on their probability of failure. The primary objective of this study is to acquire knowledge on designing a dike revetment that fulfils technical requirements and has the lowest environmental cost indicator possible. The revetment types to study are loose rock, concrete elements (Basalton), interlocking elements (Verkalit), hydraulic asphalt concrete and grass. The following main research question is defined:

"What sea dike revetment design fulfils safety requirements and has the lowest environmental impact for the Lauwersmeerdijk-Vierhuizergat dike reinforcement project?"

To answer this question, a Python-based model was made. The model evaluates the probability of failure of each design option and calculates the corresponding ECI and financial costs. The Lauwersmeerdijk-Vierhuizergat project, a Waddenzee dike reinforcement, is used as a case study. The required safety level for the Lauwersmeerdijk-Vierhuizergat outer revetment is 1/60.000 years. The model requires input for the design equations. The input consists of decision variables, control variables and hydraulic boundary conditions. The decision variables are the variables in the design equations that the designer can alter. The control variables are the variables to which the designer has no influence. The hydraulic boundary conditions are determined for each water level discretised in steps of 0.2m. Next to the input for the probabilistic calculation, the input for the ECI and financial costs are required. The ECI data is obtained from the 'Milieudatabase' (Schipper et al., 2022). The financial cost data is obtained from cost experts from Arcadis.

For loose rock, the probability of failure is calculated with the equations as defined by van der Meer (1988a). For the placed elements, the probability of failure is calculated with the equation defined by Klein Breteler and Mourik (2014). The asphalt revetment is designed with the uplift and wave impact equations as defined in TAW (2002). The grass revetment is designed with the use of the 'Gras erosie buitentalud' (GEBU) tool. The equations for erosion according to Klein Breteler (2022a) are included in this tool. The design equations are evaluated using crude Monte Carlo analysis for each water level with corresponding hydraulic boundary conditions, decision parameters, and control parameters.

More than 2,000 designs, each meeting safety requirements, are made with varying transition heights. The optimal sea dike revetment design for environmental impact is the design with the lowest ECI score. When the probabilistic approach is applied, this design has loose rock revetment at the lower section, Basalton for the middle section, and grass for the upper section. In general, it is concluded that loose rock contributes most to the ECI and should be limited as much as possible. The middle section is traditionally made of hydraulic asphalt concrete. However, when replacing this with placed elements, a lower ECI is achieved. The grass revetment often requires large volumes of high-quality clay from external locations, requiring long transport distances. This results in high ECI costs for thick clay layers. When comparing the revetment with the lowest ECI to the revetment design with the lowest financial costs, it is concluded that the design with the lowest financial costs has a large section with hydraulic asphalt concrete instead of placed elements. The study design costs €1890 per meter, with an ECI of €373 per meter. The financially most attractive design costs €1439

per meter, with an ECI of €458 per meter. The difference in financial costs is €451 per meter (24%) and €85 per meter ECI costs (23%). For the revetment design made by Arcadis, deterministic and semi-probabilistic calculation methods are applied. The asphalt layer thickness is reduced by 50% when applying this method due to the large uncertainty in the probabilistic design. This results in a €12 per meter dike width lower ECI than the design with the lowest ECI made with the probabilistic approach.

Thus, when designing a sea dike revetment probabilistically, aiming to reduce the ECI as much as possible, apply as little and the smallest possible loose rock grading, and replace the hydraulic asphalt concrete layer for placed elements.

Preface

You are about to read my Master's thesis, with which I finalise the Master Civil Engineering, track Hydraulic Engineering from the TU Delft. This report is the final product I made during my full-time study career. It is only a tiny part of the nine years of studying that I have pursued. Of course, I could not do this without the support and help of my family and friends. I felt, and still feel, supported in the broadest sense of the word. Thank you!

Some special notes regarding this thesis. During the process, I learned to use my own and other people's networks for help. I spoke to many people within Arcadis, TU Delft and external companies and organisations. I was surprised by the willingness to help and am very thankful for this. First, I would like to thank Arcadis for allowing me to do this project for their company. Specifically, the Flood Management Department adopted me as their colleague, inviting me to meetings, updating me on their day-to-day work, showing interest in my thesis and taking me for drinks and a barbeque. I thank everyone who made time for me to answer all my questions. From Arcadis, I would like to thank the following people specifically for their help: Egon Bijlsma, Jan Zandbergen, Sonja Kalle, Thom Smit and Yida Tao. Richard Marijnissen, although you left Arcadis in the first weeks of my thesis, I am thankful for your guidance and availability afterwards. Special thanks to Mark Klein Breteler from Deltares, for guiding me on the GEBU tool and the equations for placed revetment you developed.

From the TU Delft, I was supervised by Cong Mai Van and Alessandro Antonini, whom I would like to thank for their supervision. I appreciate the time and effort you put into this thesis. Thank you for the critical questions and helpful feedback. From Arcadis, Leo Kwakman and Marco Aldershof were on the committee. Thank you, Leo, for your guidance and expert knowledge on the probabilistic aspect of this thesis. Marco, I would like to thank you for the daily supervision. Even after switching companies, the supervision was continued in your own time. Thank you for the weekly meetings to discuss the progress and how life was going besides the thesis, which I appreciated.

Writing a thesis is a solitary project. However, within Arcadis, a nice group of graduates formed who all went through the same process, which helped me greatly with staying motivated. I am thankful to the other graduates, Maurits van Herwijnen and Rushil Bechan in particular, for the company and the many table tennis games we played! Enjoy reading!

K. J. van Donselaar
Delft, November 2023

Contents

1	Introduction	1
1.1	Relevance	1
1.2	State of the art	2
1.3	Aim of this study	3
1.4	Research questions	3
1.5	Outline	3
2	Theoretical background	5
2.1	Revetments	5
2.2	Probabilistic techniques	18
2.3	Sustainability	21
3	Overall analysis framework and case study	23
3.1	Workflow	23
3.2	Description case study	24
3.3	Input	27
3.4	Limit state functions and probabilistic calculation	38
3.5	ECI calculation	39
3.6	Core of the model	40
3.7	Results	40
4	Model outcome and interpretation of the results	43
4.1	Results safety assessment	43
4.2	Refurbished design	47
4.3	Designs with varying transition heights	50
4.4	Sensitivity of parameters related to the ECI	57
4.5	Financial costs of the design options	61
4.6	Comparison of the study design with Arcadis' design for the Lauwersmeerdijk case	63
5	Discussion	67
5.1	Project specific design	67
5.2	Hydraulic Boundary conditions	67
5.3	Effect of interlocking on stability	67
5.4	Maintenance of revetment	67
5.5	Correlation loading duration with wave characteristics	68
5.6	Breaker parameter	68
5.7	Validity ECI	68
5.8	Recycling/reuse value revetment	68
5.9	Sample size	69
6	Conclusion	71
6.1	Recommendations	73
	Bibliography	77
A	Parameter distributions	79
B	Workflow model	83
C	Environmental cost indicator for all design options with varying transition heights	85
D	Financial costs for all design options for varying transition heights	89
E	Hydraulic boundary conditions	93
F	Input GEBU tool	95

List of Figures

2.1	Five different revetment types	6
2.2	Head difference for small and large leakage length (Schierreck and Verhagen, 2019)	7
2.3	The stability number according the design equation versus the Steentoets	11
2.4	Design groundwater level for sea dikes	12
2.5	Reduction factor R_w depending on water level relative to the phreatic surface (TAW, 2002).	13
2.6	Slope depending pressure factor Q_n (TAW, 2002).	14
2.7	Classification for the erosion resistance of clay (TAW, 1996)	16
2.8	Schematic illustration of grass erosion due to wave runoff (Klein Breteler, 2022a)	16
2.9	Schematic illustration of grass erosion due to direct wave impact (Klein Breteler, 2022a)	16
2.10	Schematic overview of the erosion profile (Klein Breteler, 2022a)	17
2.11	Graphical representation of FORM analysis (Marelli et al., 2022)	19
2.12	Generation of random samples (Jonkman et al., 2017)	20
2.13	Output example Monte Carlo analysis (Jonkman et al., 2017)	21
2.14	Output example importance sampling (Jonkman et al., 2017)	22
3.1	Simplified workflow of the model	24
3.2	Flowchart of the dike revetment model	25
3.3	Location of the sub trajectories for the dike reinforcement project Lauwersmeerdijk-Vierhuizergat	25
3.4	Sections landelijke dijk	26
3.5	Initial geometry dike	26
3.6	ECI composition per m^2/m^3 for loose rock	30
3.7	ECI composition per m^2/m^3 for Verkalit	31
3.8	ECI composition per m^2/m^3 for Basalton	31
3.9	ECI composition per m^2/m^3 for hydraulic asphalt concrete	32
3.10	ECI composition per m^2/m^3 for grass	33
3.11	Probability density function for the slope depending impact factor (de Loeff et al., 2006)	37
4.1	Probability of failure of loose rock with respect to stability number and significant wave height	44
4.2	Probability of failure of Verkalit with respect to stability number and significant wave height	45
4.3	Probability of failure of Basalton with respect to stability number and significant wave height	45
4.4	Probability of failure of asphalt due to wave impact	46
4.5	Probability of failure of asphalt due to uplift	46
4.6	ECI for each rock class in the preferred design	47
4.7	ECI for Basalton and Verkalit	48
4.8	ECI per layer thickness of hydraulic asphalt concrete stretching from +2.41 mNAP to +6.15 mNAP	49
4.9	ECI for grass revetment	49
4.10	Refurbished design	50
4.11	Varying transition heights loose rock, Verkalit and grass	51
4.12	Design with lowest ECI for loose rock, Verkalit and grass revetment	52
4.13	Varying transition heights loose rock, Basalton and grass	53
4.14	Design with lowest ECI for loose rock, Basalton and grass revetment.	53
4.15	Varying transition heights loose rock, asphalt and grass	54
4.16	Design drawing loose rock, asphalt and grass	54
4.17	Varying transition heights loose rock, Verkalit, asphalt and grass	55
4.18	Design drawing loose rock, Verkalit, asphalt and grass	56
4.19	Varying transition heights loose rock, Basalton, asphalt and grass	56
4.20	ECI composition loose rock with changing circumstances	58
4.21	ECI loose rock depending on different damage number	58
4.22	ECI composition Verkalit with changing circumstances	59

4.23 ECI composition Basalton with changing circumstances	59
4.24 ECI composition hydraulic asphalt concrete with changing circumstances	60
4.25 ECI composition grass with changing circumstances	61
4.26 Financial costs loose rock, Basalton, asphalt and grass	62
4.27 Designs sorted by financial costs	62
4.28 Arcadis design	64
4.29 Study design: Design with lowest ECI	64
6.1 Study design: Design with lowest ECI that fulfils safety requirements	73
B.1 Complete workflow of the model	84
C.1 All design options varying transition heights Verkalit	86
C.2 All design options varying transition heights Basalton	87
D.1 Financial costs all design options varying transition heights Verkalit	90
D.2 Financial costs all design options varying transition heights Basalton	91
D.3 Financial costs 100 lowest ECI design options varying transition heights Verkalit	92
D.4 Financial costs 100 lowest cost design options varying transition heights Verkalit	92
E.1 Input screen GEBU tool	96

List of Tables

2.1	Relative leakage length to wavelength ratio with indicative values	7
2.2	Damage level S corresponding to slope (van der Meer, 1988a)	8
3.1	ECI per revetment type	33
3.2	Financial costs per revetment type	34
3.3	Nominal diameter with corresponding rock class (NEN, 2015)	35
3.4	S -values for slope 1:4 until 1:6	36
4.1	Revetment design for the original design	50
4.2	Revetment design for loose rock, Verkalit and grass	51
4.3	Revetment design for loose rock, Basalton and grass	52
4.4	Revetment design for loose rock, asphalt and grass	52
4.5	Revetment design for loose rock, Verkalit, asphalt and grass	55
4.6	Original ECI composition loose rock	57
4.7	Original ECI composition Verkalit	58
4.8	Original ECI composition Basalton	59
4.9	Original ECI composition Asphalt	60
4.10	Original ECI composition grass	60
4.11	Revetment design for Loose rock, Basalton and grass with optimal transition heights	61
4.12	Arcadis design revetment composition	64
A.1	Decision parameter distributions	80
A.2	Control parameter distributions	81
E.1	Hydraulic boundary conditions	94

1

Introduction

This thesis aims to incorporate the sustainability of a dike revetment early in the design phase to optimise for both reliability and sustainability. This study measures sustainability as the CO_2 equivalent produced by the project during the entire lifetime. To study the different design possibilities on an actual dike reinforcement project, the case 'Lauwersmeerdijk-Vierhuizergat' is used.

1.1. Relevance

The relevance of this study is twofold. It is relevant from both practical (societal and business (Arcadis)) and academic perspectives.

Societal relevance

On a societal level, the relevance is embedded in the "Rijksbreed programma circulaire economie (National program circular economy)" published by the Dutch government in 2016. It was published to emphasise the necessity and set out pathways to make the transition towards a sustainable economy. The necessity for this program is threefold. Due to an increasing world population, the demand for commodities is growing. This strong growth is unsustainable and harms the environment (Dijksma and Kamp, 2016). Next to this, the Netherlands is currently very much dependent on its resources from third countries. This may result in geopolitical instabilities and fluctuating prices, resulting in an unstable economy (Dijksma and Kamp, 2016). The third reason is the negative impact of extraction and the use of resources on the environment. Due to higher concentrations of greenhouse gasses, the global climate is changing. Depending on future actions, the average global surface temperature change for the end of the 21st century will likely exceed $1.5^\circ C$ relative to 1850 to 1900 for every "Representative Concentration Pathway" (RCP). The Intergovernmental Panel on Climate Change (IPCC) has defined seven Representative Concentration Pathways (RCPs) ranging from RCP1.9 to RCP8.5, which forecast greenhouse gas concentration pathways up to 2100. For the RCP2.6 and higher, global warming likely exceeds $2^\circ C$. Global warming will have annual to decadal and regional variability (Intergovernmental panel on climate change (IPCC), 2013). During the Conference of Parties in Paris in 2015, governments agreed to limit global warming to $2^\circ C$ and to strive for $1.5^\circ C$ by 2100. (UNFCCC, 2016)

The Dutch national program for a circular economy sets a target to have a 100% circular economy by 2050 and 50% circular economy by 2030 (Dijksma and Kamp, 2016). To measure this, a clear definition of a circular economy is necessary. The most prominent definition is provided by Kirchherr et al. (2017) based on reviewing 114 definitions. A circular economy is an:

"Economic system that replaces the 'end-of-life' concept with reducing, alternatively reusing, recycling and recovering materials in production/distribution and consumption processes. It operates at the micro level (products, companies, consumers), meso level (eco-industrial parks) and macro level (city, region, nation and beyond) to accomplish sustainable development, thus simultaneously creating environmental quality, economic prosperity and social equity, to the benefit of current and future generations."

The Dutch government focuses on five different sectors, with each their vision to achieve the overarching goal of full circularity by the year 2050. One of the sectors is the built environment. The following vision by (Dijksma and Kamp, 2016) is defined:

"By 2050, the design, development, use, management, and dismantling of structures are organised in such a way that these objects are built, (re)used, maintained, and dismantled. Construction will use sustainable materials and respond to the dynamic wishes of the users. The aim is to achieve an energy-neutral built environment by 2050 following European agreements. Buildings make maximum use of ecosystem services (natural capital such as the water-storage capacity of the subsoil)."

One of the challenges of making a more circular design compared to traditional design is quantifying circularity. To do so, Rijkswaterstaat developed a tool called DuboCalc, where a project's Environmental Cost Indicator (ECI) is calculated. The ECI indicates the emissions produced by calculating the CO_2 equivalent for each component during the project's life cycle. This is then converted to a monetary value of Euro. The lower the score, the lower the emissions.

Operational relevance

On an operational level, this new vision is to be implemented by companies in their organization. One of the companies this vision applies to is Arcadis. Arcadis is an engineering consultancy firm that operates in the entire built environment spectrum. This study focuses on the design of dike revetments. The most important parameter that dikes are optimised for is the probability of failure per year. In the Waterwet (2009) art. 2.2 and Appendix III, the probability of failure is defined for each trajectory ranging from 1:300 years to 1:100.000 years depending on the economic, social, and environmental consequences of failure.

Arcadis is involved in two important stages of renovating a dike to which this study applies. First, the assessment of the dike, and second, the design of the reinforcement. The highest form of circularity is to prevent reinforcement. The situation is most sharply assessed by assessing dike sections probabilistically, approving as many dike sections as possible. Currently, dikes are assessed according to the 'Wettelijk Beoordelingsinstrumentarium 2017' (Legal assessment tools 2017) (Rijkswaterstaat, 2017) including a mix of deterministic and (semi) probabilistic assessment methods.

Academic relevance

The academic relevance of this study is threefold. The first aspect is the fact that all different revetment types are taken as one, and the design is based on the properties of the revetment. Currently, revetment design is based on preliminary decisions on what type of revetment to use. The design formula exists for the different revetment types, but an overarching approach is missing. The second aspect of this study that makes it academically relevant is the optimization for both the probability of failure and ECI. Dike design is based on the probability of failure, costs, maintainability and constructability. To optimise for costs, research has been done for the entire dike, mainly focusing on geometry (Bischiniotis, 2013), (Daamen, 2016). The third aspect which makes this study academically relevant is the probabilistic approach. Traditionally, dike revetment is designed in a deterministic approach using safety factors. This study aims to develop a fully probabilistic approach for the design of the revetment. The advantage of this is that the design is based on the actual probability of failure and, therefore, can use a combination of materials that results in the lowest ECI possible whilst still meeting safety requirements.

1.2. State of the art

Regarding dike design, the current procedure is to design several different design proposals, which all comply with the required safety standards. For each design, the ECI is determined to evaluate sustainability. However, this way, the circularity is of secondary importance as the designs cannot be adjusted much to increase circularity. Regarding implementing probabilistic methods, the basic assessment is based on deterministic and semi-probabilistic calculations, using safety factors (Rijkswaterstaat, 2017). This often results in overdimensioned constructions. When dikes are assessed to be unsafe by a small margin, it is worth making an expert judgment. In this judgment, the engineer has much flexibility to find a way to prove the dike section is safe. An important tool in this judgment is the application of probabilistic calculations. By calculating the actual probability of failure, some dike sections that would have been rejected can be approved. These probabilistic approaches for revetments are currently only available for grass revetment. During the design phase,

there are fewer possibilities to include probabilistic methods. Due to restrictions by governing policies, the design method for each component of the dike is determined by the local waterboards, which do not include probabilistic analysis for all components yet. (Personal communication, February 24, 2023)

1.3. Aim of this study

The primary objective of this study is to acquire knowledge on designing a dike revetment that fulfils technical requirements and has the lowest environmental cost indicator possible. The focus of the study is specifically on sea dikes. The revetment of the dike is designed using various combinations of parameters. There is a range of revetment types, each with advantages and disadvantages. Due to time limitations, a selection of revetment types is made to study. The chosen revetment types are:

1. Loose rock;
2. Concrete elements (Basalton);
3. Interlocking elements (Verkaliet);
4. Hydraulic Asphalt Concrete;
5. Grass.

These specific revetment types are selected because these are the types of revetment chosen in the final design of the Lauwersmeerdijk. Basalton and Verkaliet were selected as these were the two options considered during the design phase. For Asphalt, Hydraulic Asphalt concrete is specifically chosen as this type of asphalt is applied at the Lauwersmeerdijk.

1.4. Research questions

The following main research question is defined:

What sea dike revetment design fulfils safety requirements and has the lowest environmental impact for the Lauwersmeerdijk-Vierhuizergat dike reinforcement project?

To answer this research question, the following sub-questions are defined:

1. Which probabilistic technique is the most practical for designing a sea dike revetment?
2. What parameter combination of each type of revetment fulfils safety requirements and has the lowest environmental impact under governing loading conditions?
3. What are the optimal transition heights with respect to ECI of each type of revetment under governing loading conditions?
4. What is the sensitivity of related variables to the ECI?
5. How does the optimal sea dike revetment design with respect to ECI compare to the financially optimal sea dike revetment?
6. How does the revetment design with the lowest ECI compare to the existing design, given a case study of the Lauwersmeerdijk?

1.5. Outline

This Master's thesis is structured in the following manner: First, the theory necessary to address the research questions is presented; second, the methodology, including the case study and the model structure and its various components; subsequently, the model is applied to the Lauwersmeer-Vierhuizergat case after which the results are analysed and interpreted; finally, the thesis concludes with an extensive discussion and concluding remarks.

2

Theoretical background

The research questions presented in the introduction will be addressed by developing a probabilistic model. A thorough examination of the relevant theory is essential to construct this model. This entails studying the revetment types and exploring the design equations that currently govern them. The case Lauwersmeerdijk-Vierhuizergat is discussed, and various probabilistic approaches are reviewed to identify the most suitable method to create the probabilistic model. Finally, the concept of sustainability, concerning this Master's thesis, is discussed.

2.1. Revetments

When the outer slope of a dike is left unprotected, it is vulnerable to erosion caused by waves and currents. This erosion can lead to instability of the geometry and, ultimately, failure of the dike. In this study, five types of revetments are selected to prevent erosion:

1. Loose rock;
2. Concrete column elements (Basalton);
3. Interlocking concrete elements (Verkaliet);
4. Hydraulic asphalt concrete;
5. Grass.

The five types of revetments are shown in figure 2.1.



(a) Loose rock (Deltaexpertise, 2015)



(b) Hydraulic asphalt concrete (Deltares, 2015b)



(c) Verkalit (Noppert Beton, 2019)



(d) Basalton (Ruthin Precast concrete Ltd, 2023)



(e) Grass (Jilmer Postma, 2018)

Figure 2.1: Five different revetment types

Although the loads on all five revetment types are similar, there is a significant difference in how the external load is transferred to the internal load and how each structure responds. This distinction can be best illustrated by the concept of leakage length, denoted as Λ .

$$\Lambda = \sqrt{\frac{k_F d_F d_T}{k_T}} \quad (2.1)$$

The leakage length indicates the interaction between external and internal loads caused by waves. It is influenced by the filter and top layer's permeability (k_F and k_T) and the thickness (d_F and d_T). When the leakage length is significantly larger than the length of the wavefront, there is a limited exchange between external and internal loading due to the low permeability. In such cases, the waves retrieve much faster than the internal piezometric level can adjust. When the leakage length is much smaller than the length of the wavefront, there is an easier exchange of external and internal loading. The permeable conditions allow the piezometric level within the dike to track the wave movements effectively (Schierreck and Verhagen, 2019). In figure 2.2, small and large leakage lengths are illustrated where the dashed line is the piezometric level, and the continuing line is the outer water level. For the revetment types mentioned above, table 2.1 shows the relative leakage to wavefront ratios, which explains why the failure mechanisms are entirely different.

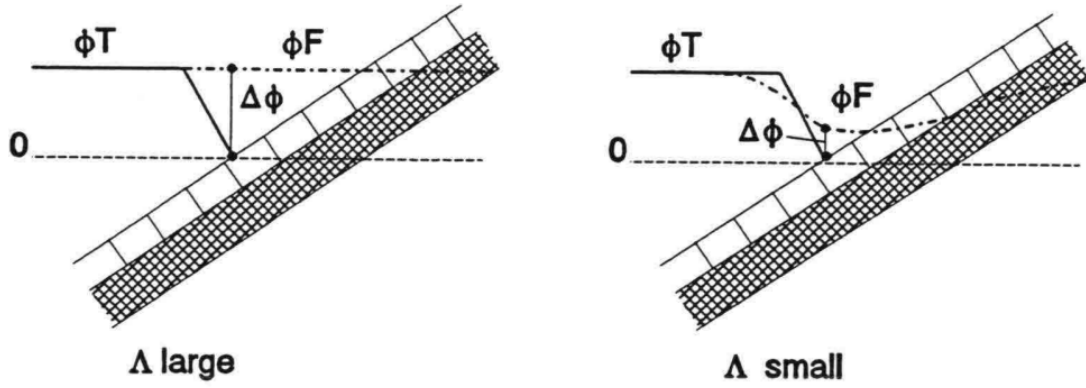


Figure 2.2: Head difference for small and large leakage length (Schierreck and Verhagen, 2019)

Table 2.1: Relative leakage length to wavelength ratio with indicative values

Loose rock	Concrete and interlocking elements	Asphalt, grass
$\Lambda \ll L$	$\Lambda \approx L$	$\Lambda \gg L$
0.15	1.5	∞

As each revetment type is subject to a different type of failure, each has its design formula developed. The governing design formulas are discussed in the following sections.

2.1.1. Loose rock

Loose rock revetment is primarily designed to withstand wave impact. Due to the high porosity of the rock layer, the leakage length associated with this type of revetment is minimal. The wavelength of the waves influences the pressure gradients within the revetment, resulting in uprush and downflow velocities that exert drag forces on the individual stones. The strength of the rock layer is derived from the weight and interlocking of the stones. (Schierreck and Verhagen, 2019). To design the loose rock revetment, the Wettelijk beoordelingsinstrumentarium (WBI), (legal assessment tool), (Rijkswaterstaat, 2017) prescribes the use of design equations developed by van der Meer in 1988. These equations are widely accepted and, therefore, used in this study. The two equations proposed by van der Meer (1988a) are provided below. Depending on the value of the Iribarren number denoted as ζ , one of the two equations governs the design process.

For plunging waves ($\zeta = 0.5 - 3$):

$$\frac{H_s}{\Delta D_{n50}} = C_{pl} P^{0.18} \left(\frac{S}{\sqrt{N}}\right)^{0.2} \zeta_m^{-0.5} \quad (2.2)$$

For surging waves ($\zeta = 3 - 5$):

$$\frac{H_s}{\Delta D_{n50}} = C_s P^{-0.13} \left(\frac{S}{\sqrt{N}}\right)^{0.2} \sqrt{\cot(\alpha)} \zeta_m^P \quad (2.3)$$

The Iribarren number, ζ , indicates the ratio between slope steepness and wave steepness and is defined by the following equation (Battjes, 1974):

$$\zeta_m = \frac{\tan(\alpha)}{\sqrt{\frac{H_s}{L_0}}} \quad (2.4)$$

The highest load on the slope is exactly at the transition between the two equations (collapsing regime) and can be expressed with the equation presented below. The Iribarren number is compared to this value. When it is lower, the plunging waves equation is applied. When it is larger, the surging waves equation is applied.

$$\zeta_{m,transition} = \left(\frac{C_{pl}}{C_s} P^{0.31} \sqrt{\tan(\alpha)}\right)^{\frac{1}{P+0.5}} \quad (2.5)$$

Depending on the permeability and slope angle, the transition lies between $\zeta = 2.5$ and 4 (van der Meer, 1988b).

Table 2.2: Damage level S corresponding to slope (van der Meer, 1988a)

Slope	Start of damage $2 \cdot D_{n50}$	Filter layer visible $2 \cdot D_{n50}$
1:1.5	2	8
1:2	2	8
1:3	2	12
1:4	3	17
1:6	3	17

Governing parameters

- Significant wave height (H_s) [m]
For the Significant wave height, the local significant wave height is applied. This relates to the average of the one-third highest waves. This can also be derived from the energy density spectrum by $H_s = 4\sqrt{m_0}$, where m_0 is the zeroth order moment (van der Meer, 1988b).
- Wavelength (L_0) [m]
For the wavelength, the mean deep water wavelength is applied. In this specific equation, the offshore mean wave period is used. Therefore, the breaker parameter ζ becomes a 'fictive' breaker parameter as it does not rely only on local circumstances (van der Meer, 1988b).
- Relative mass density of rock (Δ_m) [T/m^3]
The relative density of rock relates to the submerged weight of the rock. This value depends on the density of rock and seawater and is generally around 1.65. Loose rock is a natural product so the values may range from 1 – 3 (van der Meer, 1988b).
- Coefficient for plunging and surging waves (C_{pl} , C_s) [–]
The coefficients are the results of curve-fitting and have no physical meaning. C_{pl} ranges approximately from 5.2 to 7, 6.2 is suggested. C_s ranges approximately from 0.84 to 1.16, 1.0 is suggested by van der Meer (1988b).
- Permeability (P) [–]
The permeability coefficient describes the influence of the permeability of the structure on the stability. The lower boundary is for an impermeable structure (clay or sand) where $P = 0.1$. The upper limit is for a homogeneous structure of armour rock, where $P = 0.6$ (van der Meer, 1988b).
- Damage level (S) [–]
The damage level S indicates the number of stones with diameter D_{n50} eroded around the water level within one D_{n50} width. The lower and upper bounds of S depend on the slope angle. The values corresponding to different slope angles are presented in table 2.2. van der Meer (1988b) defined the start of damage as $S = 2$ or $S = 3$ and failure, defined as visibility of the filter, as $S = 8$ to $S = 17$ depending on the slope.
- Number of waves (N) [–]
The storm duration and mean wave period determine the number of waves. The equations are valid for $N = 1000 - 7000$. When more waves are used, the damage is overestimated (van der Meer, 1988b). Deltares (2015c) suggests using a maximum of 7500 waves.
- Slope angle (α) [–]
The equations are valid for slope angles ranging from 1 : 1.5 to 1 : 6 (van der Meer, 1988b).

2.1.2. Placed elements

Placed rock revetments, unlike loose rock revetments, typically do not fail due to direct wave impact but have different failure mechanisms. The following failure mechanisms are defined for placed elements (Deltares, 2015a):

- Toplayer instability due to wave retraction;
- Toplayer instability due to wave impact;

- Toplayer instability due to wave runup;
- Toplayer instability due to longitudinal flow;
- Shearing of the top layer;
- Material transport from the soil to the granular layer;
- Material transport from the granular layer to the top layer.

As a wave hits the revetment, the water level within the underlying dike rises with the wave. However, due to the lower permeability, the water level inside the dike recedes slower than the waves. As a result, a net pressure is exerted from beneath the elements of the revetment. The two resisting forces are the relative element weight and friction between the blocks. For the failure mechanisms mentioned above, specific design formulas are available (Deltares, 2015a). For designing placed elements as revetment, the software 'Steentoets' (Klein Breteler, 2022a) is prescribed by the WBI (Rijkswaterstaat, 2017). However, 'Steentoets' is unsuitable for probabilistic calculations due to the discontinuities in the equations and calculation time. To enable probabilistic analyses, Klein Breteler and Mourik (2014) derived a design equation that approximates the results obtained from 'Steentoets' to design the top layer. The equation is based on the parameters critical to the revetment's stability number. The deviation of the equation with respect to Steentoets is less than 10% in 97% of the results. Furthermore, the equation complies with flume experiments to prove its validity. This equation is preferred over the traditional equation developed by Pilarczyk and Klein Breteler (1998) because it considers more aspects that influence the stability of the elements. The equation presented below is derived for the column type of revetment.

$$\frac{H_s}{\Delta D} = \min \left[4,93 \cdot p_{Z_b} \cdot p_{\tan\alpha} \cdot p_{\Lambda} \cdot p_{\Delta} \cdot p_N \cdot p_{\beta} \cdot p_{S_{op}} \cdot p_D; \left(\frac{H_s}{\Delta D} \right)_{max} \right] \quad (2.6)$$

With the following equations representing the different influencing parameters.

- Dimensionless level of the upper transition height: The influence of the upper transition height (Z_b) is determined by varying the transition height while keeping the design water level the same. For lower stability numbers, the transition height shows a step-wise pattern. A smooth line is plotted through the points. The tested domain is $-1 \leq (Z_b - h_d)/H_s \leq 2$. The influencing factor ranges from $1 \leq P_{Z_b} \leq 2.5$.

$$P_{Z_b} = \max \left[1,06 \cdot \left(\max \left[\frac{Z_b - h_{MWS}}{H_s}; -0,3 \right] + 0,3 \right)^{0,125}; 5 \cdot \left(\min \left[\frac{Z_b - h_{MWS}}{H_s}; -0,2 \right] + 0,2 \right)^4 + 0,9 \right] \quad (2.7)$$

- Slope angle: The stability decreases with an increasing slope angle. The following equation is plotted through the results. The tested domain is from $0.15 \leq \tan\alpha \leq 0.4$. The influencing factor ranges from $1.6 \leq P_{\tan\alpha} \leq 0.8$.

$$P_{\tan\alpha} = 0,54 \cdot (\tan\alpha)^{-0,49} \quad (2.8)$$

- dimensionless leakage length: The influence of the leakage length is tested by changing the top layer thickness ($0.15 \leq D \leq 0.55m$), open space in the top layer ($8 \leq \Omega \leq 15\%$), the thickness of the filter layer ($0.03 \leq b_1 \leq 0.50m$) and diameter of the filter layer ($5 \leq D_{f15,1} \leq 40mm$). The lower leakage length to top layer thickness ratios are approaching the maximum stability number defined in Steentoets and are, therefore, not considered in the equation. This upper boundary is considered in the final equation 2.6. The tested domain ranges from $0.75 \leq \Lambda/D \leq 2.5$. The influencing factor ranges from $0.8 \leq P_{\Lambda} \leq 1.4$.

$$P_{\Lambda} = 0,42 \cdot \left(\frac{\Lambda}{D} \right)^{-2,4} + 0,81 \quad (2.9)$$

- Dimensionless specific mass: The dimensionless specific mass indicates the effect of the submerged weight of the elements. The tested domain ranges from $0.75 \leq \Delta \leq 2.25$. The influencing factor ranges from $0.75 \leq P_{\Delta} \leq 1$.

$$P_{\Delta} = 0,25 \cdot (\Delta - 1,7)^2 + 0,98 \quad (2.10)$$

- **Duration of loading:** Loading duration is expressed in the number of waves hitting the revetment. The top layer thickness and slope do not influence the factor for the number of waves. The tested domain ranges from $1500 \leq N \leq 10000$. The influencing factor ranges from $0.8 \leq P_N \leq 1.4$. The lower boundary seems asymptotic to a factor of 0.8, which is the lower boundary of the equation.

$$P_N = \max(3, 1 \cdot N^{-0,141}; 0, 8) \quad (2.11)$$

- **Angle of incoming waves:** The angle of incidence of incoming waves with respect to the dike's orientation influences the waves' impact on the dike. The tested domain ranges from $0 \leq \beta \leq 90$. The influencing factor ranges from $1 \leq P_\beta \leq 2.5$.

$$P_\beta = 5,5 \cdot 10^{-22} \cdot (\beta + 90)^{9,5} + 1 \quad (2.12)$$

- **Wave steepness:** Wave steepness is the ratio between significant wave height and wavelength. When wave steepness is below 0.02, the maximum stability number limits it. The tested domain ranges from $0.01 \leq S_{op} \leq 0.07$. The influencing factor ranges from $1 \leq P_{Sop} \leq 1.1$.

$$P_{Sop} = \max[0,032 \cdot (S_{op} + 0,3)^{-3}; 1,66 \cdot (S_{op} + 0,3)^{0,47}] \quad (2.13)$$

- **Element thickness:** The factor for element thickness corrects for the spreading in the results between Steentoets and the formula.

$$P_D = \frac{1}{0,054 \cdot D^{-1,3} + 0,79} \quad (2.14)$$

Steentoets uses a maximum stability number. The maximum stability number is related to the loading duration and the breaker parameter. It is determined with the following equation:

$$\left[\frac{H_s}{\Delta D} \right]_{\max} = \frac{\left(7(\min(\zeta_{op}; 2))^{-\frac{1}{3}} + \max(0,5(\min(\zeta_{op}; 5) - 2); 0) \right)}{\max((\cos\beta)^{\frac{2}{3}}; 0,4)} \cdot f_{s,front} \quad (2.15)$$

Where: ζ_{op} is the Iribarren number as described in equation 2.4. However, unlike loose rock, the local wave parameters are used. The factor for the loading duration derived from Steentoets is given by:

$$f_{s,front} = \max\left(1 - c_1 \cdot \log \frac{N}{1000}; c_2\right) \quad (2.16)$$

For columns, $c_1 = 0,15$ and $c_2 = 0,85$ and N the number of waves.

The following parameters are used in the equations mentioned above:

H_s = Significant wave height [m];

D = Thickness of the elements [m];

Z_b = Upper transition height of the element revetment [mNAP];

H_{MWS} = Mean water level [mNAP];

α = Slope of the revetment [-];

Λ = Leakage length [m];

Δ = Relative density of the elements [kg/m^3];

N = Number of incoming waves [-];

β = Angle of incoming waves [$^\circ$];

S_{op} = Wave steepness [-];

ζ_{op} = Iribarren number [-].

To apply these equations, the leakage length and the number of waves experienced during maximum loading conditions need to be calculated. The formulas for determining these parameters are provided in equation 2.17 and 2.18. The derivation of these equations can be found in Chapter 6 and Appendix A of the work by Klein Breteler and Mourik (2014).

$$\Lambda = \max\left(\sqrt{\frac{D(b_1 k_1 + b_2 k_2)}{k'}}; 0,5D\right) \quad (2.17)$$

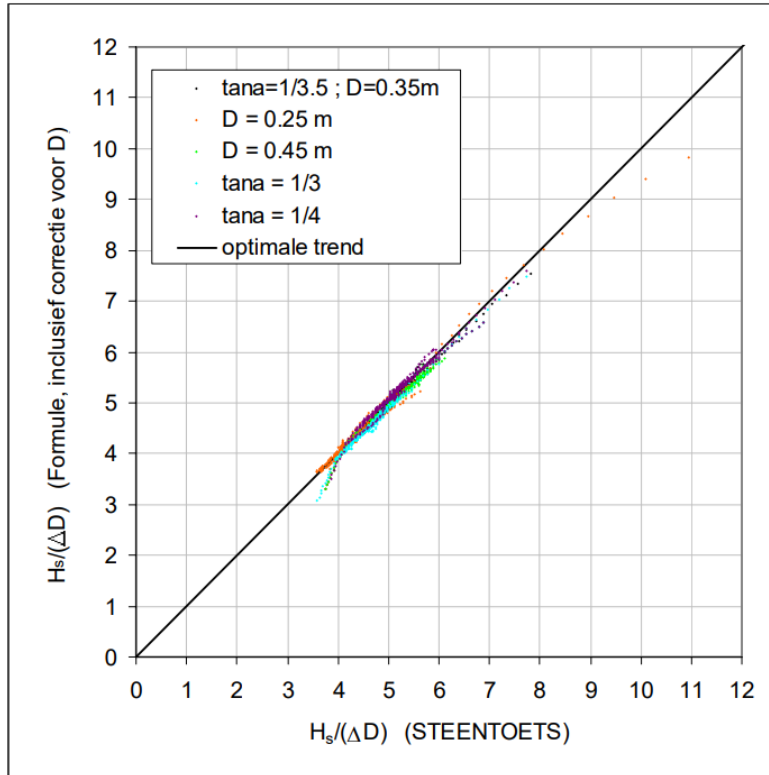


Figure 2.3: The stability number according equation 2.6 versus the stability number derived by Steentoets (Klein Breteler and Mourik, 2014)

Where:

- b_1 = thickness of the first filter layer [m];
- k_1 = Permeability of the first filter layer [m/s];
- b_2 = thickness of the second filter layer [m];
- k_2 = Permeability of the second filter layer [m/s];
- k' = Permeability of the top layer [m/s].

$$N = \frac{t_{load}}{\frac{T_p}{1,1}} \quad (2.18)$$

Where:

- t_{load} = Maximum duration of wave loading [s];
- T_p = Peak period [s]

Figure 2.3 shows the stability number derived by Steentoets and by the design equation 2.6. The correlation is considered high.

Since the previously mentioned design equation is specifically derived for column-type blocks, it cannot be directly applied to other types of revetments. To calculate the interlocking type of placed revetment (Verkalit), M. Klein Breteler from Deltares was consulted for advice. He developed the approximated design equations and 'Steentoets' and has years of experience studying different types of revetments. It was concluded to apply a factor for Verkalit to the existing design equations. The factor is determined by comparing the required block thickness of Verkalit to Basalton in 'Steentoets'. After evaluation, the safety factor determined for Verkalit is $F_v = 1.14$ compared to the Basalton equation. Therefore, the design equation for Verkalit becomes:

$$\frac{H_s}{\Delta D} = \min \left[4,93 \cdot p_{Z_b} \cdot p_{tana} \cdot p_{\Lambda} \cdot p_{\Delta} \cdot p_N \cdot p_{\beta} \cdot p_{S_{op}} \cdot p_D \cdot F_v; \left(\frac{H_s}{\Delta D} \right)_{max} \right] \quad (2.19)$$

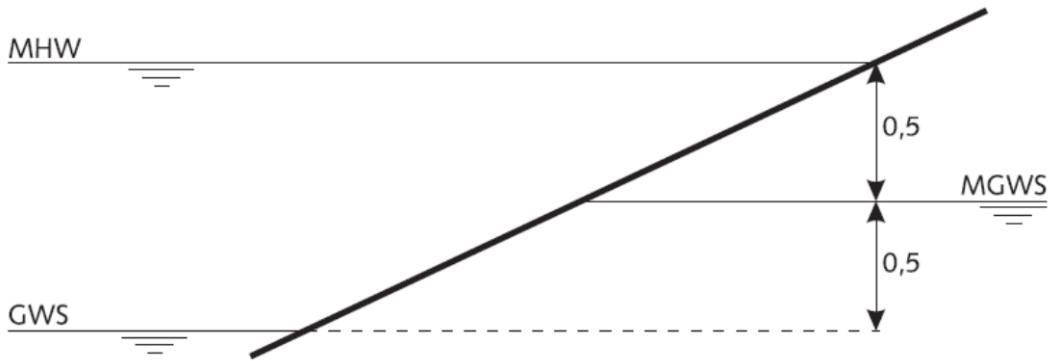


Figure 2.4: Design groundwater level for sea dikes (Deltares, 2015b). MHW: outer water level, GWS: average water level, MGWS: design groundwater level

2.1.3. Asphalt

Asphalt differentiates from other revetment types because it is considered an impermeable layer. Asphalt is designed for two failure mechanisms: uplift and wave impact. The WBI (Wettelijk beoordelingsinstrumentarium / Legal assessment tool) (Rijkswaterstaat, 2017) prescribes the equations developed in TAW (2002). These equations are therefore applied in this study. The two failure mechanisms and the accompanying design equations are further discussed.

Uplift

Uplift can occur when the water level remains high for a longer period (storm surge), causing the phreatic surface inside the dike to reach the same level as the external water level. Subsequently, when the water level outside the dike drops, the phreatic surface inside the dike cannot adjust at the same rate due to the impermeability of the asphalt layer. As a result, water pressure builds up from beneath the asphalt layer, leading to the potential for uplift failure. This failure mechanism can only occur when the outer water level is lower than the phreatic water surface and when the phreatic surface is above the lower boundary of the impermeable layer. The asphalt layer must be of a certain weight to prevent this failure mechanism. The design formula to determine the required layer thickness is (TAW, 2002):

$$d = 0,21 \cdot Q_n(a + v) \cdot \frac{\rho_w}{\rho_a - \rho_w} \cdot R_w \quad (2.20)$$

Where:

d = Layer thickness [m];

a = Vertical distance between the lower bound of the impermeable layer to the outer water level [m];

v = Vertical distance between the outer water level and design level of the phreatic surface [m];

ρ_a = Density hydraulic asphalt concrete [kg/m^3];

R_w = Reduction factor due to the relative position of the outer water level to the phreatic surface [-].

The slope depending factor Q_n is defined by (Deltares, 2015b):

$$Q_n = \frac{0.96}{\cos(\alpha)} \quad (2.21)$$

Where α is the slope.

The design level of the phreatic surface is determined according to figure 2.4 (Deltares, 2015b).

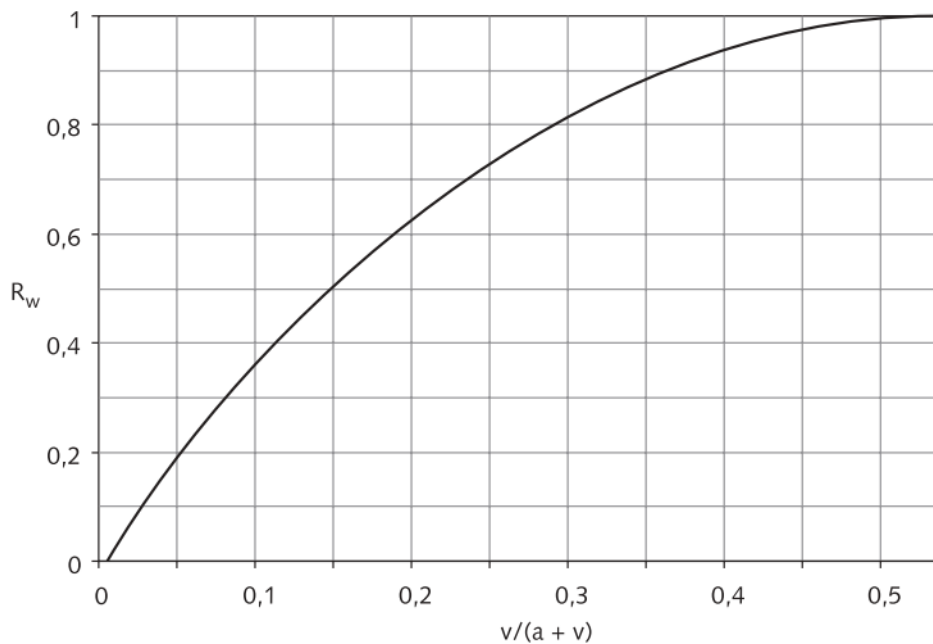


Figure 2.5: Reduction factor R_w depending on water level relative to the phreatic surface (TAW, 2002).

Governing parameters

- Pressure build up parameters (a and v)
The pressure parameter a indicates the vertical distance between the lower bound of the impermeable layer and the outer water level. The pressure parameter v indicates the vertical distance between the design groundwater and outer water levels. Together, a and v indicate the possibility of build-up water pressure under the impermeable layer. The design situation occurs when $a = 47\%$ and $v = 53\%$ of $(a+v)$ (Davidse, 2010).
- Reduction factor (R_w)
The reduction factor indicates the influence of the relative position of the outer water level to the design groundwater level. If the design water level is lower than the average water level, a reduction factor R_w is applied. This depends on the outer water level relative to the phreatic water level. Figure 2.5 presents the graph with which the reduction factor is determined. The factor ranges from 0 to 1.
- Density hydraulic asphalt concrete (ρ_a)
The density of hydraulic asphalt concrete ranges from $2300\text{kg}/\text{m}^3$ to $2350\text{kg}/\text{m}^3$ TAW (2002).
- Slope depending factor (Q_n)
The build-up water pressure is partially dependent on the slope angle. The influence of the slope is included in this factor and is determined using equation 2.21. The factor ranges from 0.96 for gentle slopes to 1.12 for steep slopes. Figure 2.6 presents the relationship.

Wave impact

Wave impact on the asphalt layer can be schematised as a cushioned-spring system. The waves induce peak pressure on the asphalt. The asphalt layer is modelled as a slab. The behaviour of the asphalt layer is influenced by the characteristics of the subsoil and the stiffness of the asphalt layer (Schierck and Verhagen, 2019). Asphalt is a material sensitive to fatigue. Failure occurs when the number of waves acting on the slope exceeds the maximum capacity of the asphalt layer to withstand. Or, in other words, when the Miner-sum exceeds one (TAW, 2002):

$$\sum \frac{n_i}{N_f} \leq 1 \quad (2.22)$$

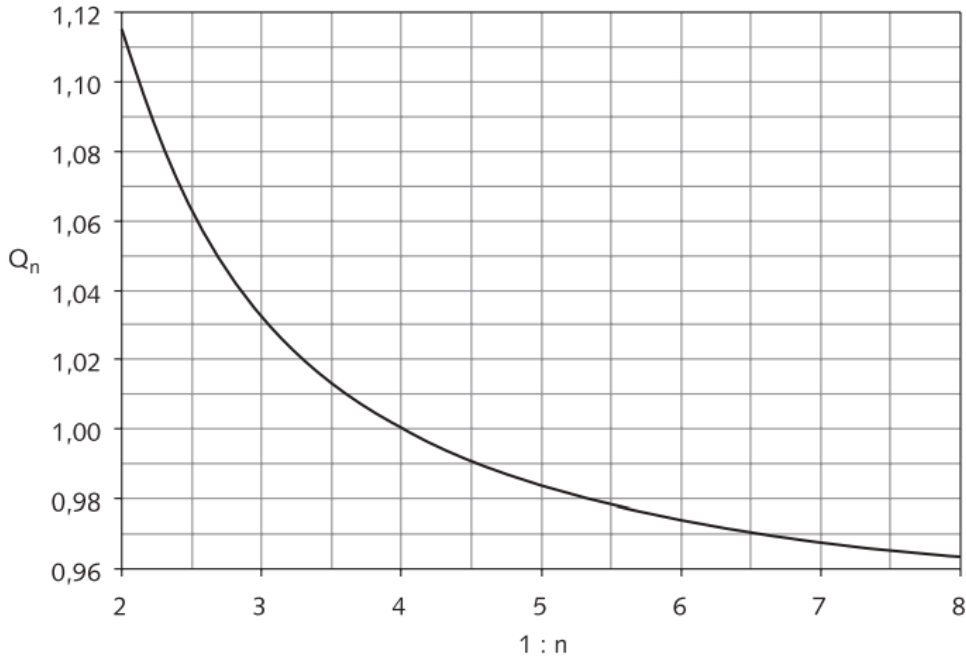


Figure 2.6: Slope depending pressure factor Q_n (TAW, 2002).

Where N_f is the number of loads leading to failure and n_i is the number of actual load repetitions during a storm. The number of loads leading to failure is determined by the fatigue line described with the following equation (Davidse, 2010):

$$\log(N_f) = \beta_f (\log(\sigma_b) - \log(\sigma))^{\alpha_f} \quad (2.23)$$

Where β_f and α_f are fatigue parameters of the asphalt. β_f ranges from 4.8 for assessing and 5.4 for design purposes. α_f ranges from 0.2 to 0.6. σ_b is the cracking strength, ranging from 2.4 to 3.6 (Davidse, 2010).

The critical stress σ is determined with the following equation (Davidse, 2010):

$$\sigma = \frac{P_{max}}{4\beta^3 z} [1 - \exp(-\beta z)(\cos(\beta z) + \sin(\beta z))] \cdot \frac{6}{d^2} \quad (2.24)$$

With:

$$\beta = \sqrt[4]{\frac{3c(1-\nu^2)}{Ed^3}} \quad (2.25)$$

$$P_{max} = \frac{0.25}{\tan(\alpha)} \rho_w \cdot g \cdot q \cdot H_s \quad (2.26)$$

Where:

- P_{max} = Maximum peak water pressure [MPa];
- c = Soil modulus [MPa/m];
- E = Elasticity modulus of asphalt [MPa];
- ν = Transverse contraction coefficient [0.35 [-]];
- H_s = Significant wave height [m];
- q = Slope depending impact factor [-].
- z = Loading width [m]

$$z = \frac{1.3355}{\beta} \quad (2.27)$$

Governing parameters

- Soil modulus (c)
The subsoil's stiffness indicates the subsoil's dampening effect on the impact of waves. It is determined with laboratory tests. The value range depends on the type of subsoil. For sand, the expected values range between 70 and 160 MPa (Klerk and Kanning, 2014).
- Elasticity modulus (Young's modulus) (E)
The elasticity modulus is an important strength parameter of the asphalt layer. It is determined with laboratory experiments. The values range from 4000 to 10000 MPa (Klerk and Kanning, 2014).
- Transverse contraction coefficient or Poisson's ratio (ν)
The transverse contraction coefficient indicates the deformation of the asphalt from wave impact. It is a fixed value of 0.35 (Klerk and Kanning, 2014).
- Slope-depending impact factor (q)
The slope-depending impact factor indicates the influence of the slope. It is based on a factor determined for slope 1:4 = 6.

2.1.4. Grass

A grass revetment on the outer slope of a dike comprises two layers: the top layer, consisting of grass and roots and the sub-layer, consisting of clay. To design a grass revetment, the WBI (Wettelijk beoordelingsinstrumentarium / Legal assessment tool) (Rijkswaterstaat, 2017) prescribes the use of the software 'Riskeer' and 'BM - gras buitentalud'. However, these two software packages are not able to perform probabilistic calculations. This study applies the 'GEBU faalkanstool' developed by M. Klein Breteler. With this software, the clay layer thickness and transition height of the clay layer are determined probabilistically. The strength of the grass revetment depends on the grass's quality and the clay layer's erodibility and thickness. Failure of the top layer is defined as (Deltares, 2015d):

1. The grass sod and part of the top layer may be damaged and even removed over large areas, but the remaining part still contains roots that hold the remainder together, providing strength and stability until the erosion depth exceeds 0.2 meters.;
2. A hole in the top layer of up to 0.15m x 0.15m can be present without causing failure, as the flow has little impact on these small damages. Such small damage may occur due to the removal of a post during a large wave overtopping event or a small initial damage caused by a mole. However, if the hole in the top layer becomes larger, the top layer will fail.

Upon failure of the grass revetment, the residual strength is determined by the thickness of the underlying clay layer. If the clay layer is eroded, the revetment is considered failed (Deltares, 2015d). The quality and composition of the clay layer play a crucial role in its ability to resist erosion. Clay can be composed of different materials and exhibit various sand, silt, and loam compositions. Based on its characteristics, clay is categorised into three distinct classes (Senhorst, 2018):

1. Erosion resistant;
2. moderately erosion resistant;
3. little erosion resistant.

The classes are a function of yield strength and plasticity index as shown in figure 2.7.

The erosion process

The erosion process of the grass layer comprises two main aspects. First, erosion due to wave run up and second, erosion due to the direct wave impact. The water level relative to the transition point from the hard structure to the grass layer determines the dominant erosion process. Wave runup is dominant when the water level is below the transition point. Direct wave impact is dominant when the water level is above the transition point. It is important to note that the transition between these two processes is not abrupt. A transition zone exists where a combination of wave impact absorbed by the hard revetment runs up to affect the grass layer, while some waves directly hit the grass. The two processes are illustrated in figure 2.8 and 2.9.

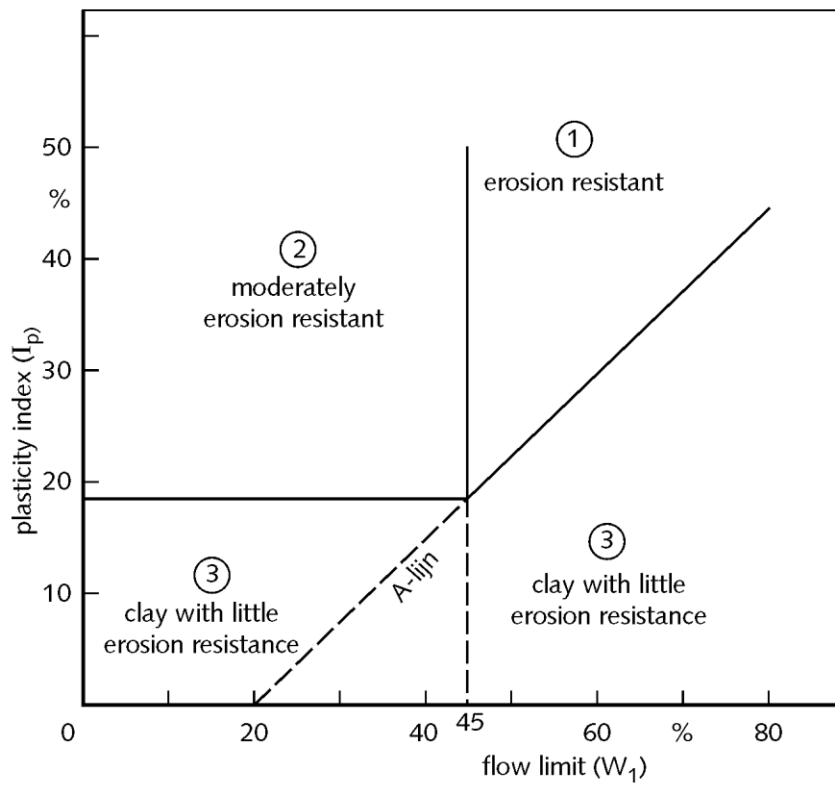


Figure 2.7: Classification for the erosion resistance of clay (TAW, 1996)

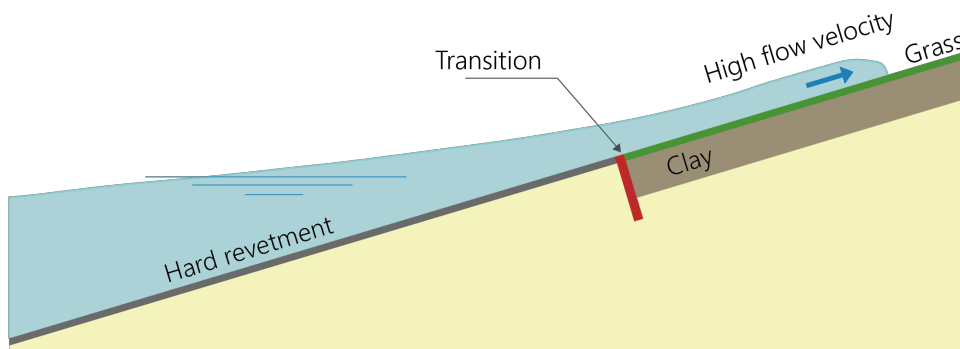


Figure 2.8: Schematic illustration of grass erosion due to wave runup (Klein Breteler, 2022a)

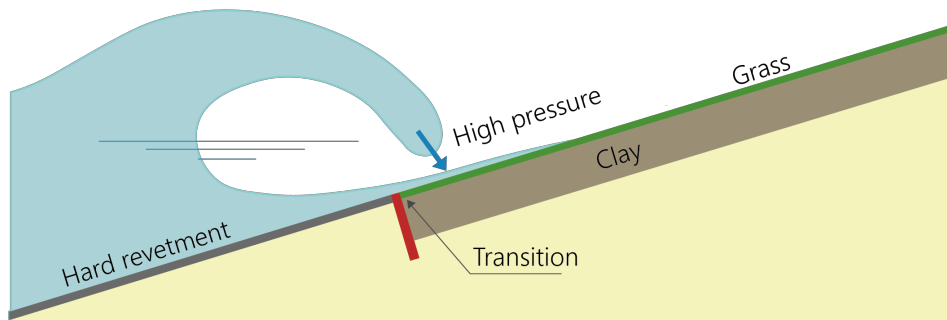


Figure 2.9: Schematic illustration of grass erosion due to direct wave impact (Klein Breteler, 2022a)

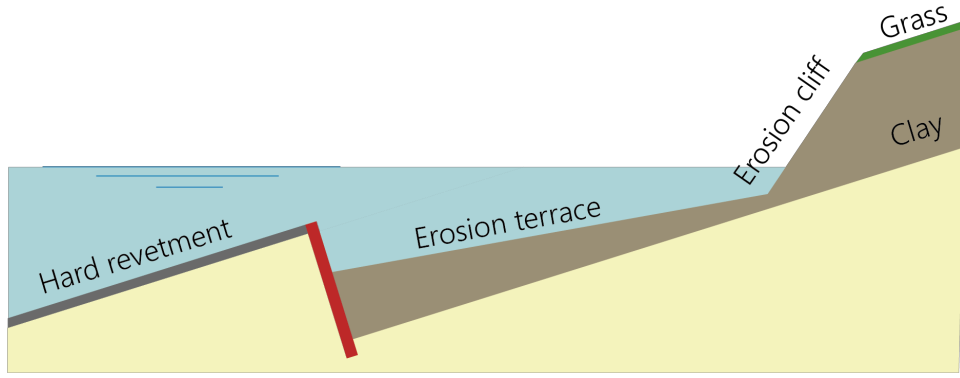


Figure 2.10: Schematic overview of the erosion profile (Klein Breteler, 2022a)

Klein Breteler (2022a) found that the erosion process of the grass and clay layer is non-linear and comprises two distinct phases. The first phase is characterised by limited damage, resulting in a scour hole with a depth of approximately 0.5 meters. During this phase, the erosion process is relatively slow. The presence of the grass layer in the top layer plays a significant role in reducing the erosion rate during this phase. The second stage is a scour hole of 0.5m deep until the underlying sand layer. The second phase is defined by forming a scour hole that extends from the initial 0.5-meter depth to the underlying sand layer. In this phase, a scour cliff becomes evident. The erosion speed increases significantly during the second stage due to the direct impact of waves on the cliff. In figure 2.10, the erosion profile is schematised.

Through the analysis of physical experiments conducted in the Delta flume and numerical simulations using software OpenFOAM (The OpenFOAM Foundation, 2023), design formulas have been derived for both phases of the erosion process. It is important to note that these design formulas are derived under the assumption of initial damage to the grass layer of approximately 15x15cm and 5cm deep. The design formulas for the erosion depth and volume derived by Klein Breteler (2022a) are:

Phase 1:

The erosion depth per time step is:

$$d_{e,growth} = m_1 \cdot f_{transition} \cdot c_d \cdot \max(0; H_{m0,ire} - 0.5) \tan(\alpha)^{1.5} \cdot t_{step} \quad (2.28)$$

The cumulative erosion depth is:

$$d_{e,i} = d_{e,i-1} + d_{e,growth} \quad (2.29)$$

The erosion volume at the end of step one is:

$$V_{e,1-2} = \frac{d_{e,1-2}^2 - d_0^2}{2 \cdot \tan(\alpha - \alpha_{terras})} + \frac{d_{e,1-2}^2}{2 \cdot \tan(\alpha_{cliff} - \alpha)} \quad (2.30)$$

Phase 2:

The final erosion depth at the end of the storm is:

$$d_e = \sqrt{\frac{2V_{e,i} \tan(\alpha - \alpha_{terras}) + d_{0,i}^2}{(1 + \frac{\tan(\alpha - \alpha_{terras})}{\tan(\alpha_{cliff} - \alpha)})}} \quad (2.31)$$

The erosion volume per time step is:

$$V_{e,growth} = 0,068 \cdot m_2 \cdot \frac{(\max(0; H_{m0,ire} - 0,25))^2}{\sqrt{(s_{op})}} \cdot \min(2,4; \max(0; 1,2 + 1,6 \cdot \frac{h_{transition}}{H_{m0,ire}})) \cdot (\frac{13}{\frac{B_{berm}}{H_{m0,ire}} \cdot \min(1; \max(0; 2 - \frac{h_{berm}}{H_{m0,ire}})) + 8} - 0,5) \cdot (1,69 - \frac{0,17}{\tan(\alpha)}) \cdot t_{stap} \quad (2.32)$$

The cumulative erosion volume is:

$$V_{e,i} = V_{e,i-1} + V_{e,increase} \quad (2.33)$$

The following parameters are used in the equations mentioned above:

$d_{e,growth}$ = Increase in erosion depth during time step i [m];

$d_{e,1 \rightarrow 2}$ = Erosion depth at the start of the second phase [m];

d_0 = Erosion depth at the transition point from hard to soft revetment [m];

m_1 = Stochastic variable from Hydra-Ring [-];

$f_{transition}$ = Influence factor for transition height [-];

c_d = coefficient for the erosion in the first phase (0,67 if sand content < 45% and including the effect of a dry and hot summer once every five years. [-];

$H_{mo,ire}$ = Significant wave height at the peak of the storm [m];

α = Slope of the dike [-];

$d_{e,i}$ = Erosion depth at the end of step i [m];

V_e = Erosion volume per meter [m^2];

d_0 = Erosion depth at the transition from hard to grass revetment [m];

S_{op} = Wave steepness [-];

$h_{transition}$ = Water depth at the transition point from hard to grass revetment [m];

B_{berm} = Width of the berm [m];

h_{berm} = Water depth on the edge of the berm [m];

t_{stap} = Time step .

2.2. Probabilistic techniques

To design the various revetment types, a probabilistic approach is applied. This results in the most precise design outcomes. This approach is based on the assumption that the more precise the outcome, the amount of materials reduces, which leads to a decrease in the ECI. The conventional deterministic approach relies on safety factors that tend to result in structures being overly dimensioned. The probability of failure is defined as follows:

$$P_f = P(S > R) \quad (2.34)$$

This is often rewritten towards the so-called limit state- or Z-function:

$$Z = R - S \quad (2.35)$$

Various probabilistic approaches can be employed to test this equation. When selecting a method, important factors to consider include implementability, efficiency, accuracy, and precision. Three potential methods have been chosen: FORM, Crude Monte Carlo, and Importance Sampling. The OpenTurns package in Python (Van Rossum and Drake Jr, 2022) is used for the probabilistic analysis (Baudin et al., 2017). This package offers numerous predefined statistical functions. The following section will discuss the theory regarding these three probabilistic techniques.

2.2.1. First-Order Reliability Method (FORM)

The first-order reliability method (FORM) estimates the probability of failure of the limit-state function. It uses an iterative approach combined with the linearization of the limit-state function. This method involves complex mathematical calculations. This section broadly covers the general method without extensively elaborating on the mathematical details. For a more in-depth understanding of the mathematical background, reference can be made to Ditlevsen and Madsen (2007). FORM is based on the following three steps, which are further discussed below:

1. Transformation of the input random vector into a standard normal vector;
2. Determination of the design point;
3. Linearization of the limit-state function at the design point and the computation of the probability of failure.

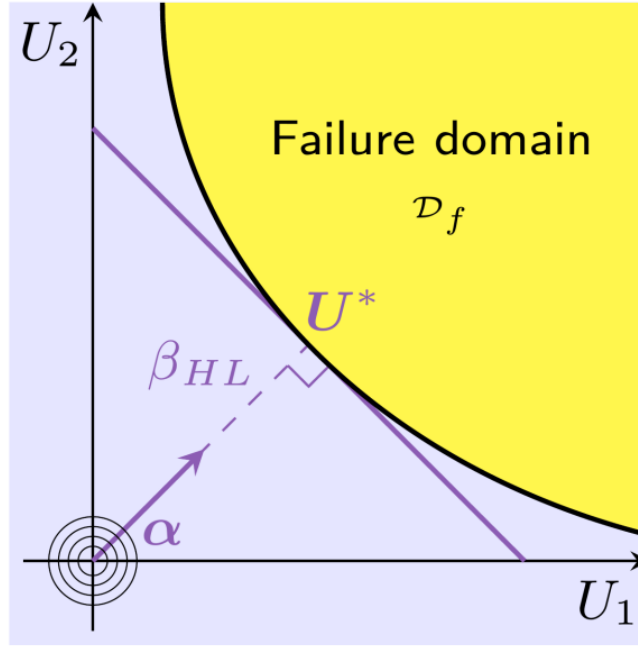


Figure 2.11: Graphical representation of FORM analysis (Marelli et al., 2022)

All parameters together that describe the limit-state function form the input random vector. First, An isoprobabilistic transform τ is done to transform the original input vector to a standard normal vector. This transformation allows for the utilization of normal Gaussian probability distributions. The values closer to the origin of the standard normal space (Φ) have a more significant influence on the overall probability of failure. Next, the design point (U^*) is defined as the point in the failure domain closest to the origin of the standard normal space (Φ). This point is considered the point where the function most likely fails. The distance from the origin of the standard normal space towards the design point is the reliability index and is directly related to the probability of failure by:

$$P_f = \Phi(-\beta_{HL}) \quad (2.36)$$

Where β_{HL} is the vector from the origin to the design point, and Φ is the standard normal space. When the original limit state function is non-linear, an iterative process determines the design point. Specifically, the Rackwitz-Fiessler algorithm is used for the iteration procedure (Rackwitz and Fiessler, 1978). The limit state function is approximated using a first-order Taylor expansion. Throughout the iterative process, the unit vector (α^2) is extracted, indicating each parameter's contribution to the input vector. With this vector, the influence of each parameter on the overall failure probability is assessed. The FORM method for a simple two-dimensional case is graphically presented in figure 2.11. (Marelli et al., 2022)

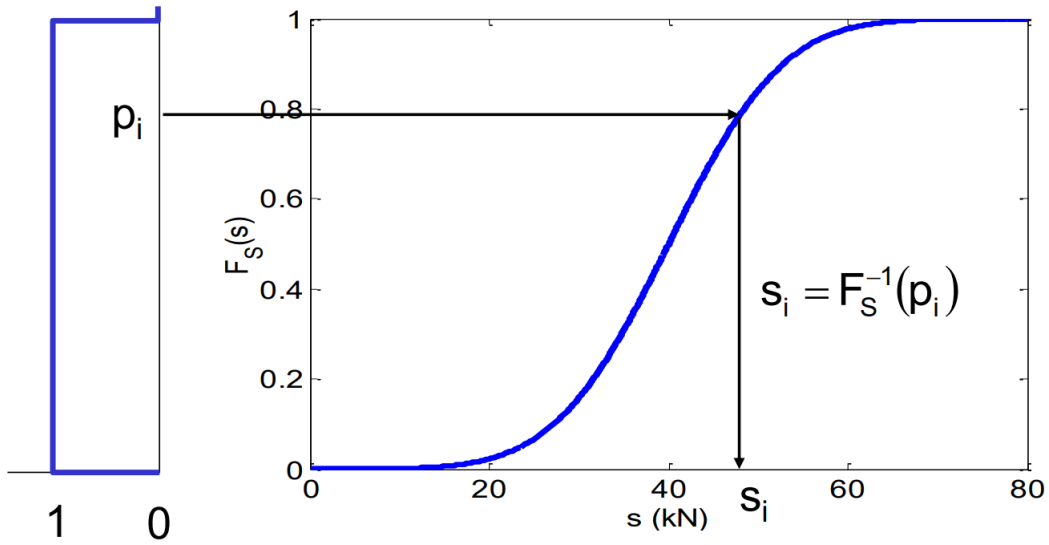


Figure 2.12: Generation of random samples (Jonkman et al., 2017)

2.2.2. Crude Monte Carlo

Crude Monte Carlo analysis is a level III probabilistic method. It does not involve linearization or other methods to simplify the limit state function. The Crude Monte Carlo method entails sampling random values from the cumulative distribution function. Random numbers x_i between 0 and 1 are drawn from a uniform probability density function. This random number x_i is then treated as the cumulative probability of an arbitrary cumulative density function $F_x(x)$. By applying the inverse of the cumulative probability density function, a realization x can be assigned to the corresponding cumulative probability (Jonkman et al., 2017). This approach allows evaluation of the limit state function using many randomly generated samples, providing a statistical assessment of the probability of failure.

$$x = F_x^{-1}(x_i) \quad (2.37)$$

This procedure is graphically presented in figure 2.12

For each random variable, N realizations are simulated. Then, for each set of realizations, the Z-function is evaluated. If $Z < 0$, a counter N_f is increased by one. The probability of failure is then obtained with:

$$P_f = \frac{N_f}{N} \quad (2.38)$$

The number of realizations N is determined by an accuracy criterion and a maximum number of evaluations. The accuracy is determined based on the coefficient of variation, which is obtained with the following:

$$COV = \frac{1}{\sqrt{NP_f}} \quad (2.39)$$

The Crude Monte Carlo analysis continues until the target accuracy is achieved. However, when the target probability of failure is very low, and the target accuracy cannot be achieved, the simulation stops once the maximum number of evaluations is reached. The output of a simple model is graphically presented in figure 2.13. (Jonkman et al., 2017)

2.2.3. Importance sampling

Compared to Crude Monte Carlo, importance sampling aims to get more realizations in the failure domain to converge faster to the required accuracy of probability of failure. This is realised by taking a sampling function $f_s(x)$ with its maximum located in the domain that contributes most to P_f . The efficiency of importance sampling compared to Crude Monte Carlo depends on the choice of $f_s(x)$ and the corresponding expected value μ . The expected value μ is often chosen in the design point (U^*). The design point is where $Z(x) = 0$ with the highest probability of occurrence. The design point can be obtained by employing FORM analysis as

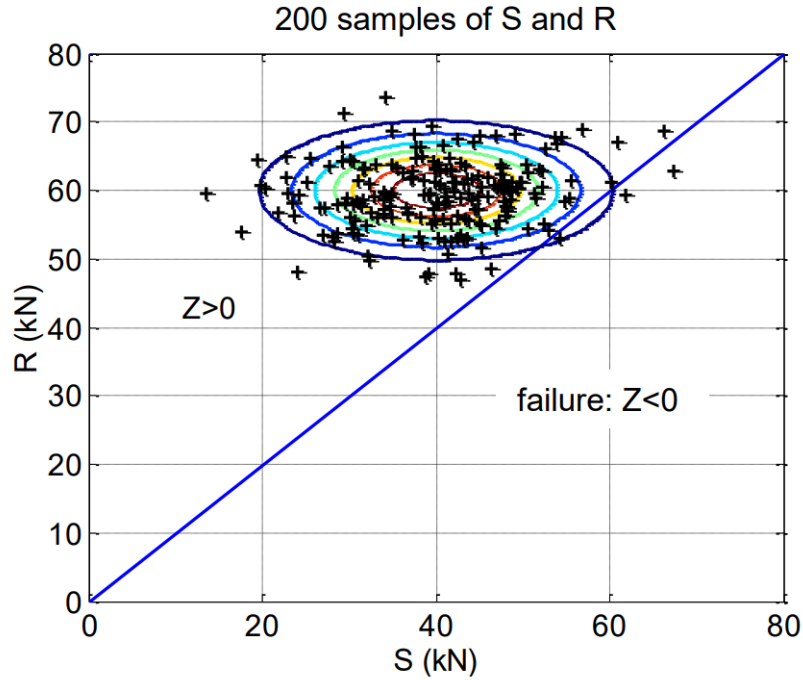


Figure 2.13: Output example Monte Carlo analysis (Jonkman et al., 2017)

described in section 2.2.1. A distribution is assigned to all parameters with mean μ corresponding to the design point, and standard deviation σ is derived from the original standard deviation. As described in section 2.2.2, the same sampling process is then applied using these distributions for each parameter. The individual sampling functions are substituted in the joint sampling distribution $f_s(x)$ (Jonkman et al., 2017):

$$f_s(x) = f_s(x_1) \cdot f_s(x_2) \cdot f_s(x_n) \quad (2.40)$$

And into the real joint probability density function:

$$f_x(x) = f_{x1}(x_1) \cdot f_{x2}(x_2) \cdot f_{xn}(x_n) \quad (2.41)$$

When taking the ratio of the real and the sampling joint probability density functions, the probability of failure is obtained with equation 2.42. This is the same equation as equation 2.38 but rewritten such that each failure is multiplied with a factor determined by the ratio as described in equation 2.41.

$$P_f = \frac{1}{N} \sum_{j=1}^N I[(g(x) < 0)] \frac{f_x(x)}{f_s(x)} \quad (2.42)$$

Convergence to the required accuracy using importance sampling is generally much faster than Crude Monte Carlo. This results in much lower computational costs. Figure 2.14 illustrates an output of a simple model using importance sampling (Jonkman et al., 2017).

2.3. Sustainability

This study aims to optimise the design for 'sustainability'. However, sustainability is an umbrella term encompassing a broad spectrum of aspects. Therefore, it is crucial to specify a definition for this study. Sustainability is often described using Social, economic, and environmental pillars. Whether these aspects overlap or support each other is subject to debate (Purvis et al., 2019). This Master's thesis focuses on the emission part of the environmental/economic aspect, expressed in the Environmental cost indicator (ECI).

Environmental Cost Indicator (ECI)

The ECI quantifies the environmental impact of a design's material and energy consumption throughout the life cycle. This includes its construction, usage, maintenance, and eventual removal, reuse, or recycling

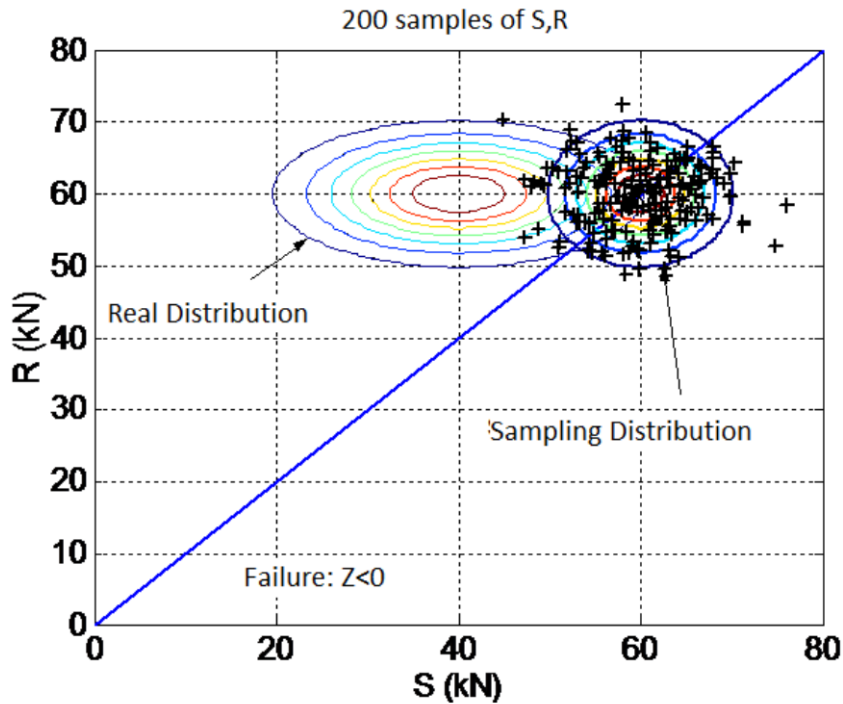


Figure 2.14: Output example importance sampling (Jonkman et al., 2017)

processes (Zandbergen, 2021). It is a single-value score indicator expressed in Euros. The lower the score, the more sustainable the design is. To make the ECI calculations, Rijkswaterstaat developed the tool called DuboCalc (Schipper et al., 2022).

The phases mentioned above for which the ECI is calculated are all subdivided into sub-phases. Additionally, the ECI accounts for environmental costs and benefits associated with the project that may not directly correspond to any specific phase. An ECI includes 11 environmental impact aspects, each with its shadow costs expressed in €/kg equivalent (van der Klauw et al., 2018). The shadow costs represent the value society is willing to pay to achieve environmental goals. The calculation methodology is based on the life cycle analysis specified in the "Determination Method for the Environmental Performance of Structures"¹ (Stichting Nationale Milieudatabase, 2022). The shadow costs for each aspect of the project are based on the "National Environmental Database", which is maintained and updated by the "Foundation National Environmental Database". Within DuboCalc, several standard objects are defined. The things relevant to this thesis are 'hard revetment' and 'soft revetment'. Hard revetment is subdivided into 'the removal of the top layer' and 'the construction of the top layer'. The soft revetment is subdivided into 'sowing of the revetment' and 'maintenance of the revetment' (Drok et al., 2021). Next to these standard objects, there is a possibility to add custom objects to the library.

¹Bepalingsmethode Milieuprestatie Bouwwerken

3

Overall analysis framework and case study

The method to answer the research questions is to develop a Python-based tool. This tool aims to systematically test all possible combinations of revetment types for their probability of failure. The tool is applied to the Lauwersmeerdijk-Vierhuizergat case, serving as a case study (3.2). For each combination that fulfils the safety requirement, the ECI is calculated. When sorting the results from low to high ECI, the design with the lowest ECI can be selected.

This chapter provides a detailed description of the model. To understand how the model works, first, the workflow and the structure of the model are discussed. The case study to which the model is applied is described and followed by the input, the probabilistic technique, the ECI calculation, and the result.

3.1. Workflow

The workflow visually describes the method and the steps required to answer the research questions as stated in section 1.4. A literature study answers the first sub-question, and the preferred probabilistic technique is applied in the model. To answer the second and third research questions, the model tests the different parameter combinations and transition heights in a structured manner for the technical requirements. Subsequently, the ECI for each parameter combination is calculated. When comparing different design outcomes, the influence of the parameters on the ECI is determined. Finally, the design with the lowest ECI is compared with Arcadis's design for the Lauwersmeerdijk.

Figure 3.1 illustrates a simplified version of the entire workflow of the model with which the research questions are answered. Appendix B presents a more elaborate workflow. This section elaborates further on the blocks and their interaction as presented in the workflow. There are four different blocks distinguished, with each its function. It starts with the total length of the slope that has to be covered with revetment. The four blocks are further explained below.

1. Grass revetment: The first block represents the probabilistic analysis of the grass revetment. The GEBU tool is used to determine the thickness and transition height from hard to grass revetment (Klein Breteler, 2022b). This tool is specifically developed to make probabilistic calculations for outer grass revetment. It is based on the equations as described in section 2.1.4. The model is validated using the Lauwersmeerdijk, which makes it very well applicable to this study. Important to note are the limitations of the tool:

- The transition height from hard revetment to grass has to be above +5mNAP.
- The model uses FORM analysis and can not be changed to a level three probabilistic method.
- The model assumes a grass cover with damages of 15 x 15 cm (Klein Breteler, 2022a).

This block is a stand-alone part of the model concerning the assessment of the technical requirements. It is not included in the Python-based model like the other blocks, but the result table is generated separately, which is manually included in the Python model. Two parameters are tested: The clay layer thickness and transition height with respect to NAP. Both parameters are discretised into steps of 0.2 m. For all combinations, the probability of failure is calculated. The corresponding ECI and financial costs are calculated for the designs that fulfil safety requirements.

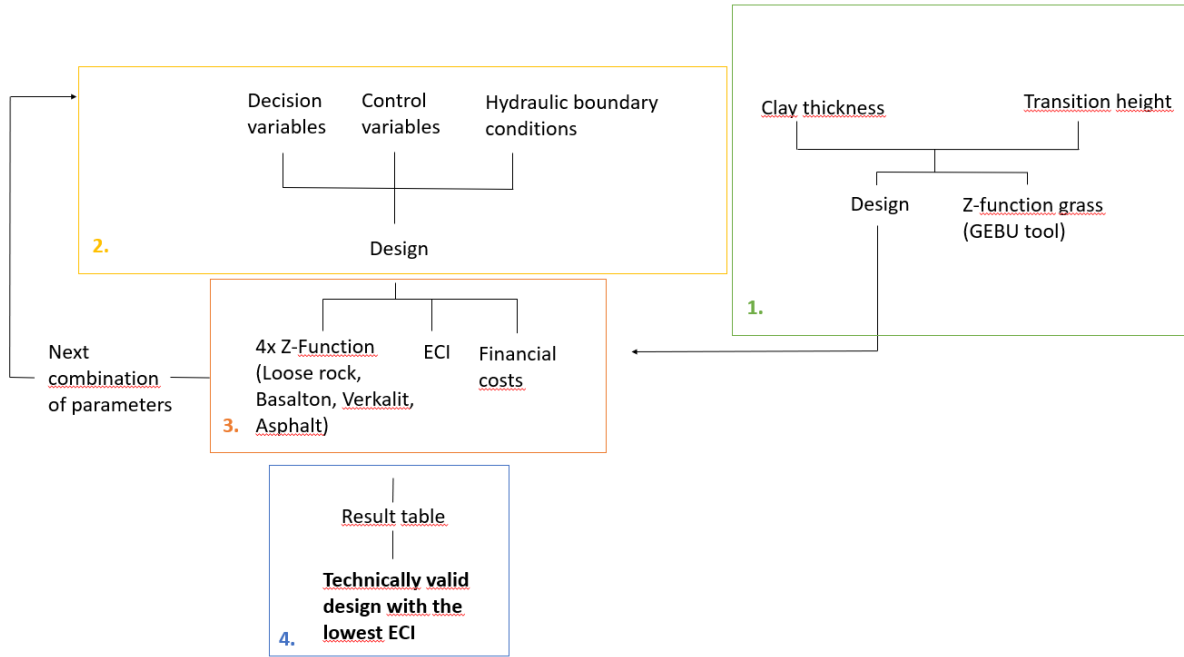


Figure 3.1: Simplified workflow of the model

2. Parameter selection: All different parameters required for the design equations described in section 3.3.5 are stored here. The parameter combinations to be tested are created and used as input for block 3. The parameters are split into three groups: the decision parameters, control parameters and hydraulic boundary conditions. Those are further elaborated in section 3.3. For each revetment type, the slope length and transition height are altered by selecting the range of hydraulic boundary conditions.

3. Testing z-function and ECI: The resulting parameter combinations from block two are evaluated here for the corresponding Z-function. For the same parameter combination, the ECI and financial costs are calculated. After completing block 3, the loop for the parameter combination begins again, and the Z-functions are evaluated for the next set of parameters. This process continues until all combinations are evaluated.

4. Merging to one table: The final block merges all designs with their probability of failure, ECI score and financial costs. The combinations that do not fulfil the safety requirements are filtered out. Next, the obtained data set is sorted based on the ECI score. The designs with the lowest ECI scores, indicating lower emissions during their lifetime, are prioritised.

3.1.1. Structure of the model in Python

The Python model is structured using object-oriented programming. It consists of input, probabilistic calculations, ECI calculations, financial calculations, the constructor to merge and the results to obtain the required output. Figure 3.2 presents the flow chart of the model's structure. The 'main' is located in the model's center. This functions as the model's constructor, where all components are merged, and the calculations are performed.

3.2. Description case study

The Lauwersmeerdijk - Vierhuizergat dike reinforcement project is chosen as a case study. The choice to use a case is twofold. Firstly, selecting a specific case allows for applying real-world geometry with hydraulic boundary conditions and failure probabilities. Secondly, the case study enables a comparison of the chosen design and the design outcome of this study. From this, lessons can be learned on the effect of early implementation of the ECI in the design process. The project is situated in the northern part of the Netherlands, in the province of Groningen. It comprises two sub-trajectories: the 'Havendijk' and the 'Landelijke dijk', as depicted in figure 3.3. For this study, the Landelijke dijk is selected, as this section is directly adjacent to the Waddenzee (Wadden Sea).

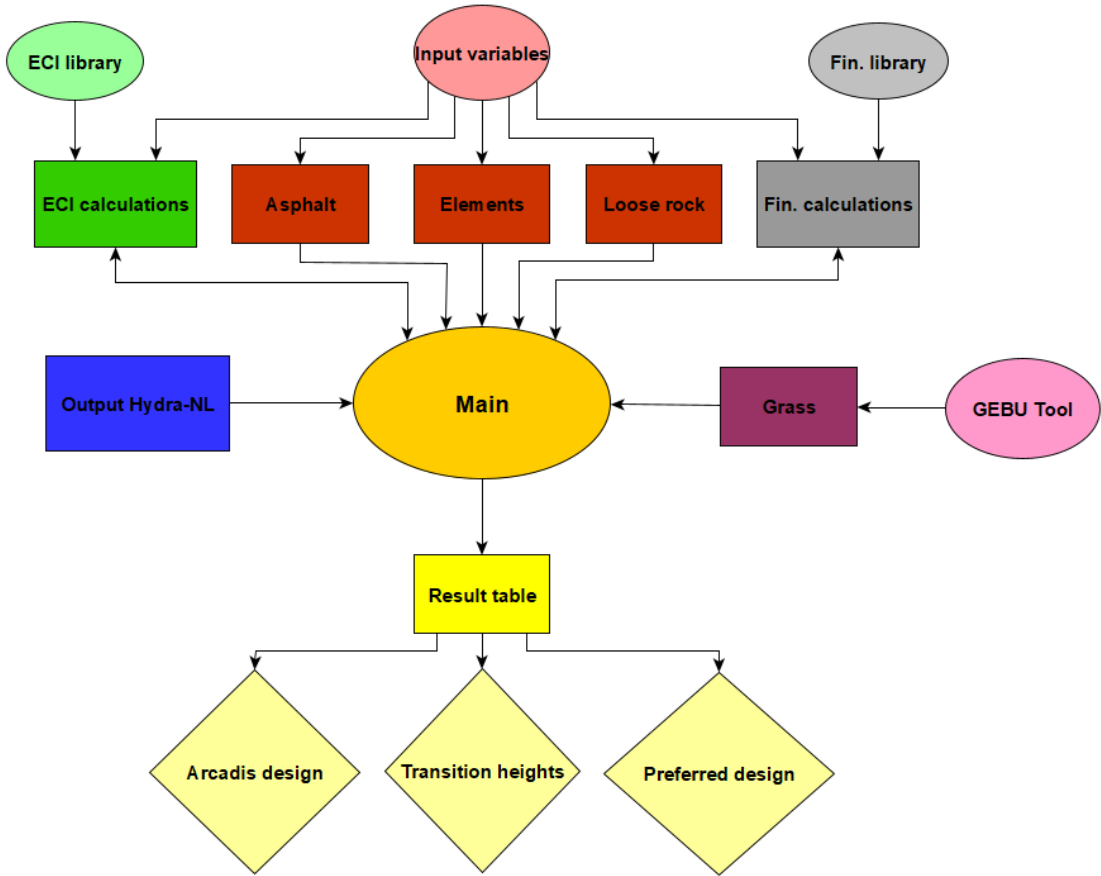


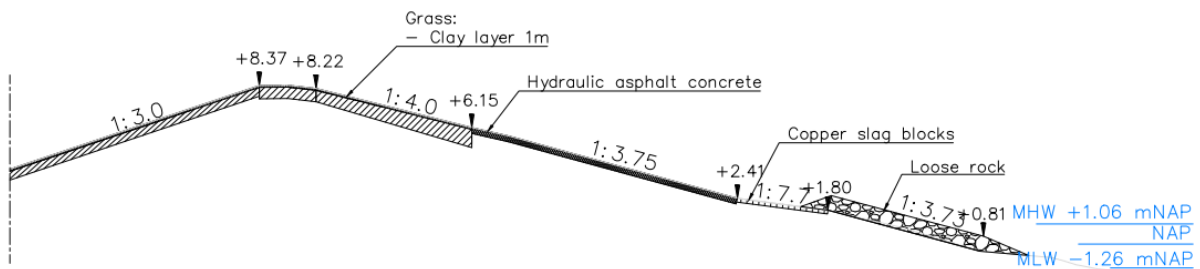
Figure 3.2: Flowchart of the dike revetment model. The blue block represents the hydraulic boundary conditions. The green blocks represent the ECI calculation, the red blocks represent the probabilistic calculations, the grey blocks represent the financial calculation, the pink blocks represent the grass calculation, and the yellow blocks represent the main constructor and the final result.



Figure 3.3: Location of the sub trajectories for the dike reinforcement project Lauwersmeerdijk-Vierhuizergat



Figure 3.4: Sections landelijke dijk



Cross-section: Original design
Scale 1:200

Dike profile	Height (+mNAP)	+8.37	+8.22	+6.15	+2.41	+1.80	+1.00	+0.81	+0.75
	Distance (m)	-33.43	-30.43	-22.19	-8.14	-3.36	0.00	4.70	8.59

Figure 3.5: Initial geometry dike

Description Landelijke Dijk

The dike is subdivided into 12 sections. For this study, one section is taken as representative of the entire dike. This is a simplification but does not influence the developed design methodology. The difference with other sections is the boundary conditions. Section 11 is selected as this is a straight section without dike transition or very shallow foreland see figure 3.4.

In general, the original dike revetment is designed as follows:

- Tow of loose rock;
- Lower slope of copper slag blocks, slope 1:3,5;
- Berm of asphalt, slope 1:10;
- Asphalt revetment, slope 1:4;
- Grass revetment on ca. 1,00 m clay to the crest of the dike.

The geometry of the dike is presented in figure 3.5.

Probability of failure

The maximum allowable probability of failure of the Lauwersmeerdijk, as prescribed in the Waterwet (2009), is 1/1000 year. The dike can fail due to several different failure mechanisms. The sum of the different failure mechanisms should equal the failure mechanism prescribed by the Waterwet (2009). As not all the failure mechanisms are equally important, a certain weighting factor to each one is applied (ω). The failure probability distribution is distributed as prescribed by (Rijkswaterstaat, 2017). The following failure mechanisms and their associated contribution to the failure probability apply to this study:

- Damage hard revetment, $\omega = 0.045$;
- Damage to grass revetment, $\omega = 0.05$.

The probability of failure per mechanism is calculated with the following equation:

$$P_{mech} = \frac{P_{max} \cdot \omega}{N} \quad (3.1)$$

Where N is the length effect factor and P_{max} is the probability of failure of the entire dike. This results in the following probability of failure for each mechanism:

- Damage hard revetment ($N = 3$), $P_f = 1/60.000$;
- Damage to grass revetment ($N = 3$), $P_f = 1/66.666$.

3.3. Input

The model's input variables are classified into Hydraulic conditions, ECI values, financial values, decision variables and control variables. The latter can further be categorised into stochastic variables and deterministic variables.

3.3.1. Hydraulic conditions

For the loading on the revetment, only hydraulic conditions are considered. Geotechnical and other aspects are outside the scope of this study. The hydraulic boundary conditions include the sea water level, corresponding waves and loading duration. The wave characteristics are correlated to the sea water level. The required hydraulic boundary conditions for the design equations per water level are:

- Water level (h): The water level is discretised into steps of 0.2m ranging from -0.37 mNAP until +6.24 mNAP. These are the lower boundary of the hard revetment and the maximum water level during design conditions.
- Significant wave height (H_{m0}): The significant wave height is the average of the one-third highest waves of the entire spectrum.
- Peak wave period (T_p): The peak period is the most frequently occurring period in the spectrum. As the spectrum is not normally distributed, the peak period differs from the average wave period.
- Average wave period (T_m): The average wave period is used to calculate, together with the storm duration, the number of waves attacking the revetment.
- Wavelength (L): The wavelength depends on the period and water depth. The following equations are valid depending on the relative water depth.
Shallow water depth ($d/L < 0.5$):

$$L = \sqrt{gdT} \quad (3.2)$$

Intermediate water depth ($0.05 < d/L < 0.5$)

$$L = \frac{gT^2}{2\pi} \tanh\left(2\pi \frac{d}{L}\right) \quad (3.3)$$

Deep water ($d/L > 0.5$)

$$L = \frac{gT^2}{2\pi} \quad (3.4)$$

- Storm duration (t): The duration the waves act on the revetment.

The hydraulic boundary conditions are correlated. Therefore, Hydra-NL (Duits, 2020) is used to calculate the conditions. Hydra-NL uses a fully probabilistic wave field generated by Hydra-Ring (Diermanse et al., 2013). Hydra ring uses Swan to calculate the wave characteristics for the different combinations of wind speed and direction and water level (van den Bos, 2018). In Swan, the following processes are considered to determine the wave characteristics.

$$S_{tot} = S_{in} + S_{nl3} + S_{nl4} + S_{ds,w} + S_{ds,b} + S_{ds,br} \quad (3.5)$$

These terms represent wave growth due to wind and the nonlinear transfer of wave energy through three and four wave-wave interactions. Wave dissipation due to wave white capping, bottom friction and depth-induced wave breaking (van den Bos, 2018). The input for the model requires wind and water level statistics. The Dutch coast is divided into sections of similar conditions. The Lauwersmeerdijk-Vierhuizergat case is located in the Western Waddenzee region. The water level statistics from the station near Lauwersmeer are used for this region. The wind statistics from Terschelling are used (Diermanse et al., 2013). Within Hydra-Ring, a wave model is generated by calculating the wave characteristics using SWAN with all possible combinations of wind speed, wind direction and water level.

Hydra-NL selects the dominating conditions for a predefined sea water level at a certain return period. For this study, a return period of 1/1000 years is used as this is the safety requirement for the Lauwersmeerdijk. This storm induces the highest loading on the upper part of the revetment. However, it is important to note that the design conditions for the lower-lying parts of the revetment do not necessarily occur during this storm event. Therefore, the maximum loading conditions for all water levels from the lowest part of the revetment up to the crest are determined. The water level is treated as a discrete variable with a step size of 0,2m. The corresponding significant wave height and peak period are determined for each water level. This step size is chosen to accurately determine the transition height of failure and non-failure for different revetment types. A site-specific Hydra-Ring model was developed to ensure realistic hydraulic conditions at the Lauwersmeerdijk project site. This was necessary as the existing models split exactly at the project site, leading to unrealistic values for hydraulic conditions.

Wave parameters

This study aims to develop a probabilistic model for the design of dike revetments. Therefore, it is essential to implement the hydraulic boundary conditions as stochastic variables in the model. With Hydra-NL, it is possible to obtain the deterministic wave characteristics corresponding to the dominant wind direction. The wave characteristics include a safety factor as a result of the probabilistic model Hydra-Ring (Diermanse et al., 2013). The total uncertainty of the various boundary conditions is determined by factors such as the model, wind, bathymetry, and dike profile. Hydra-NL provides the coefficient of variation for the uncertainty of the model. Estimating the uncertainty related to the other influencing factors, such as wind and bathymetry, is challenging due to the lack of available external data. The dike profile's uncertainty is considered by assigning a coefficient of variation to the slope, which is further explained in section 3.3.3. When implementing the wave parameters as stochastic and drawing random samples from this during the probabilistic analysis, combinations might not physically occur. This may lead to design errors. Therefore, a breaker parameter is included in the model to check for this requirement. The breaker parameter is described by the following equation defined by Kamphuis (1991):

$$H_{sb} = [0.095 \exp(4m)] L_{pb} \tanh\left(\frac{2\pi d}{L_{pb}}\right) \quad (3.6)$$

This equation calculates the maximum significant wave height based on the slope angle m , the wavelength corresponding to the peak period and L_{pb} and the still water depth d . The physically impossible waves are filtered out by including this breaker parameter as a check and filtering out all waves higher than H_{sb} . However, by doing so, a statistical error is made. The 'random sampling' is not completely random anymore, and the area under the probability density function of the significant wave height is not equal to 1 anymore. This error is accepted as the influence on the design outcome is expected to be lower than when including non-existent waves in the further equations.

Number of waves

The number of waves depends on the storm duration and the mean wave period. The storm, with a return period of 60,000 years, lasts approximately 44 hours, during which the water level rises and falls. The time when waves act on each part of the revetment is limited. The design storm may not cause the largest duration of wave attack on each revetment type. Hence, the revetment height is discretised into steps of 0.2 m. The maximum duration of wave attack for each water level is determined using the 'Waterstandsverloop tool' (water level variation tool) (Botterhuis et al., 2017). This tool adds a trapezoidal storm set up to the astronomical tide such that the maximum water level equals the design water level. The trapezoidal shape of the storm set-up is determined in Chbab (2015). To determine the maximum loading duration, the water level is discretised into steps of 0.2 m, ranging from +0.4 m NAP to +6.24 m NAP. The zone of wave attack is defined as $\frac{1}{6}H_s$, where H_s is the significant wave height (Deltares, 2015c). Deltares (2015c) prescribes using a maximum of 7500 waves acting on the revetment. This is included as a threshold value that can not be exceeded. The maximum number of waves is used for a revetment that is loaded during regular tidal cycles (below +1,20 m NAP). The average duration of wave attack for all water levels is about 10 hours and is assumed normally distributed with $COV = 0.05$ (Deltares, 2015c).

The number of waves is calculated with:

$$N = \frac{t}{T_m} \quad (3.7)$$

The mean wave period (T_m) is not provided by Hydra-NL. Deltares (2015c) suggests the following relationship with the peak period to determine the mean period.

$$T_m = \frac{T_p}{1.2} \quad (3.8)$$

By using the peak period derived by Hydra-NL, the peak period from the design storm is used. Therefore, a strong correlation between the loading duration and the peak period is assumed. In Appendix E, the full table of hydraulic boundary conditions is included.

3.3.2. GEBU input

The input for the GEBU tool consists of the hydraulic boundary conditions and the geometry of the dike profile. The hydraulic boundary conditions used by the GEBU tool are obtained from Hydra-Ring, the same input data used by Hydra-NL. As mentioned earlier, this database is generated explicitly for this site. Directly using the database without simplifying, like Hydra-NL, causes a slight deviation in accuracy between the grass revetment and the other types of revetments. The profile discussed in the case study section 3.2 is imported. The minimal clay layer thickness and transition height from hard to grass revetment are imported manually. Appendix F presents the input screen of the GEBU tool, providing an overview of the input parameters and settings used in the tool.

3.3.3. ECI input

To optimise the revetment for the lowest ECI, the different components of the revetment are determined, and the corresponding ECI value is stored. The ECI values are determined by the Nationale Milieudatabase (Schipper et al., 2022). Life-cycle assessments are conducted to determine the CO_2 equivalent of each component from construction to decomposition. The components are classified into three groups based on the accuracy of the defined CO_2 emission.

- Category 1: Determined by the manufacturer of the component or the equipment;
- Category 2: Determined by branch organisations;
- Category 3: Determined by third companies able to do a life cycle assessment. For this category, a 30% factor is added as these values are more uncertain.

All justifications for each value can be found in Schipper et al. (2022). This database is continuously updated. It is important to note that this study uses data until May 24, 2023.

A representative cross-section of the dike is selected. Therefore, the ECI is calculated for 1 m dike length. To implement the ECI in the model, all ECI values are calculated per m^2 or m^3 . In the database, several values are provided per hour (h), tonne (t) or tonne-kilometre (tkm). To obtain the values per m^2 or m^3 , the

construction method of the Lauwersmeerdijk is taken as a reference. The $hour/m^2$ is calculated from this, making it easy to calculate the ECI per m^2 . For the ECI values per tonne, the ECI is multiplied by the density of the material. The ECI value is multiplied by the distance and density for the tonne-kilometre. The scope for each revetment type includes the transport from the production site, the materials required and the equipment needed for installation. It does not include the removal of the existing revetment. This choice is made because removing existing revetment is done for the entire slope and does not affect the new design. Also, the calculation does not include the possible reuse of material from the existing revetment. There is no proper way to include this in the ECI calculation, as no ECI values for reused materials are available. This is taken into account implicitly by the recycling value, which is part of the final ECI outcome (Schipper et al., 2022).

The following components and assumptions are considered per revetment type; a table with all values is presented in table 3.1:

- **Loose rock:**

1. Transportation from the quarry in Norway to the site (650 km) with a bulk carrier;
2. The production of loose rock;
3. The equipment to place the rock on the slope;
4. Filter layer;
5. Maintenance.

The equipment used by the contractor for the Lauwersmeerdijk project is known. Therefore, specific ECI values for these machines are used instead of the standard installation values from the Milieudatabase. The values are determined using the consumption of diesel by the equipment. As the Milieudatabase does not provide different ECI values for different rock sizes, this is taken into account by assuming a layer thickness of $2d_{n50}$ and calculating the volume of the protection. The actual ECI value shall be higher as more rock has to be produced to create the largest gradings. A standard filter layer is assumed with standard values from the Milieudatabase. Maintenance is considered separately and depends on the damage number allowed for the design. The ECI value used is the standard value for loose rock maintenance prescribed by the Milieudatabase. The distribution of the ECI is presented in figure 3.6.

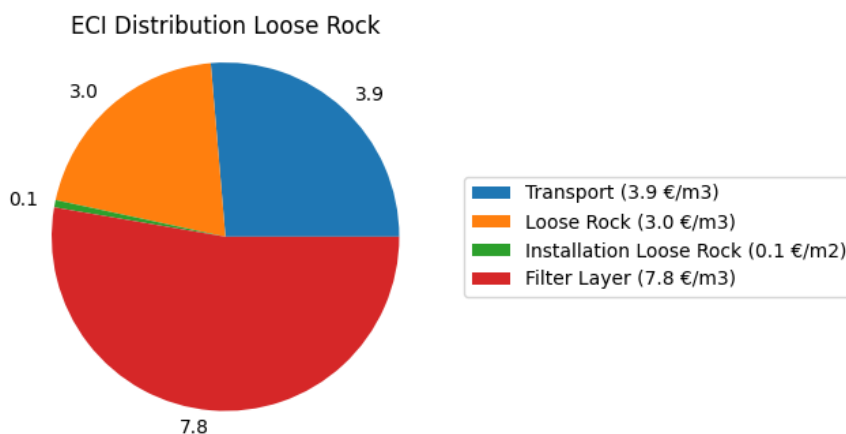


Figure 3.6: ECI composition per m^2/m^3 for loose rock

- **Placed elements (Verkalit and Basalton):**

1. Transport from the factory for Verkalit in Burgum (Friesland) to the site (38 km) and transport from the factory for Basalton in Alphen aan den Rijn to the site (228 km), both by truck;
2. The production of the elements;
3. The filter material;
4. The geotextile;
5. The equipment to apply the elements;
6. For Basalton, the split applied in the gaps and cracks of the elements is included.

As for loose rock, the equipment used by the contractor for the Lauwersmeerdijk project is known, and therefore, specific ECI values for these machines are used instead of the standard installation values from the Milieudatabase. The values are determined using the consumption of diesel by the equipment. The thickness of the elements is considered by calculating the ECI per m^3 and multiplying this with the volume of the elements. For the split, standard ECI values for installation are assumed here. The distribution of the ECI is presented in figures 3.7 and 3.8.

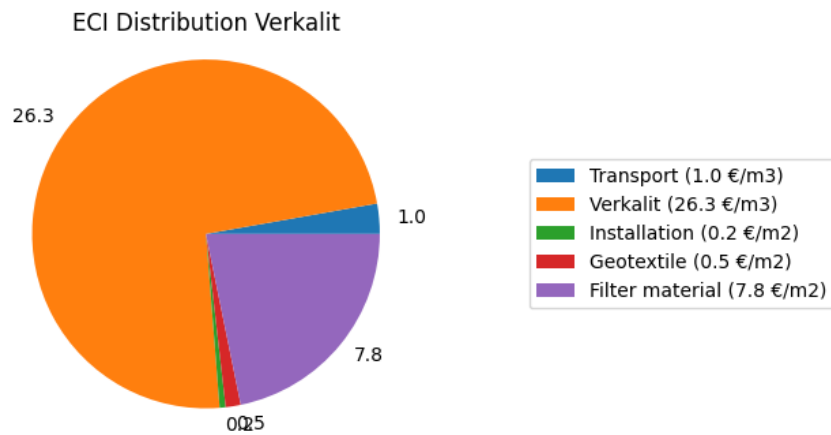


Figure 3.7: ECI composition per m^2/m^3 for Verkalit

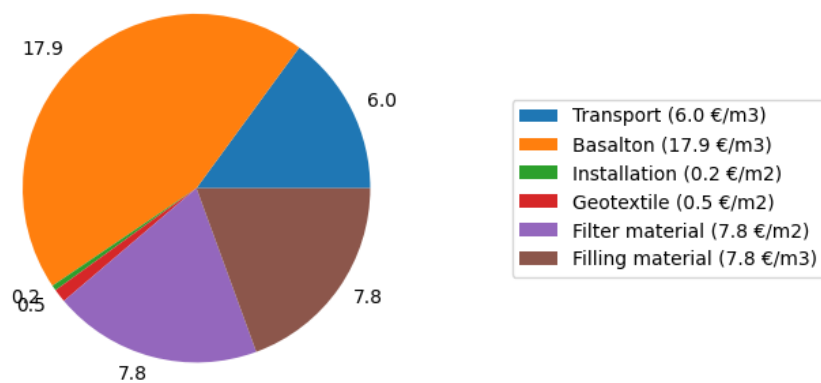


Figure 3.8: ECI composition per m^2/m^3 for Basalton

- **Hydraulic asphalt concrete:**

1. Transport from the factory to the dike (36 km) by truck;
2. The production of Hydraulic asphalt concrete;
3. The equipment to apply the hydraulic asphalt concrete;
4. Sand for the foundation;
5. Adhesive coating.

For the production of hydraulic asphalt concrete, the Milieudatabase does not provide ECI values for the entire life cycle other than production (A1-A3). The equipment used by the contractor is known, and specific ECI values for these machines are used. For the foundation, sand is applied. Hydraulic asphalt concrete has no recycling value (Bak et al., 2022). For the adhesive coating, default Milieudatabase values are assumed. The layer thickness of the asphalt is considered by calculating the required volume. The distribution of the ECI is presented in figure 3.9.

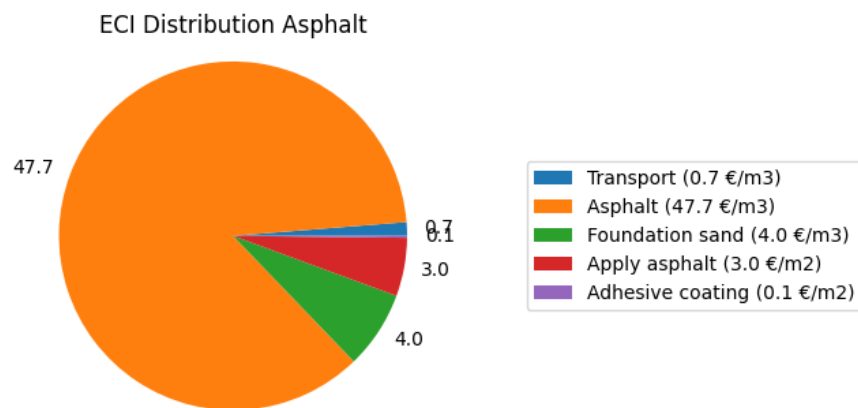


Figure 3.9: ECI composition per m^2/m^3 for hydraulic asphalt concrete

- **Grass:**

1. Transport of clay from the Betuwe area to the site (312 km) by inland vessel;
2. The production of the clay;
3. The equipment to apply the clay;
4. The sowing of the grass by tractor;
5. Maintenance by sheep.

For grass revetment, the equipment used by the contractor for the Lauwersmeerdijk project is known. Therefore, specific ECI values for these machines are used instead of the standard installation values from the Milieudatabase. Maintenance for the grass revetment is assumed to be carried out by sheep, a common practice on Waddenzee dikes. Since the calculation of the grass revetment is based on the residual strength of the clay, the ECI is considered by considering the clay's volume. The distribution of the ECI is presented in figure 3.10.

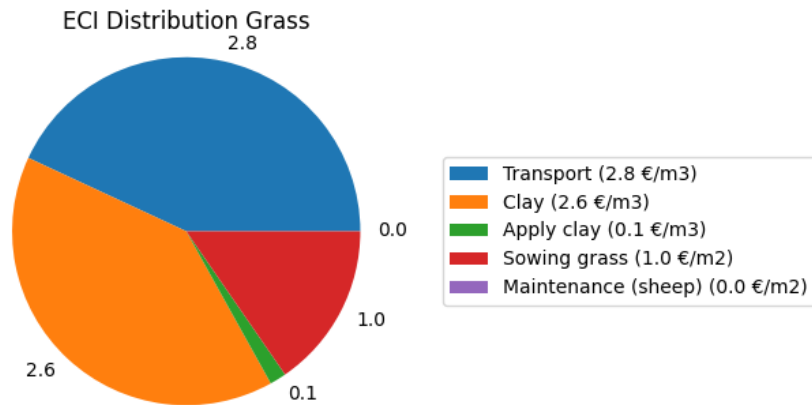
Figure 3.10: ECI composition per m^2/m^3 for grass

Table 3.1: ECI per revetment type

Revetment	Activity	Financial costs (€)	Unit
Loose rock	Transport per bulk carrier from Norway	3.89	m^3
	Production loose rock	2.95	m^3
	Installation loose rock (crawler crane)	0.04	m^2
	Installation loose rock (excavator)	0.003	m^2
	Filter layer	7.80	m^3
	Maintenance	3.94	m^3
Verkalit	Transport per truck from the factory (38 km)	1	m^3
	Production Verkalit	26.30	m^3
	Installation Verkalit (crawler crane)	0.11	m^2
	Shaping slope (excavator)	0.07	m^2
	Geotextile	0.45	m^2
	Filter layer	7.80	m^3
Basalton	Transport per truck from the factory (228 km)	6.04	m^3
	Production Basalton	17.88	m^3
	Installation Basalton (crawler crane)	0.11	m^2
	Shaping slope (excavator)	0.07	m^2
	Geotextile	0.45	m^2
	Filter layer	7.80	m^3
Asphalt	Split (filling material)	7.80	m^3
	Transport asphalt (36 km)	0.86	m^3
	Production asphalt	47.71	m^3
	Foundation sand	4.04	m^3
	Profiling slope and apply asphalt	2.57	m^2
	Densify asphalt	0.47	m^2
Grass	Bitumnous toplayer	0.12	m^2
	Transport clay with inland vessel (312 km)	2.78	m^3
	Clay (class 1)	2.56	m^3
	Excavation works (crawler crane)	0.03	m^3
	Excavation works (bulldozer)	0.03	m^3
	Densify clay (bulldozer)	0.02	m^3
	Profiling (bulldozer)	0.02	m^3
	Sowing grass	0.01	m^2
Maintenance (sheep)	0.00	m^2	

3.3.4. Financial cost input

To assess the feasibility of the different design options, the financial costs of the designs are estimated. To assign the costs to the different revetment types, the same components that are used for the ECI calculation are used. The prices are estimated by cost experts from Arcadis (M. Deltrap and S. Reuling). Also, the cost estimate from a cost indication by Royal Haskoning DHV and HKV for the Lauwersmeerdijk (Post and van der Laar, 2021) is used. For Basalton, only the price for elements with heights of 0.25, 0.35 and 0.45 meters is known. The price for the other diameters is estimated by inter- or extrapolation. For Verkalit, only the price of 0.3m thick elements is known. The price ratio with the same diameter Basalton estimates the price for other diameters Verkalit. Combining these two sources leads to the financial cost input as presented in table 3.2.

Table 3.2: Financial costs per revetment type

Revetment	Activity	Financial costs (€)	Unit
Loose rock	Purchase rock grading LMa 15 - 300 kg	73	m^3
	Purchase rock grading HMa 40-200 kg	75	m^3
	Purchase rock grading HMa 60-300 kg	77	m^3
	Purchase rock grading HMa 300 - 1000 kg	81	m^3
	Purchase rock grading HMa 1 - 3 tonnes	89	m^3
	Purchase rock grading HMa 3 - 6 tonnes	225	m^3
	Purchase rock grading HMa 6 - 10 tonnes	400	m^3
	Installation loose rock (excavator)	147	h
	Filter layer	19.45	m^2
Verkalit	Purchase Verkalit 0.10 m	43.93	m^2
	Purchase Verkalit 0.15 m	45	m^2
	Purchase Verkalit 0.20 m	47.1	m^2
	Purchase Verkalit 0.25 m	51.4	m^2
	Purchase Verkalit 0.30 m	60	m^2
	Purchase Verkalit 0.35 m	68.6	m^2
	Purchase Verkalit 0.40 m	79.4	m^2
	Purchase Verkalit 0.45 m	90.3	m^2
	Installation Verkalit	10.73	m^2
	Purchase geotextile	3	m^2
	Filter layer	19.45	m^2
Basalton	Purchase Basalton 0.10 m	38.44	m^2
	Purchase Basalton 0.15 m	39	m^2
	Purchase Basalton 0.20 m	41	m^2
	Purchase Basalton 0.25 m	45	m^2
	Purchase Basalton 0.30 m	53	m^2
	Purchase Basalton 0.35 m	60	m^2
	Purchase Basalton 0.40 m	70	m^2
	Purchase Bassalton 0.45 m	79	m^2
	Purchase geotextile	3	m^2
	Filter layer	19	m^2
	Purchase split	8.21	m^2
Asphalt	Purchase hydraulic asphalt concrete	178	m^3
	Purchase sand	39	m^3
	Apply sand	2	m^3
	Bitumneus top layer and gravel	2.35	m^2
Grass	Purchase clay class 1	17	m^3
	Install clay layer	2	m^3
	Purchase grass seed	1	m^2

Table 3.3: Nominal diameter with corresponding rock class (NEN, 2015)

Nominal diameter (m)	Rock class
0.31	LMa 15-300
0.34	LMa 40-200
0.38	LMa 60-300
0.59	HMa 300-1000
0.9	HMa 1000-3000
1.18	HMa 3000-6000
1.44	HMa 6000-10000

3.3.5. Decision variables

The decision variables in the design are the parameters that can be altered to optimise the design. Different values are assigned to these parameters based on practical considerations. Most of these variables are stochastic variables with a specific distribution. Since the uncertainty changes when the expected value changes, the coefficient of variation is used to characterise the variability of each variable. The different decision variables for which the design is optimised are discussed below.

- **Density concrete (ρ_c)**

The manufacturer determines the density of the concrete. It has to comply with product requirements set by the Kiwa Kiwa (2016). In this document, the production tolerances are described. The manufacturer can manipulate the density. Densities ranging from 2650 to 3000 kg/m^3 with steps of 50 kg/m^3 are tested for this study. The density of concrete is distributed according to a normal distribution. The uncertainty is quantified as: $-2\% < \rho_c < 6,5\%$ and $\rho_c \geq \mu - 1.645\sigma$. In the case of the lower boundary (-2%), this means that $COV = 0.0103$. The probability density function used for this study complies with the lower limit (Kiwa, 2016).

- **Element thickness Basalton and Verkalit (D_B, D_v)**

The element thickness of Basalton and Verkalit is the most essential parameter the engineer can change to optimise the design. The thickness of the elements ranges between 0.20m to 0.60m with steps of 0.05m. The element thickness is distributed according to a normal distribution. The uncertainty is quantified as $D_{B,v} \leq 5\%$ or $D_{B,v} \leq 2mm$, where the least strict criterion is governing and where $D_B, D_v \geq \mu - 1.645\sigma$. In case the 5% norm is applied, the $COV = 0.0304$ (Kiwa, 2016).

- **Layer thickness Asphalt (d)**

The Asphalt layer thickness is the most important parameter the engineer can change to optimise the asphalt layer revetment. The thickness ranges from 0.10m to 0.40m with steps of 0.05m. The lower bound of this range is assumed because a thinner layer can not be applied. The upper boundary is assumed to be 0.40m because a larger thickness is not likely to be used. The step size is based on constructability. The layer thickness is distributed according to a Normal distribution with $COV = 0.1$ (Klerk, 2014).

- **Average nominal diameter loose rock (D_{n50})**

The average nominal diameter of loose rock is chosen such that it is a regular grading. The following gradings are tested $D_{n50}[m] = 0.31, 0.34, 0.38, 0.59, 0.90, 1.18, 1.44$ (NEN, 2015). Loose rock classes are distributed according to a normal distribution with $COV = 0.03$ (van der Meer, 1988b). The nominal diameter belongs to the rock classes as presented in table 3.3.

- **Damage number (S)**

The damage number S represents the permissible amount of damage before the structure fails, specifically for the loose rock revetment. The range of values for S is from 2 to 17. Since this parameter is subjective and its value depends on the definition of failure, it is considered deterministic in this study. This is in line with van der Meer (1988b). The allowable damage number depends on the slope. In this case, the slope is 1:5.88, for which van der Meer (1988a) defined the values for S as presented in 3.4 for slopes 1:4 and 1:6. The start of damage is defined as the movement of a couple of rocks. Intermediate damage is defined as damage after a storm which can be fixed with maintenance work. Failure is defined as the visibility of the filter layer for a $2d_{n50}$ thick layer.

Table 3.4: S-values for slope 1:4 until 1:6

Start of damage	Intermediate damage	Failure
3	8-11	17

3.3.6. Control variables

The control variables are variables that are not altered or are taken as a constant in this study. These variables are divided into two types: stochastic variables and deterministic variables. First, the stochastic variables are discussed, followed by the deterministic parameters.

- Density rock (ρ_s)**
 Rock is a natural product and can have different densities. The density used in this study is 2650 kg/m^3 . The uncertainty regarding the density of rock is not determined explicitly. However, the uncertainty of the relative density of loose rock under water is provided by van der Meer (1988b). When assuming the density of water is a deterministic value and is 1025 kg/m^3 , the $COV = 0.03$. This results in a standard deviation of $\sigma = 79.5$.
- Density water (ρ_w)**
 The density of water is not constant as it depends on temperature, salinity and sediment concentration. It is assumed to be normally distributed with an expected value of 1025 kg/m^3 , which is the average for seawater. The standard deviation is assumed to be 30.75. This is in line with the covariance of the submerged density of rock as described above. (van der Meer, 1988b)
- Slope angle 1, 2 and 3 ($\alpha_{1,2,3}$)**
 The slope angle of the dike is split into three sections as they differ along the slope. From bottom to top: loose rock [1], placed elements [2] and asphalt [3]. The slope is determined by the dike's original profile, which is described in 3.2. As the slope is not constant, the slope is assumed to be normally distributed with expected values: $\alpha_1 = 1 : 5.68$, $\alpha_2 = 1 : 7.7$, $\alpha_3 = 1 : 3.75$. The relative uncertainty of the slope is assumed to be the same for each section. From van der Meer (1988b), it is found that $COV = 0.05$.
- Notional permeability (P)**
 The notional permeability indicates the permeability of the core material of the dike. This parameter has no physical meaning and is based on curve fitting by van der Meer (1988a). For a dike with an impermeable core (sand or clay), the expected value is 0.1. van der Meer (1988b) found a normal distribution and used a value of $P = 0.5$ in his probabilistic study to which he assigned a standard deviation of $\sigma = 0.05$. The considered cross-section in this study has an impermeable core. Therefore, an assumption regarding the standard deviation is made. It is assumed that the uncertainty does not depend on the core's permeability, so the standard deviation is assumed $\sigma = 0.05$.
- Uncertainty parameter a and b (C_{pl}, C_s)**
 The uncertainty parameters C_{pl} and C_s are fitting parameters and are assumed normally distributed with expected values $C_{pl} = 6.2$, $C_s = 1.0$ and standard deviation $\sigma = 0.4$ and $\sigma = 0.08$ van der Meer (1988b)
- Density hydraulic asphalt concrete (ρ_a)**
 The density of hydraulic asphalt concrete is influenced by the densities of the composition of the asphalt and the amount of hollow space within the mixture. According to TAW (2002), the density of hydraulic asphalt concrete ranges between $2300 - 2350 \text{ kg/m}^3$. As no further literature regarding uncertainties has been found, the assumption is that the density is normally distributed and has an expected value of 2325 kg/m^3 and a standard deviation of $\sigma = 10$. This assumption ensures that the boundaries of the normal distribution lay between the limits provided by the literature.
- Soil modulus (c)**
 The stiffness of the subsoil determines how the soil reacts to loading. According to Klerk and Kanning (2014), the stiffness of the soil is log-normally distributed with an expected value of 100 MPa/m and $COV = 0.25$.

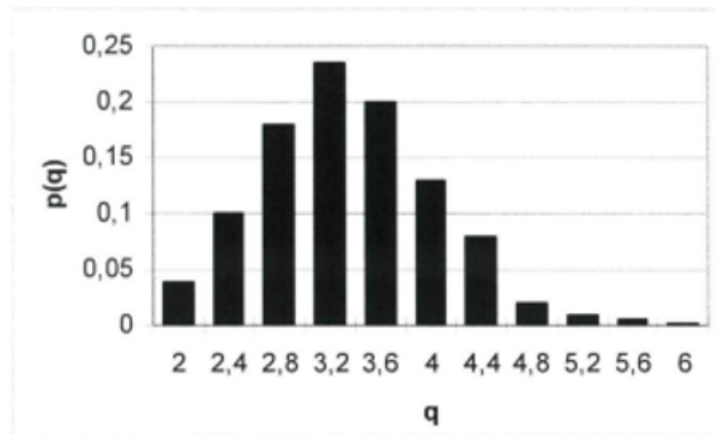


Figure 3.11: Probability density function for the slope depending impact factor (de Looff et al., 2006)

- **Elasticity modulus asphalt (Youngs modulus) (E)**

The elasticity modulus is a parameter indicating a specific aspect of the strength of the asphalt. In Klerk and Kanning (2014) appendix H, elasticity modulus data is plotted, and two possible distributions are fitted for both new and old asphalt. Based on the observations and the fact that a new asphalt layer is assumed for this study, the distribution with the least uncertainty is assumed. This results in a normal distribution with an expected value of 7000 MPa and a standard deviation of $\sigma = 1400$. This distribution captures the characteristics of the provided data set.

- **Cracking strength (σ_b)**

The cracking strength of the asphalt is an important variable regarding the resistance of asphalt to wave impact. The average varies between 5.0 and 7.6 MPa , mainly depending on the age of the asphalt. The older the asphalt, the lower the cracking strength. For a young asphalt layer, (Klerk and Kanning, 2014) suggests a normal distribution with an expected value of 6.3 and $COV = 0.2$. However, applying this considerable uncertainty in this study, with a required probability of failure of $1/60.000$, results in extremely low and high, unrealistic realisations of the cracking strength. Therefore, it is chosen to truncate the distribution at the upper and lower limits at the 2.5% and 97.5% intervals, such that 95% of the distribution is included. This results in a lower limit of 3.83 MPa and an upper limit of 8.77 MPa . Klerk and Kanning (2014) uses 216 cases of different ages from different dike sections in the Netherlands. As the data set is quite diverse and not large, the uncertainty and, therefore, the coefficient of variation is large. For this study, a new asphalt layer is designed for which the uncertainty is lower than the samples from the data set. The probability of extreme values is, therefore, smaller.

- **Slope-dependent impact factor (q)**

The slope-dependent impact factor indicates a wave's impact depending on the slope. Based on figure 3.11, de Looff et al. (2006) suggests a log-normal distribution with an expected value of 3.45 and $COV = 0.5$. This study suggests a considerable uncertainty resulting in extreme values. The distribution is based on the figure shown below. It is observed that values higher than 5.2 are rare. Therefore, the distribution is truncated at 5.2 .

The following parameters are considered deterministic:

- **Coefficient for length of loading (c_1, c_2)**

These two coefficients indicate the influence of the duration of the load. According to Klein Breteler and Mourik (2014), these are deterministic values and depend on the type of elements applied. For column types, the values are $c_1 = 0.15$, $c_2 = 0.85$.

- **Parameters related to the filter**

The stability of the top layer of the placed revetments is partially dependent on the characteristics of the filter. Therefore, a well-functioning filter is essential. However, due to time limitations, the design

of a filter layer is left out of the scope of this study. Instead, a stable filter layer is assumed. The applied filter in the Lauwersmeerdijk case is applied, and therefore, the following parameters are taken as deterministic from the design document (Arcadis, 2022). It concerns the following parameters:

- Filter thickness ($b_1 = 0.06\text{ m}$)
 - Permeability geotextile ($k_2 = 0.00286\text{ m/s}$) (Terrafix, 2007)
 - Thickness geotextile ($b_2 = 0.0053\text{ m}$)
 - Kinematic viscosity water ($\nu = 1.2 * 10^{-6}\text{ m}^2/\text{s}$)
 - Porosity granular material ($N_f = 0.35$)
 - 15% fraction diameter filter material Verkalit ($d_{V,f15} = 0.004\text{ m}$)
 - 15% fraction diameter filter material Basalton ($d_{B,f15} = 0.017\text{ m}$)
- **Gravity (g)**
Gravity is considered constant and deterministic as the space and time fluctuations are irrelevant to this study; $g = 9.81\text{ m/s}^2$.
 - **Slope-depending uplift factor (Q_n)**
The slope-depending uplift factor indicates the influence of the slope on the water pressure from inside the dike to the asphalt layer. This is determined from graph 7.10 on pg. 122 of (TAW, 2002). For a slope of 1:3.75, $Q_N = 1.005$.
 - **Reduction factor due to relative position design water level to the phreatic surface (R_w)**
If the design water level for uplift of asphalt is lower than the average water level, a reduction factor R_w is applied. This depends on the outer water level relative to the phreatic water level. The factor is determined by graph 7.9 on page 120 of (TAW, 2002).
 - **Fatigue parameters asphalt (β, α)**
The fatigue parameters α and β range from 0.23 to 0.63 and 3.8 to 7, respectively. They have considerable influence on the probability of failure. However, as these parameters are coupled with the cracking strength, their uncertainty is considered in this parameter Klerk and Kanning (2014). The values used for calibrating the original design equation are also applied to this study. These are, $\alpha = 0.5$ and $\beta = 5.4$ (Davidse, 2010).
 - **Transverse contraction coefficient / Poisson's ratio (ν)**
The transverse contraction coefficient determines the deformation by normal forces resulting from wave impact acting on the asphalt. This coefficient is determined to be $\nu = 0.35$ by both (Klerk and Kanning, 2014) and (Davidse, 2010).
 - **Vertical distance between the lower transition of the impermeable revetment to the outer water level (a) and vertical distance between the outer water level and phreatic water level (ν)**
Together, a and ν indicate the possibility of build-up water pressure under the impermeable layer. This depends on the phreatic line, outer water level and lower transition point of the impermeable layer. The design situation occurs when $a = 47\%$ and $\nu = 53\%$ of $(a + \nu)$ (Davidse, 2010). The design phreatic line is determined as described in section 2.1.3 and figure 2.4. The relative positions of a and ν are determined for each water level.

In appendix A, the table with decision and control parameters is included.

3.4. Limit state functions and probabilistic calculation

One of this study's objectives is to analyse the limit state functions for all revetment types fully probabilistically. Compared to level II techniques, level III techniques are more precise. However, level III probabilistic techniques generally require more calculation time. The number of computations is significant due to the numerous combinations of parameters and water levels. The probabilistic approach most suitable for this study is the Crude Monte Carlo analysis. FORM analysis can not be applied due to the discontinuous character of the limit state functions. Importance sampling would be an option if the number of different designs would be smaller. To apply importance sampling, the first step is to determine the design point. Usually,

FORM analysis is used to find the design point. However, this is not possible due to the earlier-mentioned restrictions. The design point can be estimated differently, but due to the many different design options, the design point must be determined for each parameter combination. This requires adjustment of the OpenTurns packages, which is not the goal of this study. This makes the method practically not applicable. Crude Monte Carlo is preferred due to its simplicity and the wide range of applicability. The Crude Monte Carlo module from OpenTurns (Baudin et al., 2017) has been used. It is adjusted slightly to make the calculations more efficient. A matrix is made for the random samples to which the limit-state functions are applied. This removes the feedback loop for the conversion criteria but overall increases computational speed drastically. The probabilistic analysis uses limit state functions as described in section 2.2. The limit state functions that are evaluated are listed below. For the rationale behind the functions, reference is made to section 2.1.

- Loose rock:
For plunging waves ($\zeta \approx 0.5 - 3$):

$$Z = \frac{H_s}{\Delta D_{n50}} - 6.2P^{0.18} \left(\frac{S}{\sqrt{N}} \right)^{0.2} \zeta_m^{-0.5} \quad (3.9)$$

- For surging waves ($\zeta \approx 3 - 5$):

$$Z = \frac{H_s}{\Delta D_{n50}} - 1.0P^{-0.13} \left(\frac{S}{\sqrt{N}} \right)^{0.2} \sqrt{\cot(\alpha)} \zeta_m^P \quad (3.10)$$

- Revetment (Basalton):

$$Z = \frac{H_s}{\Delta D} - \min \left[4, 93 \cdot p_{Z_b} \cdot p_{\tan\alpha} \cdot p_{\Lambda} \cdot p_{\Delta} \cdot p_N \cdot p_{\beta} \cdot p_{S_{op}} \cdot p_D; \left(\frac{H_s}{\Delta D} \right)_{max} \right] \quad (3.11)$$

- Revetment (Verkalit):

$$Z = \frac{H_s}{\Delta D} - \min \left[4, 93 \cdot p_{Z_b} \cdot p_{\tan\alpha} \cdot p_{\Lambda} \cdot p_{\Delta} \cdot p_N \cdot p_{\beta} \cdot p_{S_{op}} \cdot p_D \cdot 1.14; \left(\frac{H_s}{\Delta D} \right)_{max} \right] \quad (3.12)$$

- Hydraulic asphalt concrete:
For uplift:

$$Z = d - 0,21 \cdot Q_n(a + v) \cdot \frac{\rho_w}{\rho_a - \rho_w} \cdot R_w \quad (3.13)$$

- For impact:

$$Z = N_f - N \quad (3.14)$$

- Grass:

$$Z = d_e - \sqrt{\frac{2V_{e,i} \tan(\alpha - \alpha_{terras}) + d_{0,i}^2}{\left(1 + \frac{\tan(\alpha - \alpha_{terras})}{\tan(\alpha_{cliff} - \alpha)}\right)}} \quad (3.15)$$

3.5. ECI calculation

The environmental cost indicator (ECI) is included in the model by making a library including the different components and calculating the ECI based on volumes. Unfortunately, the Milieudatabase is not approachable from outside Dubocalc. Therefore, hardcoding the values corresponding to the different variables in the model library is required. The database is updated frequently, so the date the data is retrieved is very important. For this study, the data was retrieved on May 24, 2023.

3.5.1. Hard revetments

The ECI for all three hard revetment types is calculated based on the length of the revetment and the thickness of the specific type. Besides the installation of the hard revetment, maintenance may be required. For maintenance, equipment and materials are mobilised for a relatively small amount of work. When the option of little to no maintenance is considered during the design phase, the total ECI for the entire lifetime might be reduced. For placed revetment and asphalt, no maintenance is considered in this study because there is no suitable parameter that can be adjusted to allow for quantification of maintenance. Regarding loose rock, the maintenance is linked to the damage number S . The following assumptions are made regarding the maintenance of the loose rock revetment in consultation with K. Stoeten (senior hydraulic engineer at Arcadis):

- The waterboard maintains the rock layer when ten rocks are displaced, corresponding to damage number $S = 10$. This value is based on van der Meer (1988a) where $S = 10$ is about intermediate damage.
- The ECI value for maintenance to loose rock revetment prescribed by Schipper et al. (2022) is assigned to a design with $S = 10$.
- When the revetment is designed for other damage numbers than $S = 10$, the number of displaced rock corresponding to that number is calculated back to $S = 10$. For example, when $S = 2$ is chosen in the design, less maintenance is expected, so the factor used in this case is $2/10$. When $S = 15$ is used in the design, more maintenance is expected, so the factor used in this case is $15/10$.
- The ECI value of a design concerns the entire lifetime. Therefore, a certain frequency of maintenance during the entire lifetime has to be assumed. It is assumed that the frequency of maintenance is once every five years during the 50-year lifetime.
- The ECI for maintenance depends on the diameter of the installed rock. As the larger rock comes with higher ECI values, this is considered by multiplying the ECI with the nominal diameter of the applied grading.

The ECI value for maintenance is calculated with the following equation:

$$maintenance = D_{n50} * ECI_{maintenance} * frequency * designlifetime * \frac{S}{10} \quad (3.16)$$

The amount of required maintenance during the lifetime of the revetment is very uncertain, and therefore, the outcome has to be treated with care. This calculation only provides an indication.

3.5.2. Grass

The ECI of grass revetment is determined based on the required amount of clay and sowing of the grass. The determination of the volume follows the following procedure. First, the GEBU tool is used to establish the necessary thickness of the clay layer at the transition point from hard revetment to grass, as described earlier. This clay layer thickness is not uniformly required for the entire slope. To provide a buffer for minor damages to the top layer, a minimum clay layer thickness of 0.8m is recommended (Klein Breteler, 2022a). The required clay volume is determined by taking this minimum cover at the crest of the dike and following a straight line towards the required thickness at the transition height.

3.6. Core of the model

The components are merged in the constructor, and probabilistic, ECI and financial cost calculations are executed. The revetment is tested for each parameter combination, and the probability of failure is calculated. The results obtained from the GEBU tool are imported, and the ECI and financial costs calculation is performed. This results in data files for each revetment type where all design options for each water level are stored. The interaction of the core with the other elements of the model is shown in figure 3.2.

3.7. Results

The results section evaluates the data files created in the constructor section. The results are filtered based on the following criteria. First, the designs with a failure probability above $1/60000$ are filtered out. Next, the results are sorted by water level and ECI score. The design with the lowest ECI score for each water level is

selected. To design the revetment with the lowest emission for the original situation, the revetment sections are selected, and the design with the lowest ECI that fulfils the safety requirements for the entire section is selected. This is done for all five revetment types. The best transition height for the ECI score depends on several factors. The ECI depends strongly on the amount (tonnes or m^3) of material placed. This is influenced by the revetment's size (diameter or thickness) and the covered section. For the top and bottom sections the revetment is predefined, and the lower-, respectively, upper boundaries are defined. This concerns the loose rock and grass revetment. The lower and upper boundaries are not fixed for the sections in between (placed elements and asphalt). The ECI depends on the diameter or thickness, which depends on the specific section on the slope. Therefore, it is not possible to solve the transition heights analytically. There are four revetment designs for the entire slope possible, from toe to crest:

- Loose rock - grass;
- Loose rock - placed elements - grass;
- Loose rock - asphalt - grass;
- Loose rock - placed elements - asphalt - grass.

For the bottom three designs, all different design combinations are generated for which the ECI is calculated. The designs are then ordered based on ECI, and the design with the lowest ECI is selected. For placed elements, a distinction is made between Verkalit and Basalton.

4

Model outcome and interpretation of the results

The results and findings derived from the model described in the previous chapter are presented in this chapter. First, the outcome of the probabilistic analysis is presented. Then, an analysis and evaluation of the model results is conducted. The optimal parameter combination for the original design is discussed first. The best transition heights are studied based on the environmental cost indicator (ECI). This results in several design options, discussed based on their ECI. Sensitivity analysis for the components of the ECI is performed to determine the dominant factors. Lastly, the design made by Arcadis is compared to the preferred design resulting from this study. In this chapter, several designs are mentioned and compared. For clarity, the following definitions for the different designs are used:

- **Original design:** The original design is the revetment design, designed around 1970. This design has been assessed and rejected. A new design is required to fulfil safety requirements.
- **Refurbished design:** The refurbished design has the same geometry, revetment types and transition heights as the original design. In this design, the revetment types are updated to fulfil safety requirements.
- **Arcadis design:** The Arcadis design is the design Arcadis made to fulfil the safety requirements. It has another geometry and transition heights. For this design, more aspects are considered than revetment only, and it is being constructed.
- **Study design:** The study design is the design which has the lowest ECI score according to this study. For this design, the geometry of the original design is used.

4.1. Results safety assessment

This section presents the probabilistic outcomes generated by the model. The relationship between the significant wave height, stability number or layer thickness and the probability of failure for the different revetment types is shown. It provides an indication of what situations the designs fulfil safety criteria and in which situation the probability of failure is large.

4.1.1. Loose rock

Figure 4.1 presents the probability of failure with respect to the stability number and significant wave height. On the x-axis, the stability number is presented. On the y-axis, the significant wave height is presented. The colour of the dot indicates the probability of failure. The darker the dot, the smaller the probability of failure. The lines that can be distinguished are for different nominal diameters of the different rock classes. The entire analysis was done for damage number S ranging from 2 to 17 with steps of 1. This figure shows data for S is 2, 6, 11 and 17 to present the influence of the damage number on the probability of failure. It is observed that the probability of failure is lowest for the lower significant wave height and lower stability numbers.

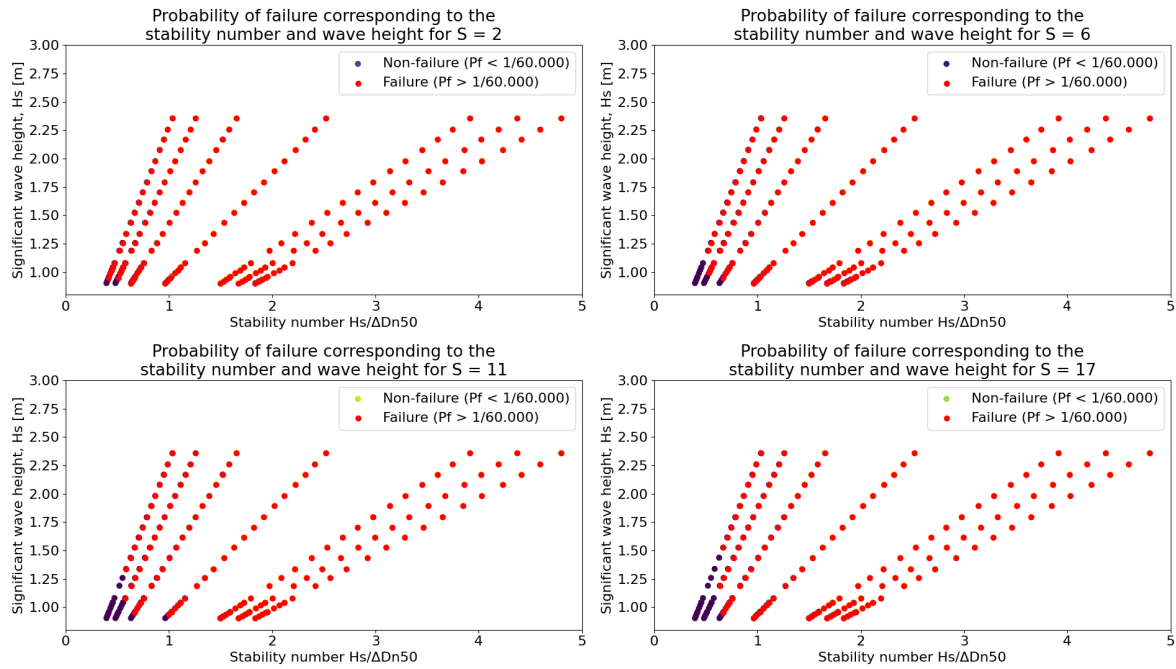


Figure 4.1: Probability of failure of loose rock with respect to stability number and significant wave height

4.1.2. Placed elements

Figures 4.2 and 4.3 present the probability of failure with respect to the stability number and significant wave height for Verkalit and Basalton. The entire calculation is done for the concrete density ranging from 2650 to 3000 kg/m^3 in steps of 50 kg/m^3 . This figure shows the data for 2650, 2750, 2850 and 3000 kg/m^3 to present the dependency on concrete density. The lines of points that can be distinguished are the different element thicknesses. It is observed that the probability of failure increases slowly, mainly with increasing stability number and depends less on the wave height compared to loose rock. The points with low significant wave height and stability number between 2 and 3 that do not follow the trend are explained by a change in slope angle in combination with a relatively long loading duration. The points with slightly larger wave heights have a shorter loading duration. There is limited difference visible between Basalton and Verkalit. In general, Verkalit has a lower probability of failure.

4.1.3. Asphalt

Figure 4.4 presents the probability of failure of the asphalt layer due to wave impact with respect to the layer thickness and the significant wave height. All data points obtained by running the model are presented. The layer thickness ranges from 0.1 to 0.4 m. It is observed that, as expected, the probability of failure increases with higher significant wave height and decreases with larger layer thickness.

Figure 4.5 presents the probability of failure of the asphalt layer due to uplift with respect to the layer thickness and the significant wave height. It is observed that uplift may occur for the waves corresponding to the water levels below the design phreatic surface (+3.1 mNAP).

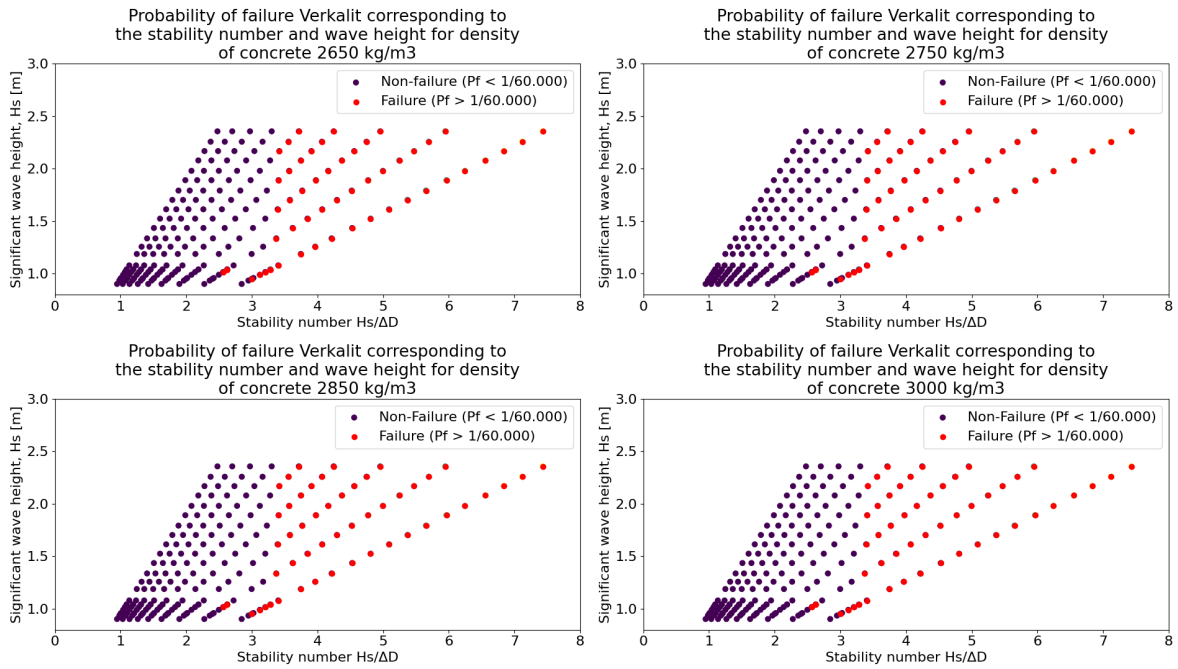


Figure 4.2: Probability of failure of Verkalit with respect to stability number and significant wave height

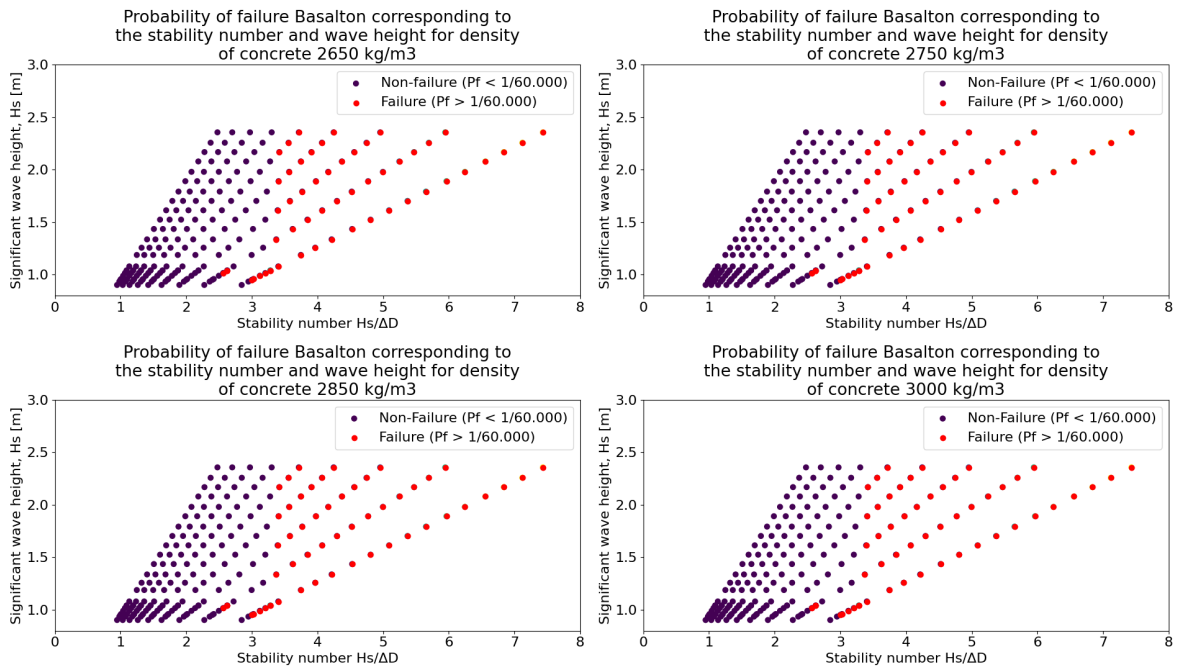


Figure 4.3: Probability of failure of Basalton with respect to stability number and significant wave height

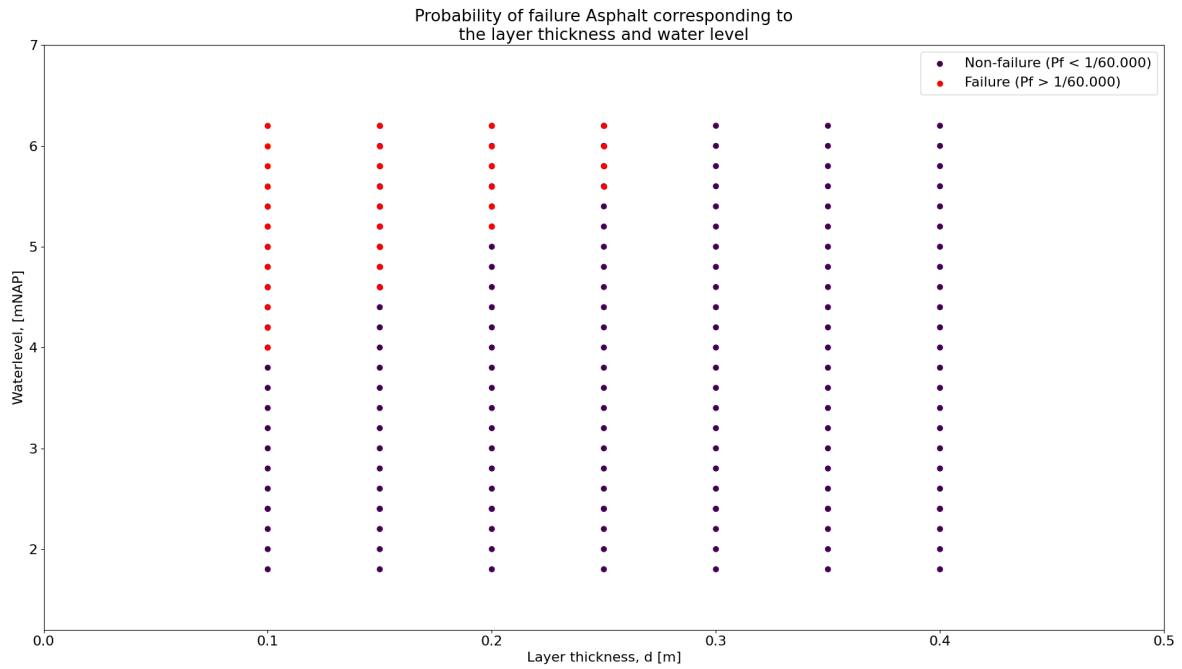


Figure 4.4: Probability of failure of asphalt due to wave impact with respect to layer thickness and significant wave height

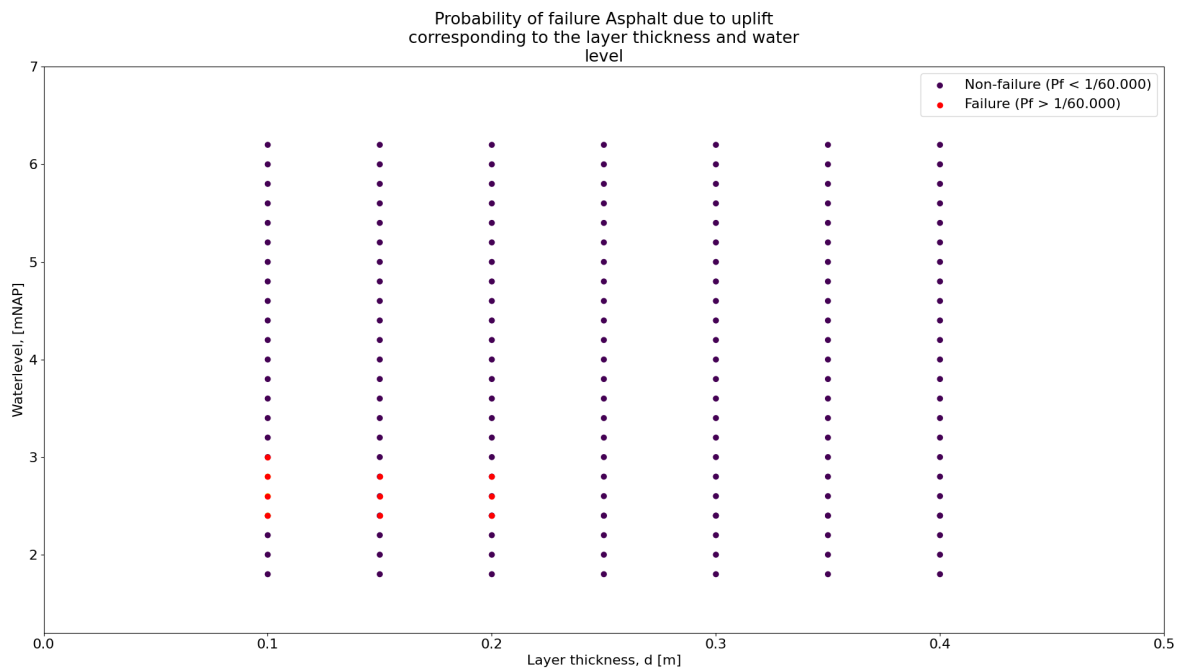


Figure 4.5: Probability of failure of asphalt due to uplift with respect to layer thickness and water level

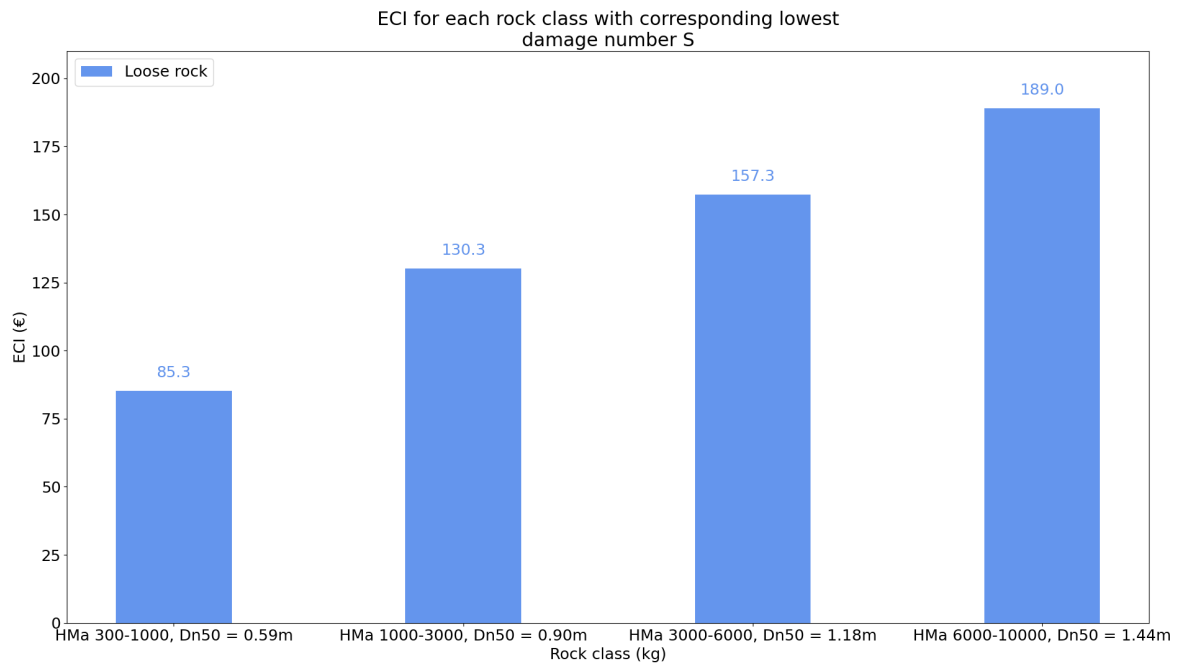


Figure 4.6: ECI for each rock class in the preferred design

4.2. Refurbished design

From the above-presented data, the design options that do not fulfil safety requirements of 1/60.000 are filtered out. With the designs that fulfil the safety requirement, further analysis is performed. First, the optimal parameter combination for the refurbished design is considered. The optimal parameter combination is the design that fulfils the safety requirements and has the lowest ECI score. For each revetment type, this parameter combination is presented and discussed. This results in a design for the entire revetment with the lowest ECI possible whilst fulfilling safety requirements. All data presented in these graphs fulfil safety requirements. The graphs present the ECI corresponding to different designs, all for the same hydraulic boundary conditions. The different nominal diameters, element thicknesses or layer thicknesses are shown in the graphs to indicate the influence of increasing thickness on the ECI.

4.2.1. Loose Rock

The original slope, protected by loose rock, ranges from -0.37 to +1.79 mNAP. Figure 4.6 presents the probabilistic analysis results and ECI calculation results. On the x-axis, the rock class and corresponding nominal rock diameter are shown. The y-axis shows the ECI score in euros. The four rock classes fulfil safety requirements and can be applied on the slope. As described in section 3.3.5, the damage number S indicates the amount of maintenance. The graph shows that the HM_a 300-1000 rock class can be applied for limited damage ($S=2$). When applying rock classes higher, the protection requires less maintenance. For the case of the Lauwersmeerdijk, the rock grading HM_a 300-1000 is the preferred design with respect to the ECI score.

4.2.2. Placed elements

For placed concrete elements, there are two options: Basalton and Verkalit. In the original design, placed elements range from +1.80 mNAP to +2.41 mNAP. The slope is 1:7.7, which results in a cover of 4.82m. The decision variables are the element's thickness and the concrete's density. The combinations that fulfil the safety requirements are then selected, for which the ECI is calculated. Figure 4.7 presents the results. On the x-axis, the element thickness is shown. On the y-axis, the ECI in euros is shown. The graph shows that the option with the lowest ECI is a Verkalit revetment of 0.2m thick. The required concrete density is 2750 kg/m^3 . The larger element thicknesses are not interesting for the preferred design to apply. However, a trend is observed which is interesting in general. Where both Basalton and Verkalit fulfil safety requirements, Verkalit has lower ECI until a thickness of 0.25m. From this point, with increasing layer thickness, the ECI for Basalton is lower than for Verkalit. This indicates that for situations where larger elements are required, Basalton is the

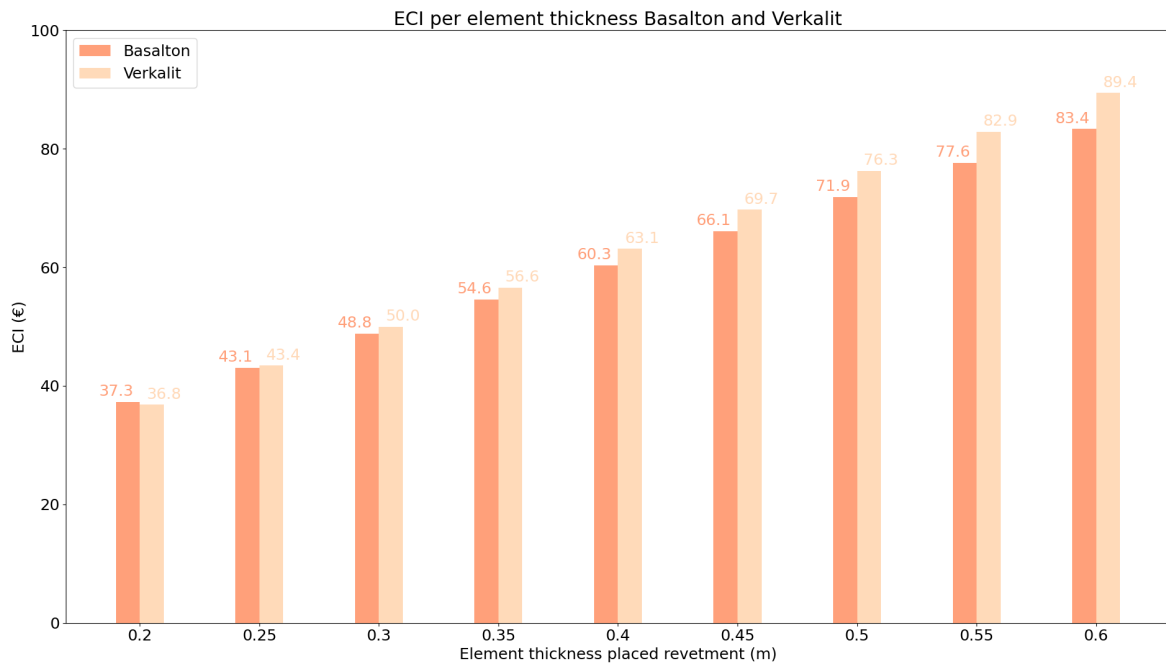


Figure 4.7: ECI for Basalton and Verkalit

option with lower emission during its lifetime. This is explained by the components from which the ECI is constructed. The ECI for Verkalit is $26.30 \text{ Euro}/m^3$, whereas the ECI for Basalton is $17.88 \text{ Euro}/m^3$. This means that the total ECI for Verkalit rises faster with the required thickness than for Basalton. The ECI for Verkalit is lower for the required thickness due to the shorter transport distance and extra materials needed for Basalton, which depend less on the required thickness, like a thicker filter layer and filling material to fill the cracks.

4.2.3. Asphalt

The asphalt revetment ranges from +2.41 mNAP to +6.15 mNAP in the original design. The angle of the slope is 1:3.75, covering 14.54 meters. The decision parameter is the thickness of the asphalt layer. The minimum required asphalt layer thickness is calculated probabilistically for failure due to wave impact and uplift from high water pressure. Figure 4.8 presents the asphalt layer thicknesses that fulfil the safety requirements. As can be observed, the minimum required layer thickness is 0.3 meters. As expected, when applying a thicker asphalt layer, the ECI increases.

4.2.4. Grass

In the original design, the grass revetment ranges from +6.15 mNAP to +8.22 mNAP. With a slope of 1:4, this covers 8.49m. The decision parameter for the grass revetment is the clay layer thickness. Due to changing hydraulic boundary conditions per water level, the required clay layer thickness changes with each level. With the GEBU tool, the required clay layer thickness for each water level is determined. Based on the required clay layer thickness, the ECI is calculated. The result is presented in figure 4.9. On the x-axis, the required clay layer thickness is shown. The left y-axis shows the ECI in euros, the right y-axis shows the transition height from hard to grass revetment. The blue bars show the relation between the clay layer thickness and ECI. The red line shows the relation between the clay layer thickness and the transition height. There is a clear relation between the transition height and the ECI visible. The lower the transition, the higher the ECI. The kink in the red line indicates the transition height of the original design at +6.15 mNAP. This value is added as an extra point to the graph. At this point, the required clay layer thickness is 1.4m, resulting in an ECI value of €72.8.

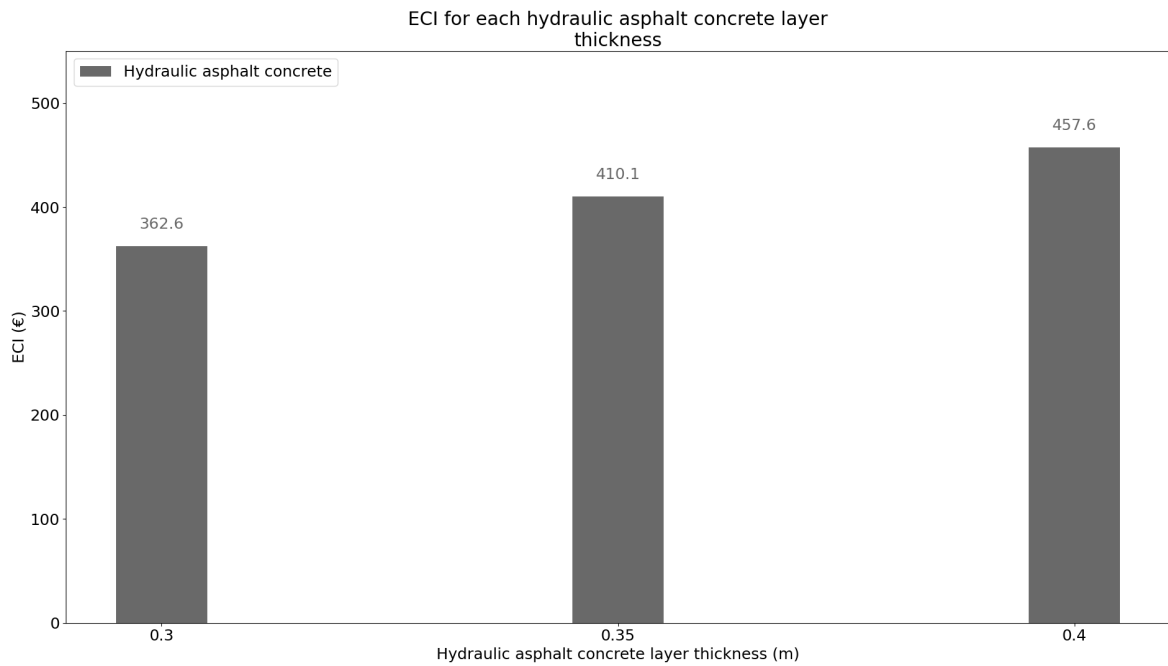


Figure 4.8: ECI per layer thickness of hydraulic asphalt concrete stretching from +2.41 mNAP to +6.15 mNAP

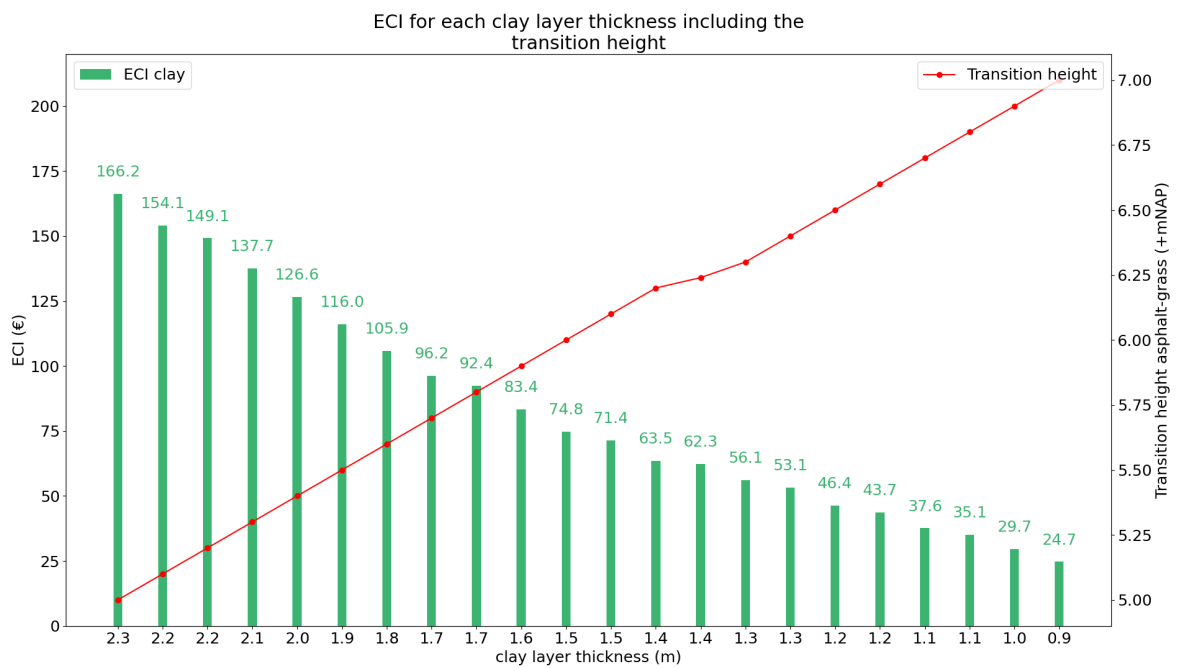


Figure 4.9: ECI for grass revetment

Table 4.1: Revetment design for the original design

Transition height (mNAP)	Section length (m)	Revetment	ECI (€)
-0.37 - +1.79	8.34	Loose rock, HMa 1000-3000	85.7
+1.79 - +2.41	4.82	Verkalit, 0.2 m	36.8
+2.41 - +6.15	14.54	Asphalt, 0.3 m	273.4
+6.15 - +8.22	8.49	Grass, 1.4m clay	62.3
Total	36.19		455.2

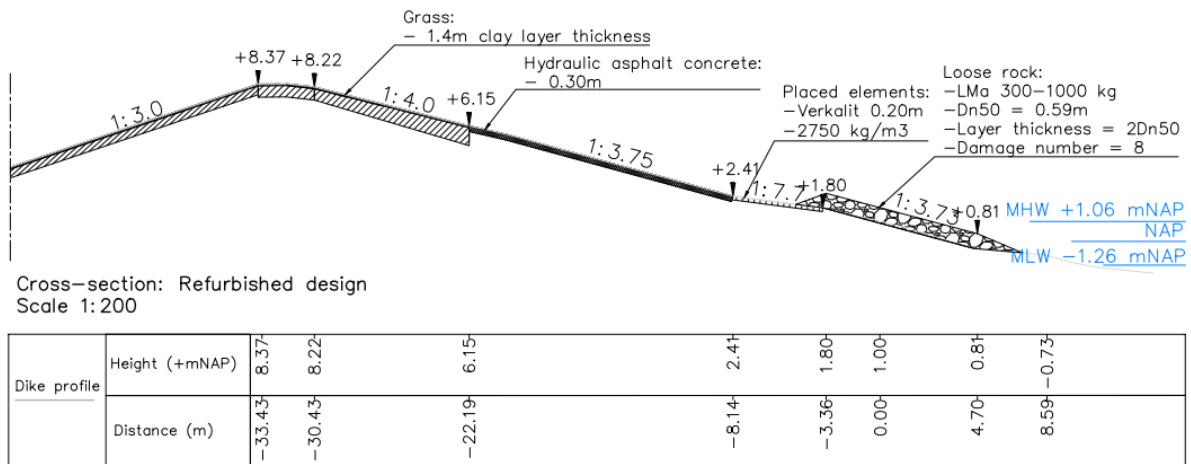


Figure 4.10: Refurbished design

4.2.5. Complete design

The complete dike revetment design is made by combining the preferred design options for each above-mentioned revetment type. The preferred options are summarized and presented in table 4.1. The total ECI of the revetment is €455.2. The asphalt section has the most significant contribution to the total ECI.

4.3. Designs with varying transition heights

This study aims to determine optimal transition heights between revetment types. There are many design options possible. First, the combination where only loose rock and grass revetment are applied is discussed. An asphalt or placed element section can be added to this revetment. Finally, the combination, including placed elements and asphalt, is studied. To study the combinations, all different options with corresponding ECI are made. The best combinations are selected. To do so, the following assumptions are made:

- The parameter combination selected for each revetment type per design options is the parameter combination that fulfils safety requirements and has the lowest ECI. In practice, this means the section with higher transition heights generally has larger diameters or thicknesses.
- Below +1.8 mNAP, only loose rock revetment is applied due to construction limitations. This area is situated in the inter-tidal zone, limiting installation methods. Loose rock can be installed with an excavator from a pontoon or land and does not require precise positioning of the individual rocks. Therefore, +1.8 mNAP is taken as the lower boundary for all other types of revetment.
- The lower boundary for grass is +5 mNAP. The model might produce unreliable results when the design water level exceeds the transition height too much.
- Within one revetment type, for example, Verkalit, the general trend is that the higher on the slope, the larger elements are required. However, using different sizes of the same revetment type within one design is impractical. Therefore, it is assumed that for each specific section, the largest element, which satisfies the safety requirements, is applied to the entire section.
- The design with the four different revetment types is ordered traditionally (loose rock, placed elements, asphalt, grass).

4.3.1. Loose rock - Grass

The first option is to apply only loose rock and grass revetment. However, it turns out that the largest rock size tested (HMa 6000 - 10000) does not fulfil safety requirements at the upper part of the dike where the grass begins (+5 mNAP). The loose rock revetment might fulfil safety requirements when a larger rock grading than tested in this study is applied (HMa 10000 - 15000). This grading is so large, that the corresponding ECI increases drastically. As this study aims to find the design with the lowest ECI, this is not further studied.

4.3.2. Loose rock - Verkalit - Grass

Figure 4.11 presents the design options with three revetment types. On the x-axis, the designs are numbered. The left y-axis presents the height with respect to NAP. The right y-axis presents the ECI. The blue bars represent the section covered with loose rock, the beige section represents the Verkalit, and the upper green section represents the grass revetment. The red line shows the total ECI score for the entire revetment. The different design options are ordered from low ECI to high ECI. Regarding the loose rock revetment, it is observed that the ECI is strongly dependent on the amount and diameter of rock applied. When the transition to Verkalit is higher, the required rock class and amount of rock both increase. Regarding the Verkalit, it is observed that the more Verkalit applied, the lower the ECI score. This is explained by the fact that the difference in element thickness between the lower and higher transitions is limited, and therefore, it does not have a large influence on the ECI. Regarding the grass revetment, it is observed that the lower the transition height with Verkalit, the higher the ECI becomes. However, it is not dominant over loose rock and shows a step-wise pattern. From design 20 to 21, a significant increase in ECI is shown due to increasing rock class, from HMa 1000-3000 to HMa 6000-10000. The optimal design (number 1) for a design with only Verkalit in between loose rock and grass results is presented in table 4.2 and shown in figure 4.11

Table 4.2: Revetment design for Loose rock, Verkalit and grass with optimal transition heights

Transition height (mNAP)	Section length (m)	Revetment	ECI (€)
-0.37 - +1.80	8.34	Loose rock, HMa 1000-3000	85.7
+1.80 - +6.00	18.7	Verkalit, 0.35m	220.2
+6.00 - +8.22	9.15	Grass, 1.5m clay	74.8
Total	36.19		380.7

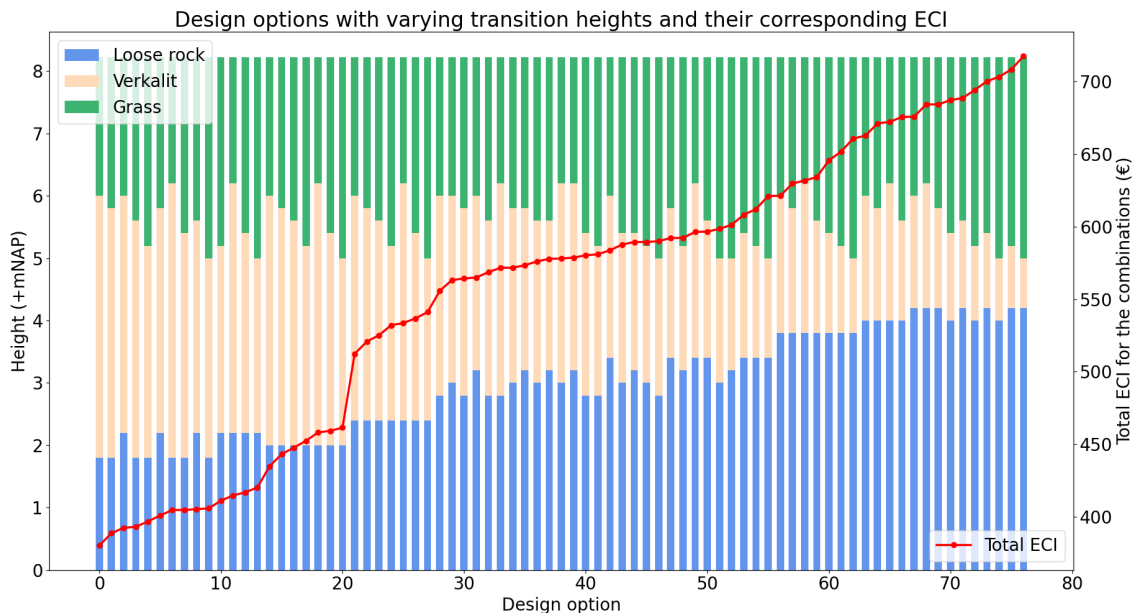


Figure 4.11: Design options with varying transition heights for loose rock, Verkalit and grass revetment. Designs sorted by ECI, increasing to the right

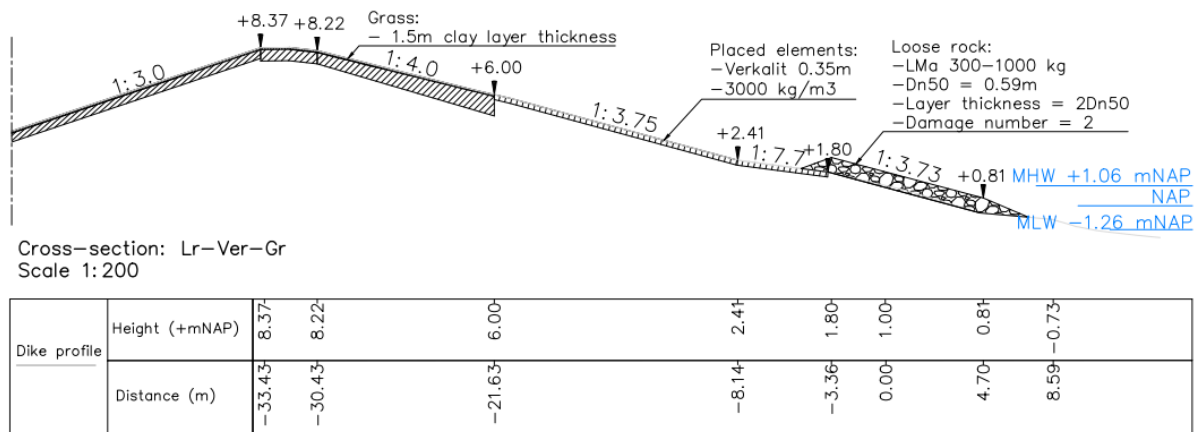


Figure 4.12: Design with lowest ECI for loose rock, Verkalit and grass revetment

Table 4.3: Revetment design for Loose rock, Basalton and grass with optimal transition heights. Designs sorted by ECI, increasing to the right

Transition height (mNAP)	Section length (m)	Revetment	ECI (€)
-0.37 - +1.80	8.34	Loose rock, HMa 1000-3000	85.7
+1.80 - +6.00	18.7	Basalton, 0.35m	212.6
+6.00 - +8.22	9.15	Grass, 1.5m clay	74.8
Total	36.19		373.1

4.3.3. Loose rock - Basalton - Grass

Figure 4.13 presents the design options for the revetment when Basalton is applied. The axes are the same as for the options with Verkalit. The graph looks similar to the one with Verkalit. However, the design with the lowest ECI score has a lower ECI value than Verkalit. This is due to the larger diameter required for the larger stretch. As shown in figure 4.7, Basalton has lower ECI for larger element thicknesses. This is due to the lower ECI value per m^3 . The preferred design is described in table 4.11, and a design drawing is presented in figure 4.14.

4.3.4. Loose rock - Asphalt - Grass

In figure 4.15, the different design options for the designs with asphalt between loose rock and grass are presented. The axes are the same as in the previous two sections. The figure shows that the ECI of this type of design strongly depends on the loose rock revetment. In contrast to the designs with placed elements, the designs with the lowest ECI have low transitions from asphalt to grass. This results in a relatively thick clay layer. The higher the transition from asphalt to grass, the larger the thickness it requires. This means that when a revetment with only asphalt is preferred over a combination with placed elements, a low transition from loose rock to asphalt and a low transition from asphalt to grass has the lowest ECI score.

4.3.5. Loose rock - Verkalit - Asphalt - Grass

Appendix C shows the graph with all 1273 design options. For clarity, the first 100 designs are selected and presented in figure 4.18. The figure in Appendix C shows that different designs lead to significant differences in ECI value. Like the previous three sections, the ECI depends strongly on the loose rock section. When

Table 4.4: Revetment design for Loose rock, Hydraulic asphalt concrete and grass with optimal transition heights. Designs are sorted by ECI, increasing to the right.

Transition height (mNAP)	Section length (m)	Revetment	ECI (€)
-0.37 - +1.80	8.34	Loose rock, HMa 1000-3000	85.7
+1.80 - +5.00	14.87	Asphalt, 0.20m	203.9
+5.00 - +8.22	12.98	Grass, 2.3m clay	166.3
Total	36.19		455.9



Figure 4.13: Design options with varying transition heights for loose rock, Basalton and grass revetment. Designs sorted by ECI, increasing to the right

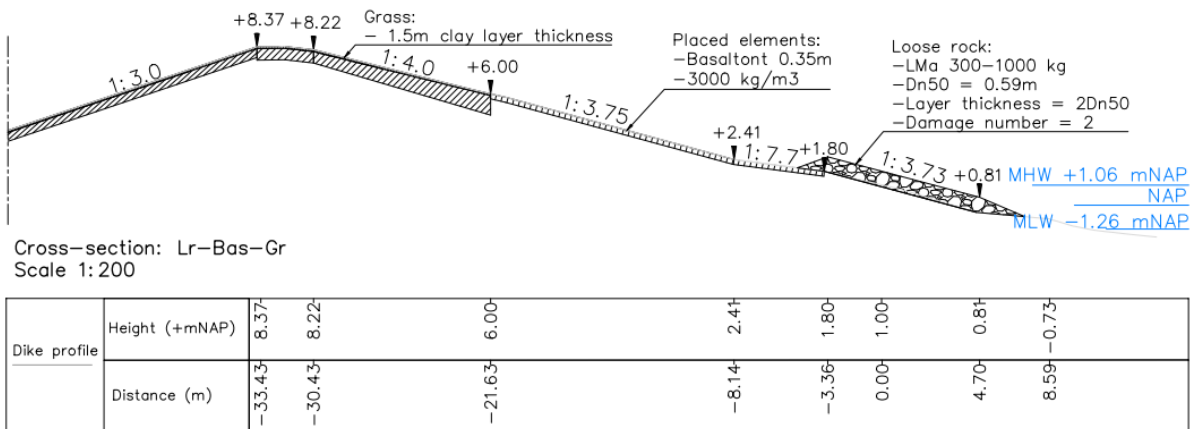


Figure 4.14: Design with lowest ECI for loose rock, Basalton and grass revetment.

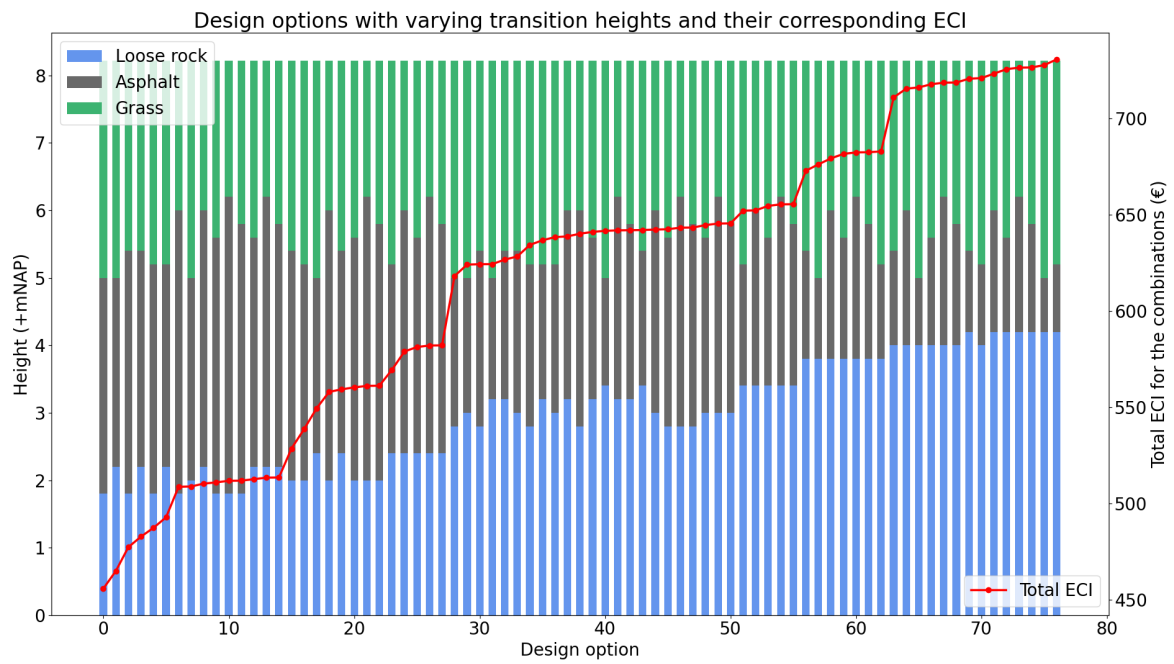


Figure 4.15: Design options with varying transition heights for loose rock, Hydraulic asphalt concrete and grass revetment. Designs are sorted by ECI, increasing to the right.

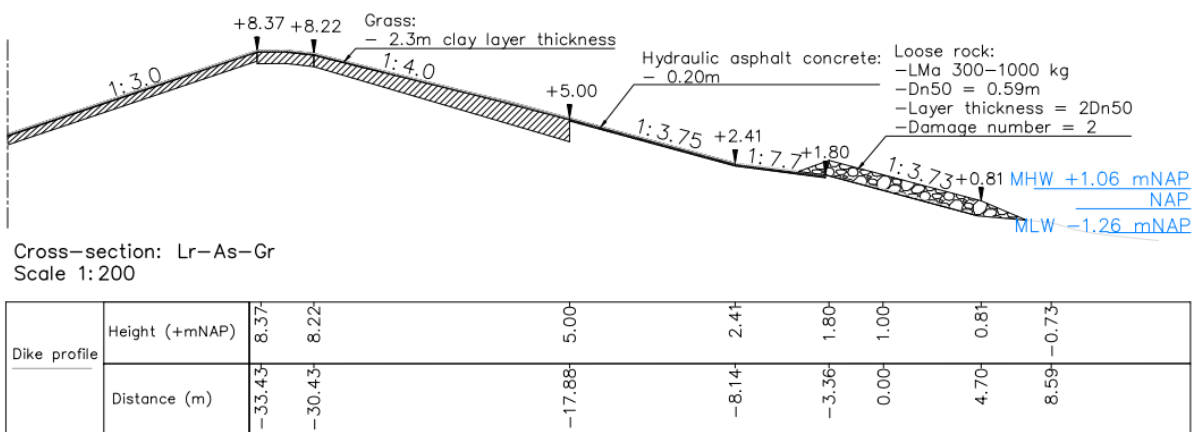


Figure 4.16: Design with lowest ECI for loose rock, Hydraulic asphalt concrete and grass revetment

Table 4.5: Revetment design for Loose rock, Verkalit, Hydraulic asphalt concrete and grass with optimal transition heights.

Transition height (mNAP)	Section length (m)	Revetment	ECI (€)
-0.37 - +1.80	8.34	Loose rock, HMa 1000-3000	85.7
+1.80 - +5.20	15.65	Verkalit, 0.30m	162.4
+5.20 - +6.00	3.05	Asphalt, 0.30m	57.6
+6.00 - +8.22	9.15	Grass, 1.5m clay	74.9
Total	36.19		380.6

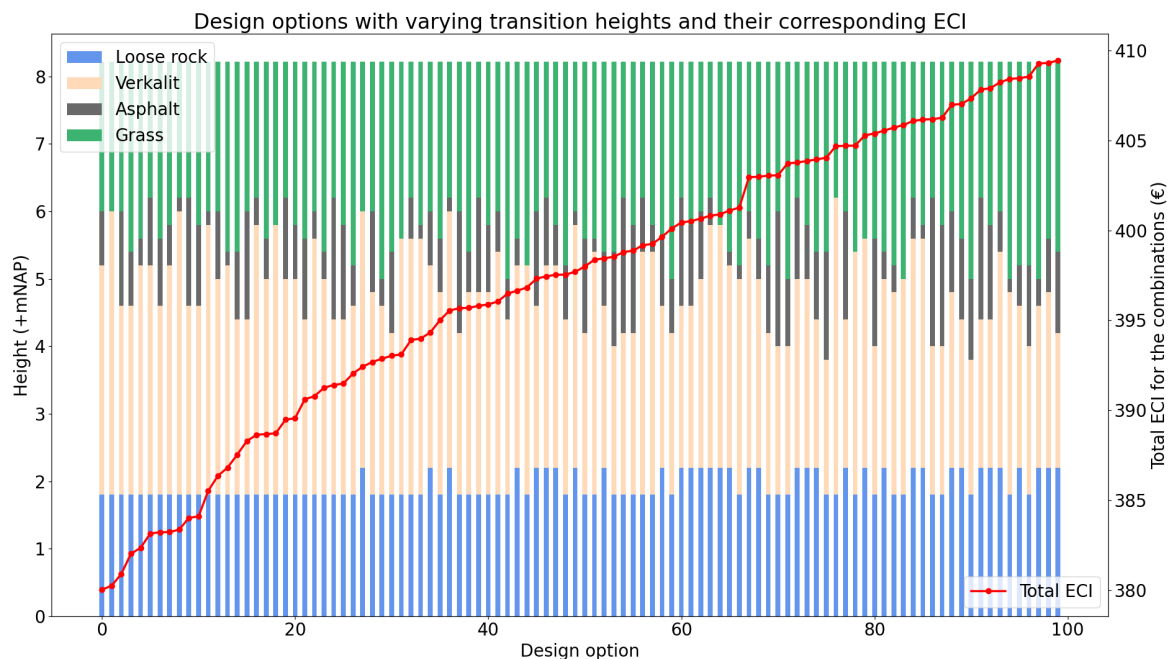


Figure 4.17: Design options with varying transition heights for loose rock, Verkalit, Hydraulic asphalt concrete and grass revetment. Designs are sorted by ECI, increasing to the right.

the loose rock increases one grading or transition height, several options exist for both Verkalit-dominated and asphalt-dominated designs. The designs with the lowest ECI are all Verkalit-dominated. Several options within the lowest 100 designs have varying transition heights from Verkalit to grass. The design with the lowest ECI has a small section of asphalt included. This section allows for five-centimetre thinner Verkalit elements compared to a design without asphalt. The design is presented in figure 4.18 and elaborated in table 4.5. The total ECI is 0.1 Euros lower than the complete Verkalit cover described in table 4.2. Apply a small section of asphalt or apply no asphalt. Both have their advantages. No specialised equipment and contractor are required when no asphalt is applied. This is beneficial for both planning and financial costs. When the small upper section of asphalt is combined with a berm, it can be used as a maintenance road.

4.3.6. Loose rock - Basalton - Asphalt - Grass

Appendix C shows the graph with all 1273 design options. For clarity, the first 100 designs are selected and presented in figure C.2. The same pattern is observed for the design with Verkalit instead of Basalton. The designs with the lowest ECI are Basalton-dominated and sometimes have a small section of asphalt in the upper region. The design with the lowest ECI consists of a loose rock, Basalton and grass revetment. In this design, the loose rock transition is at +1.8 mNAP, and the transition to grass is at +6 mNAP. The design is shown in figure 4.14 and table 4.11. This design is also the design with the lowest ECI overall and, therefore, the 'study design'.

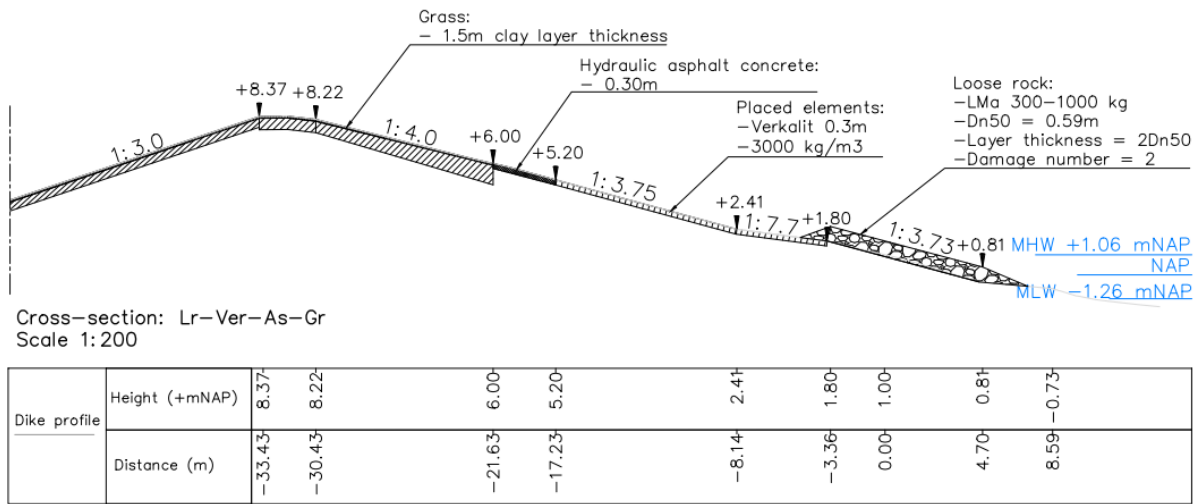


Figure 4.18: Design with lowest ECI for loose rock, Verkalit, Hydraulic asphalt concrete and grass revetment

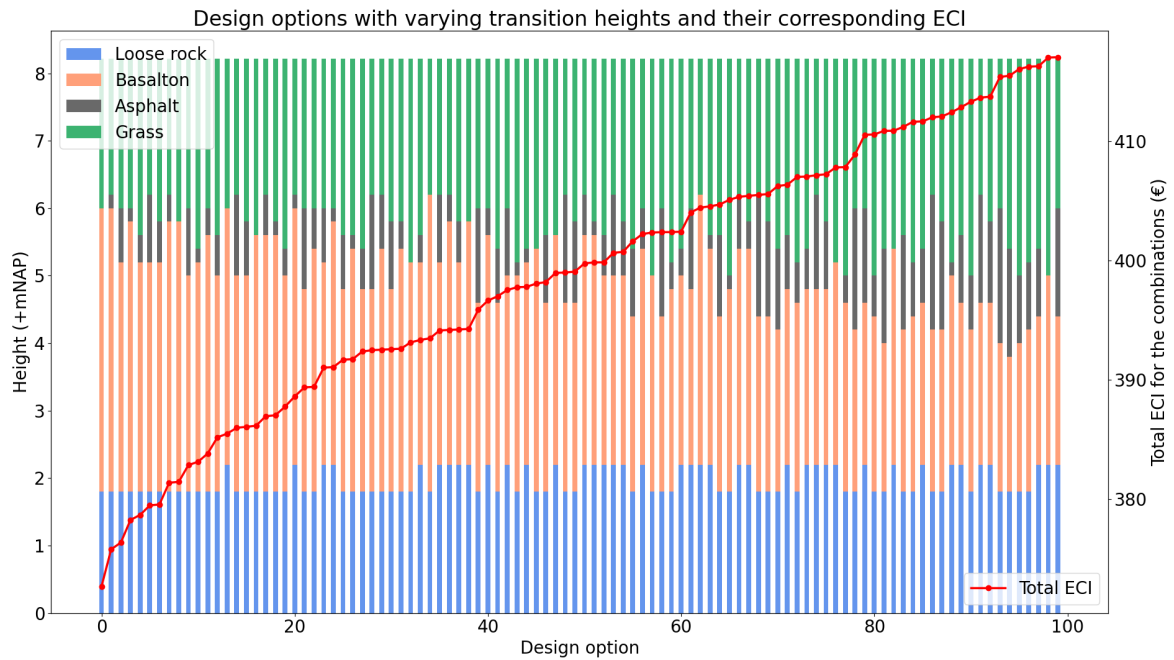


Figure 4.19: Design options with varying transition heights for loose rock, Basalton, Hydraulic asphalt concrete and grass revetment. Designs are sorted by ECI, increasing to the right.

4.4. Sensitivity of parameters related to the ECI

In section 3.3.3, the composition of the ECI is presented per revetment type. The ECI value assigned to each revetment type changes per project location. This section elaborates on the sensitivity of the different components of the ECI per revetment type. The values are all presented in m^2 or m^3 . To assess the influence of different components on the ECI outcome, the design proposed in section 4.2 is used as the base case. The impact of the specific component is assessed by changing one component and recalculating the total ECI. The ECI generally comprises the transport, material, installation and filter. The changes that are proposed that influence the outcome of the ECI are:

- Diameter/layer thickness.
- Project location relative to the production site/factory.

Installation of the revetment with equipment that produces less emissions is a possibility that results in a lower ECI. This is not considered in this sensitivity analysis because the ECI values for several components include the installation, and therefore, the ECI values without installation are difficult to determine. Installing the revetment with electrical or hydrogen-powered equipment will lead to lower emissions. The filter layer is kept constant as this is not part of this study.

4.4.1. Loose rock

Table 4.6 presents the components of the ECI for loose rock revetment in the original design. As described in section 4.2.1, the loose rock revetment covers a stretch of 8.34m consisting of a two-layer HMa 300-1000 originating from Norway with a 0.2m thick filter layer. This means that a total of $9.84m^3$ of rock is applied per meter dike. The design is based on an S value of 2, corresponding to limited maintenance.

Table 4.6: Original ECI composition loose rock

ECI Component	Value (€)
Transport	38.5
Loose rock	29.2
Installation	0.4
Filter layer	13.1
Maintenance	4.6
Total	85.8

Figure 4.20 presents three graphs where the composition of the ECI changes due to fictive changes in the circumstances. The left graph shows the distribution of the refurbished design as described above. The middle graph shows the ECI composition when the transportation distance changes from 650 km to 100 km by a bulk carrier. However, this reduction is hard to realize as the right quality rock is not produced in the Netherlands. This might be possible due to another project with rock left over or sharing transportation costs with another project nearby. This transportation reduction leads to a significant decrease in ECI costs. The right graph shows the composition of the ECI when the rock size changes from HMa 300-1000 kg ($Dn50 = 0.59m$) to HMa 1000-3000 kg ($Dn50 = 0.90m$). The layer thickness remains two times the nominal rock diameter. The ECI for transport, the loose rock itself and maintenance depend directly on the quantity of rock in m^3 applied. This leads to a significant increase in ECI. Figure 4.21 presents the ECI for each S-value per rock class. The S-values are linked to the required maintenance described in section 3.5.1. The lower three classes do not differ much due to similar Dn50 values. In a situation where a choice has to be made between class LMa 15-300 with $S = 10$ or LMa 40-200 with $S = 4$, the latter leads to a lower ECI. From the lowest three gradings to HMa 300-1000 and HMa 1000-3000, this situation does not occur. The increase in diameter is dominant over the amount of maintenance. The situation does occur for the upper three gradings. The influence of S increases with increasing grading, this is due to the fact that when large gradings are to be maintained, large rock is required.

It is concluded from the above-mentioned observations that the change in nominal rock diameter is most dominant. Reduction in transport distance for loose rock is practically impossible but can potentially lead to a significant reduction of ECI. The influence of damage number S increases with increasing grading and influences the ECI outcome. In some situations, a larger grading with a lower damage number leads to lower ECI than a smaller grading with a high damage number.

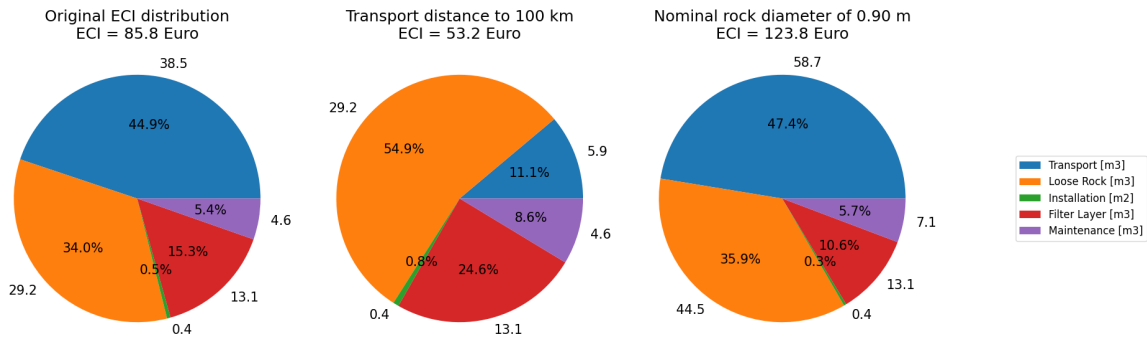


Figure 4.20: ECI composition loose rock with changing circumstances

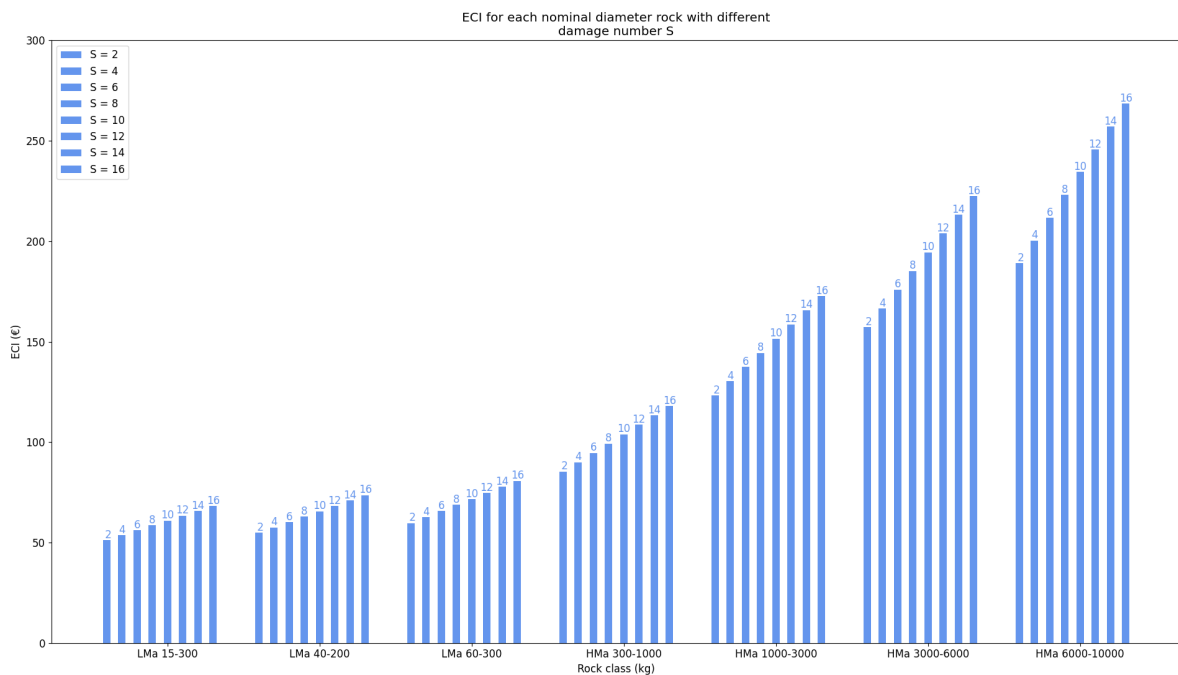


Figure 4.21: ECI loose rock depending on different damage number

4.4.2. Verkalit

Table 4.7 presents the composition of the ECI for Verkalit revetment in the original design. As described in section 4.2.2, Verkalit revetment covers a stretch of 4.52m consisting of 0.2m thick elements with a density of 2750 kg/m^3 . A total amount of 0.90 m^3 is applied per meter dike width.

Table 4.7: Original ECI composition Verkalit

ECI Component	Value (€)
Transport	1
Verkalit	24.9
Installation	0.9
Geotextile	2.1
Filter layer	7.4
Total	36.3

Figure 4.22 presents three graphs where the composition changes due to changed parameters. The left graph presents the composition for the preferred situation as presented in section 4.2.2. The middle graph shows the composition where the transport distance is changed from 38 km to 228 km, the distance that Basalton is

transported. This shows an increase of 4.7 euros compared to the preferred design. The right graph shows an increase in element thickness from 0.2 to 0.4 meters. This induced a total increase of 25.8 euros distributed over the production of Verkalit and transport costs.

It is concluded from the above-mentioned observations that the increase in element diameter has the largest effect on total ECI.

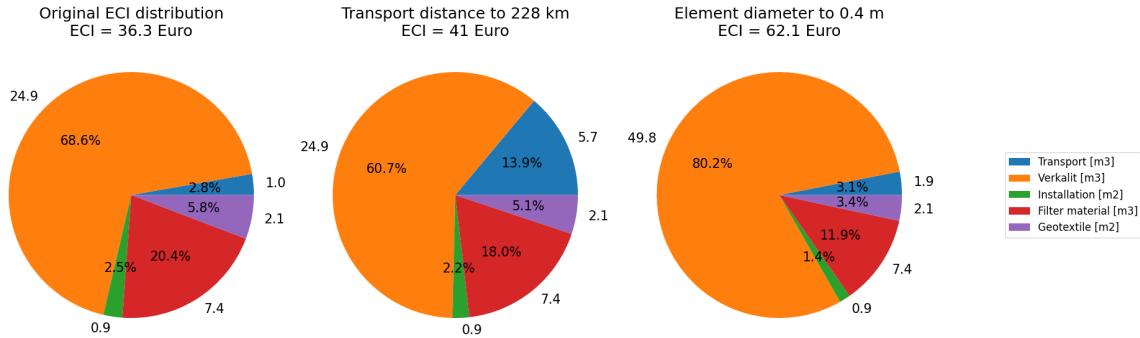


Figure 4.22: ECI composition Verkalit with changing circumstances

4.4.3. Basalton

Table 4.8 presents the composition of the ECI for Basalton revetment in the preferred design. To make a proper comparison, the exact same dimensions as Verkalit are chosen for this analysis.

Table 4.8: Original ECI composition Basalton

ECI Component	Value (€)
Transport	5.7
Basalton	16.9
Installation	0.9
Geotextile	2.1
Filter layer	7.4
Split	3.7
Total	36.7

Figure 4.23 presents three graphs where the composition changes due to changed parameters. The left graph presents the preferred design as presented in section 4.2.2. The middle figure shows the ECI composition when the transport distance is reduced to that of Verkalit (38 km). It is observed that a reduction of 4.7 euros is achieved. The total ECI is now lower than that of Verkalit due to the lower emissions during the manufacturing of the elements. The right graph presents the design with an increased element thickness from 0.2 to 0.4 meters. This induces an increase of 22.7 euros. The increase is lower than Verkalit due to the lower ECI values for Basalton.

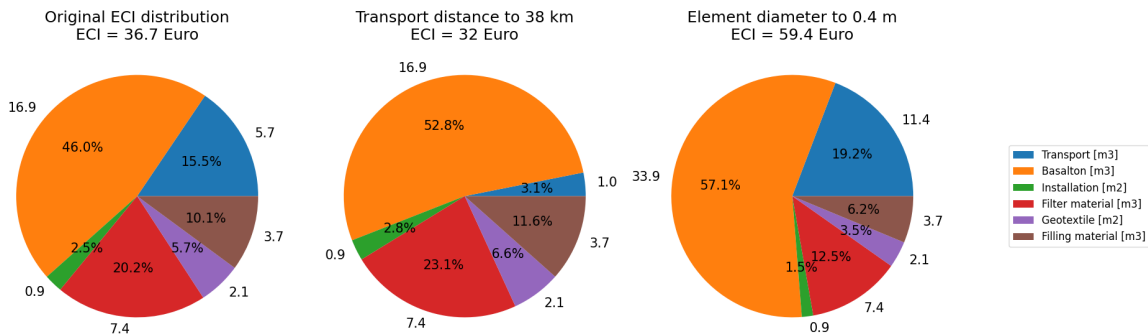


Figure 4.23: ECI composition Basalton with changing circumstances

4.4.4. Asphalt

Table 4.9 presents the composition of the ECI for the hydraulic asphalt concrete layer in the preferred design. As described in section 4.2.3, asphalt revetment covers 14.54m with a layer thickness of 0.30m. A total amount of 4.36 m³ is applied per meter dike width.

Table 4.9: Original ECI composition Asphalt

ECI Component	Value (€)
Transport	3.8
Asphalt	208.3
Installation	44.2
Foundation (sand)	11.8
Adhesive coating	1.7
Total	269.8

Figure 4.24 presents three graphs where the composition of the ECI changes due to changed parameters. The left graph shows the composition of the preferred design as presented in section 4.2.3. The middle graph shows the ECI composition when the transport distance is changed from 38 to 100 km. This leads to an increase of 6.7 Euros. The right graph shows the ECI combination when the layer thickness decreases from 0.30m to 0.15m. The ECI value for the production of asphalt halves, decreasing the total ECI by 106 Euros. It is concluded that the impact of an increased layer thickness has the largest effect on the total ECI.

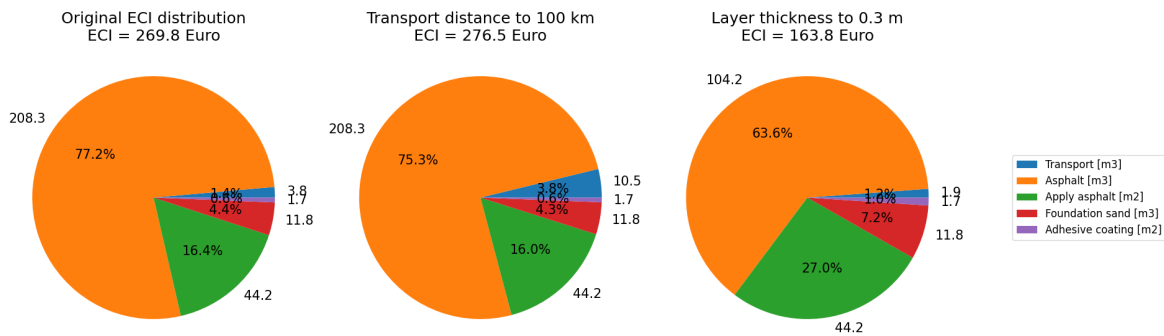


Figure 4.24: ECI composition hydraulic asphalt concrete with changing circumstances

4.4.5. Grass

Table 4.10 presents the composition of the ECI for grass revetment in the preferred design. As described in section 4.2.4, grass revetment covers a stretch of 8.49 m, starting with a clay layer thickness of 1.4m at the transition with asphalt and 0.8m at the crest.

Table 4.10: Original ECI composition grass

ECI Component	Value (€)
Transport	33.2
Clay	30.6
Installation	1.2
Sowing	0.1
Maintenance	0
Total	65.1

Figure 4.25 presents three graphs where the ECI composition changes due to changed parameters. The left graph presents the composition for the original situation as presented in section 4.2.4. The middle graph presents the situation where the transport distance decreases to 40 km, and the clay is not transported by inland vessel but by truck. This shows a significant decrease in ECI value for the entire revetment. The right graph shows the ECI when the clay layer thickness increases to 2 meters at the transition with asphalt. The increased thickness results in an increase of 27.9 euros.

It is concluded that the effect of transportation is very large. This is hard to reduce, but when local clay is an option, it reduces the ECI drastically.

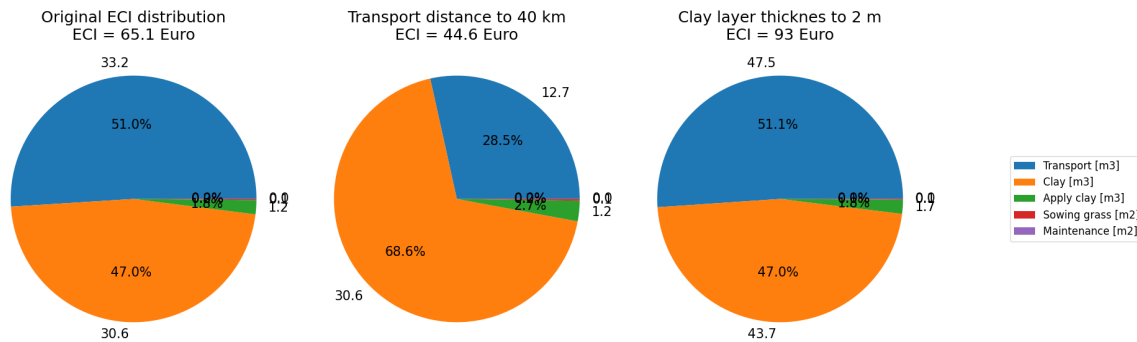


Figure 4.25: ECI composition grass with changing circumstances

4.5. Financial costs of the design options

The financial cost for the entire revetment is the sum of the costs per revetment type. In figure 4.26, the financial costs per design are plotted in the previous figure for the 100 designs with the lowest ECI. Appendix D shows the graph for all 1273 designs. The right x-axis presents the costs in euros. The financial costs are of another order than the ECI. From the graph with all the designs, it is observed that the financial costs are generally increasing when the ECI is increasing. This is because both ECI and financial costs depend most dominantly on the increasing loose rock diameter and volume. When looking at the 100 designs with the lowest ECI, it is observed that the study design does not have the lowest financial costs. The costs for the best 100 options range from €1750 to €2250 per meter dike length. For kilometres of dike lengths, this difference is significant. Loose rock has the largest influence on financial costs. For the designs where the loose rock is constant, the difference is made by the Basalton, which is more expensive than hydraulic asphalt concrete. Figure 4.27 presents the designs sorted for financial costs. It is observed that the design with the lowest financial costs looks like the design as it was in the original situation. Or, in this study, the refurbished design. Asphalt is a relatively cheap option and is dominant in this situation.

The study design costs €1890 per meter, with an ECI of €373 per meter. The financially most attractive design costs €1439 per meter, with an ECI of €458 per meter. The difference in financial costs is €451 per meter (24%) and €85 per meter ECI costs (23%). To compare both costs is complex as the ECI costs are a cost per kg CO₂ and are not corrected for inflation or fluctuation of the CO₂ price in the past. In practice, the ECI is multiplied with a certain factor to be able to make a summation. This factor differs per project/tender and depends on how important the ECI is considered. To find the design with the combined lowest financial costs and ECI score, this factor has to be determined, which is a political choice the client has to make. The graphs for the designs with Verkalit instead of Basalton are presented in Appendix D. The trends are very similar. Only Verkalit is more expensive per m^3 .

Table 4.11: Revetment design for Loose rock, Basalton and grass with optimal transition heights

Transition height (mNAP)	Section length (m)	Revetment	Costs (€/m)
-0.37 - +1.80	8.34	Loose rock, HMa 1000-3000	960
+1.80 - +6.00	18.7	Basalton, 0.35m	720
+6.00 - +8.22	9.15	Grass, 1.5m clay	209
Total	36.19		1890

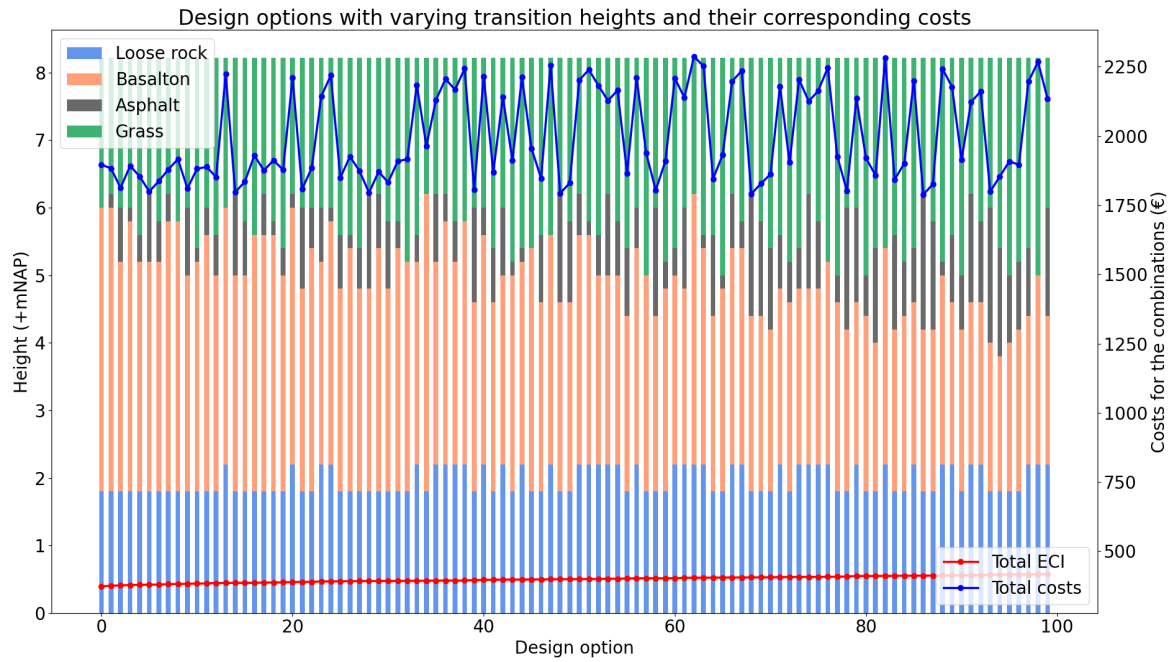


Figure 4.26: Financial costs corresponding to the design options for loose rock, Basalton, asphalt and grass revetment. Designs are sorted by ECI, increasing to the right.

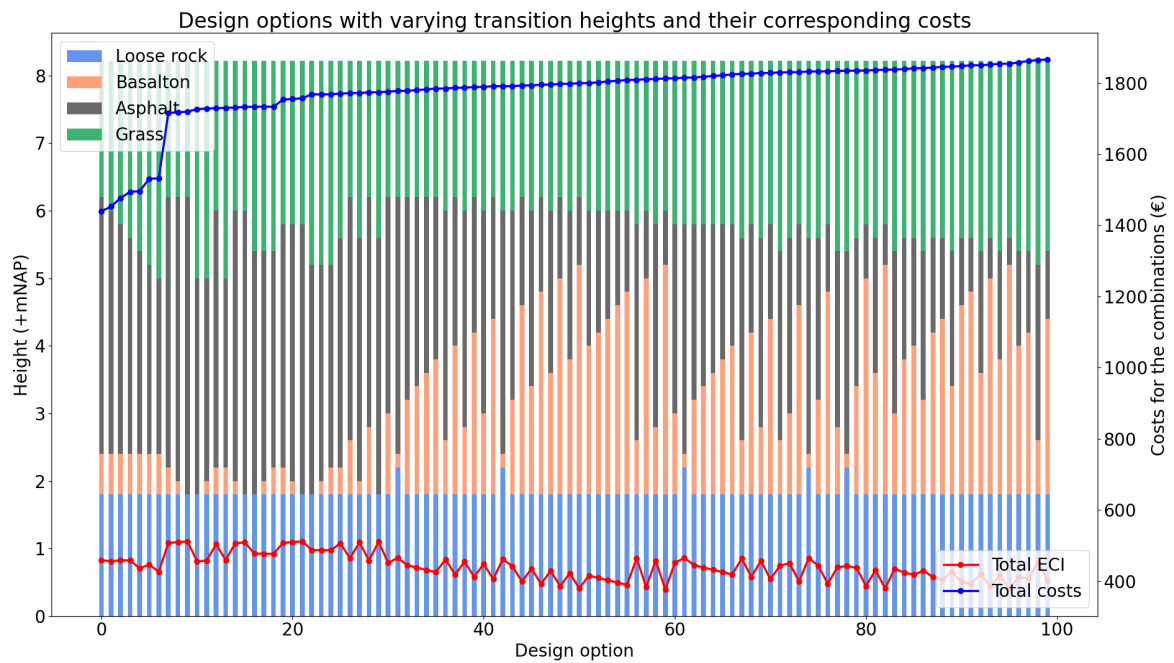


Figure 4.27: Financial costs corresponding to the design options for loose rock, Basalton, asphalt and grass revetment. Designs are sorted by financial costs, increasing to the right.

4.6. Comparison of the study design with Arcadis' design for the Lauwersmeerdijk case

The fifth research question concerns comparing Arcadis's design for the Lauwersmeerdijk and the design with the lowest ECI resulting from this study. This chapter focuses on the comparison between the two designs. First, a general comparison regarding geometry and design approach is made, and then the application of different revetment types and the transition height are compared. Next, the ECI score and the financial costs are compared.

General comparison

Figures 4.28 and 4.29 present the designs proposed by Arcadis and the design proposed by this study. The dike designs differ significantly. The Arcadis design considers more aspects than the design proposed by this study. The Arcadis design is designed to fulfil all failure mechanisms. Also, the different stakeholders interested in the dike design are considered. The study design only considers the stability of the revetment and ECI.

When the geometry is compared, two differences stand out. In the study design, the berm is located around +2.4 mNAP. In the Arcadis design, the berm is located around +5.5 mNAP. Next to this, the height of the dike is different. The Arcadis design is designed with a crest level of +8.80 mNAP. The study design is designed with a crest level of +8.22 mNAP. In the Arcadis design, the height is increased to fulfil safety requirements concerning overtopping. The difference in height results in an extra slope length of 1.74m with a slope angle of 1:3. The slope angle of the dike influences the stability of the different revetment types. The different geometry results in 2.76m extra revetment length for different revetment types.

The calculation method for the two designs differs. The Arcadis design is calculated as prescribed by the Rijkswaterstaat (2017). The loose rock, placed elements and asphalt revetment in the Arcadis design are calculated deterministically. The grass revetment is calculated probabilistically. This study calculates all revetment types probabilistically. For the placed elements, loose rock and grass revetment, the designs are similar. However, for the hydraulic asphalt concrete layer, a significant discrepancy in required layer thickness is observed. The design made by Arcadis does fulfil the safety requirements as prescribed by the Rijkswaterstaat (2017) and is considered a safe design. The design made with the probabilistic approach requires a larger thickness due to the uncertainty of specific parameters. Exceptionally important is the cracking strength. When random samples are taken from this distribution, realizations with extremely low cracking strength are calculated, which results in failure of the asphalt layer. Combined with a small required probability of failure, like in this study, the required layer thickness is larger than the design according to the deterministic approach. Due to the differences in geometry and calculation method between the designs, the comparison cannot be made one-on-one, but a nuance must be considered.

Revetment type

From the toe to the crest of the dike, the comparison for the revetment types and the transition height is made. The loose rock revetment designed by Arcadis has the same rock class. The transition height is slightly higher. The middle section of Arcadis's design consists of Verkalit of 0.30m thickness with 2650 kg/m^3 combined with a large stretch of hydraulic asphalt concrete of 0.15m thickness. The middle part of the study design consists of Basalton of 0.35m thickness with 3000 kg/m^3 . The difference is due to the calculation method as described above. The larger element thickness of the study design is because it is placed higher on the revetment where hydraulic boundary conditions are more severe. The upper part of both designs is made of grass with a similar clay layer thickness.

ECI comparison

Table 4.12 presents the ECI values corresponding to the different revetment sections. When comparing this design to the study design as presented in table 4.11, the Arcadis design has the lowest ECI value of €361.0 versus €373.1 for the study design. The difference is mainly explained by the fact that the asphalt layer in the Arcadis design is only 0.15m thick. When applying a 0.3m thick asphalt layer, which would suffice the safety criteria according to the probabilistic approach, the ECI for the Arcadis design would be €463.9. This is €102.9 higher than the study design. It is concluded that as long as the deterministic approach for calculating the asphalt layer is applied, this probably leads to a design with lower ECI. It can not be concluded that, although the Arcadis design has a lower ECI than the study design, it is the optimal design with respect to ECI. Another design with deterministic calculation techniques likely results in a lower ECI than the Arcadis design.

When the financial costs between the two designs are assessed, the Arcadis design is more expensive. Table

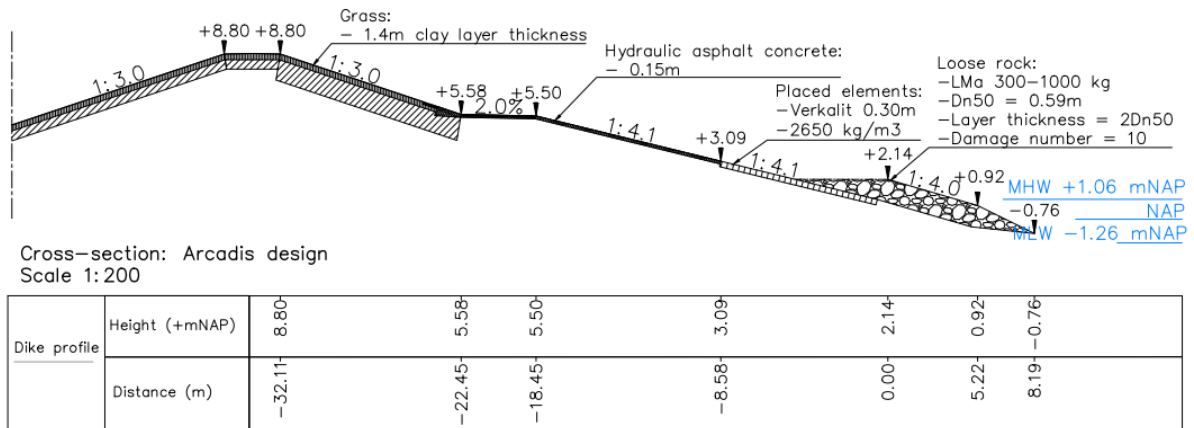


Figure 4.28: Arcadis design

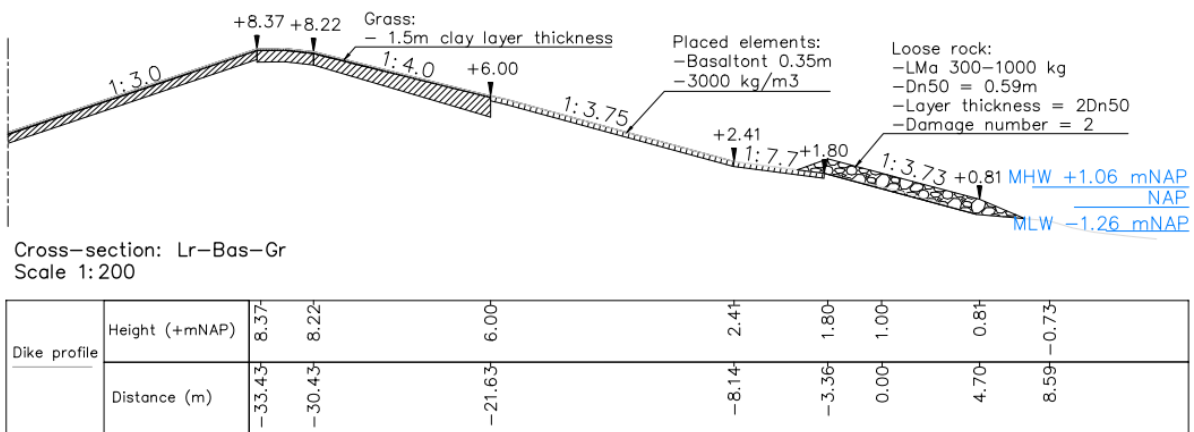


Figure 4.29: Study design: Design with lowest ECI

Table 4.12: Arcadis design revetment composition

Transition height (mNAP)	Section length (m)	Revetment	ECI (€)	Financial costs
-0.37 - +2.20	10.59	Loose rock, HMA 1000-3000	83.0	1008
+2.20 - +3.09	3.79	Verkalit, 0.30m	39.4	514
+3.09 - +5.56	14.13	Asphalt, 0.15m	159.0	287
+5.56 - +8.80	10.44	Grass, 1.4m clay	79.6	229
Total	38.95		361.0	2038

4.11 describes the financial costs for the study design. The costs are €1890 per m^1 . In table 4.12, the last column shows the financial costs for the design made by Arcadis, which is €2038. This is a difference of €148 per meter dike width. The difference is counterintuitive due to the large stretch of asphalt applied. However, the price increases due to the extra length of loose rock. Also, because asphalt is relatively cheap, the difference between 0.3 m and 0.15 m thick layer is less significant regarding financial costs.

5

Discussion

5.1. Project specific design

This study was performed based on the Lauwersmeerdijk-Vierhuizergat case study. Within this project, one cross-section is taken as representative for this study, see figure 3.5. It is therefore important to note that the design solutions as suggested by this study apply to the site conditions specifically to this project. When applying the knowledge gained from this study for future projects, it is important to check whether the site conditions and geometry at the project site are compatible with the conditions used for this study and if the governing conditions might lead to different designs.

5.2. Hydraulic Boundary conditions

Hydraulic boundary conditions for the model are generated with Hydra-NL. This model generates deterministic values based on the dominant wind direction. It simplifies the probabilistic wave field generated by Hydra-Ring (Duits, 2020; Diermanse et al., 2013). This study requires stochastic input for the wave characteristics. Therefore, the model uncertainty of Hydra-NL is used as the uncertainty of the wave characteristics. This uncertainty is not precisely the uncertainty of the significant wave height and period due to the uncertainty in water level and wind statistics used in the model. This results in uncertainty in the different components used in SWAN to determine the wave characteristics. To include this uncertainty, the entire wave field corresponding to different water levels generated by Hydra-Ring should be included in the model.

5.3. Effect of interlocking on stability

From figure 4.2 and 4.3, little difference is observed in the probability of failure. Figure 4.7 presents the required diameter with a concrete density that fulfils safety requirements. It is observed that Verkalit and Basalton behave very similarly while it is a different type of block. This is explained by the applied z-functions for both equations. The equation developed by M. Klein Breteler is used to assess the safety requirements for both Basalton and Verkalit (Klein Breteler and Mourik, 2014). Three different equations are developed for three different types of elements: column types of blocks, blocks on the side and wedged blocks. To date, no equation for interlocking blocks has been developed. To apply this equation to interlocking blocks, Steentoets was used to find a factor for the difference in element thickness between Basalton (column type) and Verkalit for the same boundary conditions. A factor of 1.14 is applied. However, this is a general approach, and the factor is not validated. When comparing the factor to the upgrade factor used in the equation developed by Pilarczyk (Pilarczyk and Klein Breteler, 1998) for interlocking blocks and loose blocks on geotextile, the factor used in this study is smaller. Pilarczyk suggests a factor of 2 for loose blocks and 2.5 for interlocking blocks, resulting in a ratio of 1.25. This means that the interlocking effect might be underestimated in this study.

5.4. Maintenance of revetment

The environmental cost indicator represents the costs in euros necessary to compensate for the emissions produced by the project during its entire design lifetime. This includes maintenance. For placed elements and hydraulic asphalt concrete, no maintenance has been assumed as it is designed for the entire lifetime,

and no parameters related to any allowable damage are included in the design equations. How to consider maintenance for loose rock and what ECI score is assigned to the maintenance is subject to discussion. An attempt has been made to include maintenance properly in the ECI calculation described in section 3.5.1. To include the effect of the damage number on the amount of maintenance, a threshold for the moment maintenance is done is applied. Figure 4.21 presents the sensitivity of the environmental cost indicator relative to the damage number. However, it has become clear that the maintenance of loose rock revetment is based on subjective observations. The waterboard Noorderzijlvest, who is the owner of the Lauwersmeerdijk-Vierhuizen project, says: "We add some extra rock to the protection every once in a while when some rocks are displaced, based on the naked eye" (JW. Nieuwenhuis). This policy cannot be used to calculate the ECI values in this study due to the subjective character. Therefore, in this study, the maintenance is linked to the damage number S . As maintenance is an important contributor to the total ECI, the assumptions applied in this study might lead to a wrong estimation of the maintenance and, therefore, over- or underestimation of the total ECI.

5.5. Correlation loading duration with wave characteristics

The number of waves acting on the revetment influences the required strength of the revetment. To assign the number of waves to the corresponding water level, the storm set-up plus the normal tide has been assessed as described in section 3.3.1. The maximum loading duration and the mean period result in a number of waves assigned to each water level. The corresponding waves assigned to the water levels are the waves calculated with Hydra-NL. These waves correspond to the design storm for the different water levels. This results in the assumption that a correlation exists between the number of waves and wave characteristics. This full correlation is likely to be not correct as the maximum duration of loading is not always simultaneous with the peak of the storm, where the largest waves occur.

5.6. Breaker parameter

The wave-breaking criteria suggested by Kamphuis Kamphuis (1991) is applied in the model to exclude waves with non-existing combinations of wavelengths and heights. This results in deleting a portion of the drawn samples. These samples are not considered in further calculating the probability of failure. This results in a not entirely randomly drawn sample set. No further studies on the effect of this are found. In this study, physical correctness is considered more important than statistical correctness. The number of samples removed by the criteria is around 5-15%, depending on the water level. This is considered when selecting the sample size, such that always more than $12 * 10^6$ valid samples are used to calculate the probability of failure.

5.7. Validity ECI

The environmental cost indicator is a relatively new method of calculating the emissions. Weekly, new or existing elements are added or updated in the database. As an effect, the ECI calculated today is likely to be different in half a year. This study presents results based on the database like it was in May 2023. The developments are not included because the model can not be linked to the database yet. As a result, the outcome of this model may be outdated quickly. When new production methods or more detailed emission assessments are performed for particular components, this might result in a different outcome. Therefore, caution should be maintained, and the latest database version must be utilized when calculating the ECI for a project.

5.8. Recycling/reuse value revetment

Within the ECI composition for all different components, a negative value represents the component's value after the lifetime has passed. This reduces the total ECI but is subjective. Loose rock has a lifetime much longer than the design lifetime of the dike. The high ECI costs for this project might weigh up to the costs of applying the same rock for another (or the same dike) project when the lifetime has passed. The recycling value of the different components should be further studied and specified to include this argument when making design choices.

5.9. Sample size

Crude Monte Carlo analysis requires a predefined sample size to acquire the right accuracy for the probability of failure necessary for the safety assessment. This study uses a rule of thumb of 200 times the probability of failure. However, no conversion criteria are included in the model for efficiency reasons. It is assumed that the required accuracy is achieved by taking a sample size large enough to capture all possible events.

6

Conclusion

This study aimed to acquire knowledge on designing a dike revetment that fulfils technical requirements and has the lowest environmental cost indicator (ECI) possible. This has been done by making a Python model to assess the safety requirements probabilistically and determine the ECI for each corresponding design.

The probabilistic technique applied for this study is crude Monte Carlo analysis. This is the preferred technique due to the simplicity and availability of the method. Crude Monte Carlo comes with large computational costs due to the many samples required. Due to the discontinuity of the limit state functions, determining the design point with FORM analysis is impossible. For importance sampling, the design point is usually estimated with FORM. When other techniques are used to estimate the design point, importance sampling might be an option that requires less computational time. For this study, this was not considered due to the large number of different designs and the necessity to adjust the module in OpenTurns to use another technique to estimate the design point.

Based on all the designs that fulfil the safety requirements, the parameter combination that fulfils the safety requirement and has the lowest ECI for the different revetment types is studied. The Lauwersmeerdijk-Vierhuizen original revetment design was updated to fulfil safety requirements. Regarding loose rock, the preferred parameter combination is the smallest grading that fulfils safety requirements. The ECI of the different gradings depends on the amount of maintenance during the lifetime. In this study, the amount of maintenance is coupled to the damage number for quantification. A grading with a high damage number leads, in some cases, to higher ECI compared to one grading larger with a lower damage number. For placed elements, Verkalit and Basalton are considered. For both, the design with the lowest element thickness is preferred with respect to ECI. The choice between the two types depends on the required element thickness. When a thickness larger than 0.20 m is required, Basalton is preferred due to the lower ECI value per m^3 . The hydraulic asphalt concrete layer is tested for both wave impact and uplift. The design with the lowest ECI has the thinnest layer. For grass, the clay layer thickness is the decision parameter that influences the ECI the most. Therefore, the thinnest possible clay layer is preferred.

The probability of failure of the different revetment types is calculated for all water levels with corresponding wave characteristics. Therefore, it is possible to make designs with all different transition heights from one revetment to another and calculate the corresponding ECI. The design with the lowest ECI combines loose rock, Basalton and grass. The transition heights for this design are +1.8 mNAP from loose rock to Basalton and +6 mNAP from Basalton to grass. Hydraulic asphalt concrete is absent in this design. When Verkalit is preferred over Basalton, asphalt is included in the design. The optimal transition for this design is +1.8 mNAP from loose rock to Verkalit, +5.2 mNAP from Verkalit to hydraulic asphalt concrete and +6.0 mNAP from hydraulic asphalt concrete to grass.

The ECI for different revetment types is composed of several factors. The ECI for loose rock depends on the rock class, transport distance and maintenance. The amount of maintenance is linked to the damage number. When the design is made with a high damage number, a larger grading with a low damage number is worth considering. The ECI for Verkalit and Basalton depend strongly on the element thickness. The choice

for an element type should depend on the ECI/m^3 and the transport distance. The ECI for hydraulic asphalt concrete depends strongly on the layer thickness. An asphalt plant close to the project site is preferred for transport. The ECI for grass revetment depends strongly on the amount of clay applied and the transport distance. The transport takes up a large part of the total ECI.

Besides the environmental costs for each design, the financial costs are estimated. This remains an important factor in the feasibility of a design. When comparing the designs with alternating transition heights, the financial costs for the revetment per meter dike length depend strongest on the loose rock class. The optimal design for both ECI and financial costs has as small and as little rock as possible. When comparing the design to the design with the lowest ECI, the financially optimal design includes a large section of hydraulic asphalt concrete instead of Basalton and a small section of Basalton between loose rock and asphalt. This results in a design similar to the refurbished design. The financial optimal design is €451 per meter dike width cheaper (24%) than the design with the lowest ECI but is €85 per meter dike width more expensive in terms of ECI (23%). To find the design that has the lowest combined financial and ECI costs, the factor with which the ECI is multiplied has to be determined by the client.

The Lauwersmeerdijk-Vierhuizen case is studied to compare the revetment design made by Arcadis and the design proposed by this study. Due to the different geometry and calculation methods applied to design both revetments, the designs are difficult to compare. The most important difference between the Arcadis design and the study design is the application of hydraulic asphalt concrete. The Arcadis design applies a large stretch of hydraulic asphalt concrete. The study design applies Basalton for the entire section between loose rock and grass. Based on the deterministic calculations for hydraulic asphalt concrete, the design Arcadis made results in a design with lower ECI compared to the preferred design by this study because the required hydraulic asphalt concrete layer thickness is reduced by 50%. Comparing the financial costs of both designs, the design made by Arcadis is €148 per meter dike width more expensive. This is due to the slightly larger section of loose rock.

Based on the above, the main research question that covers all aspects of the study is answered. The main research question is:

What sea dike revetment design fulfils safety requirements and has the lowest environmental impact for the Lauwersmeerdijk-Vierhuizen dike reinforcement project?

The preferred sea dike revetment is the design with the lowest ECI score and fulfils the safety requirement. The safety requirement for the revetment is to have a probability of failure maximum of 1/60.000. Depending on the calculation method applied, there are two different outcomes. When the design is made probabilistically, the design that satisfies this requirement with the lowest ECI consists of loose rock, Basalton and Grass revetment. The design is presented in figure 6.1. However, when a deterministic/semi-probabilistic approach is applied, the design with the lowest ECI differs from the probabilistically determined design and has a lower ECI. The design made by Arcadis has a lower ECI. However, the transition heights are not optimized. Therefore, it is likely that the ECI could be further decreased. The Lauwersmeerdijk-Vierhuizen project is currently (November 2023) under construction, and therefore, the lessons learned from this study are not implementable in this case. A study like this is too extensive for future dike reinforcement projects. Thus, the conclusions are translated into lessons learned for future sea dike revetment design.

1. Probabilistic calculation techniques for sea dike revetment design do not always lead to a design with a lower ECI score than a deterministic design. Generally, the prevailing thought is that probabilistic design leads to a sharper design that requires fewer materials and is more sustainable. However, as observed in this study, this is not always true. The probabilistic approach for the asphalt revetment tested for wave impact leads to a design requiring a larger asphalt layer thickness. In this case, one parameter, the cracking strength, dominates over the other parameters. When the uncertainty is not known well and therefore has a large interval, extreme situations are tested when the number of samples is large. Knowing this uncertainty well is important before undertaking the probabilistic approach. Therefore, a calibration study into the entire equation for wave impact on the asphalt layer is required.
2. Loose rock has the largest influence on the total ECI. Therefore, apply the smallest grading and limit the application range as much as possible to reduce the total volume.

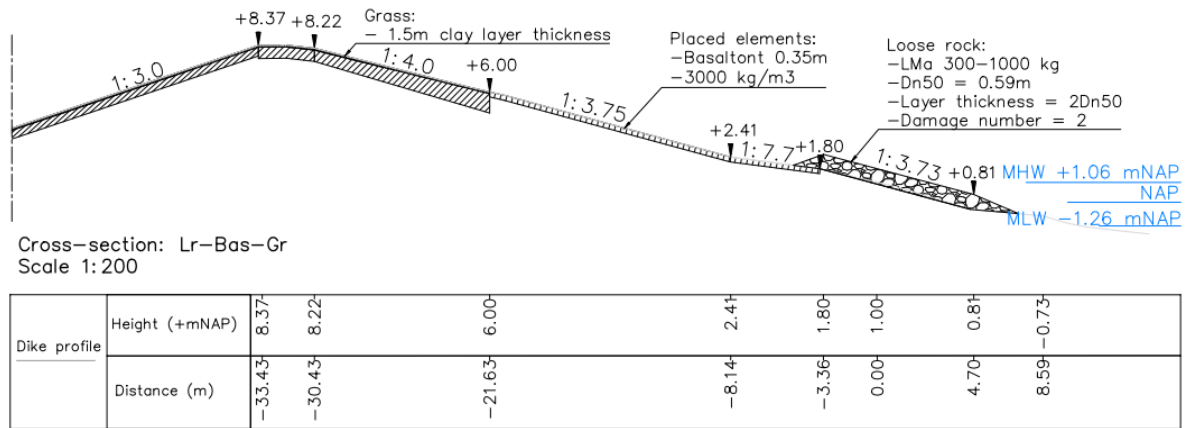


Figure 6.1: Study design: Design with lowest ECI that fulfils safety requirements

- Traditionally, the ratio of hydraulic asphalt concrete and elements is such that the asphalt is dominant. From a financial perspective, this is the cheapest solution. However, based on the probabilistic calculation, from an ECI perspective, the ratio should be reversed. Placed elements dominate the designs with the lowest ECI score. Asphalt is absent or only applied in the upper section. When the deterministic calculation method is applied, the required asphalt layer is reduced by 50%.
- An interlocking type of element (Verkalit) or a column type of element (Basaltont) does not result in a significantly different range in applicability based on the probability of failure.
- The preferred element type for placed elements depends on the diameter and the transport distance. When the ECI score per m^3 differs much for Verkalit and Basaltont, the ECI per volume is dominant. However, when the considered options have similar ECI values, the best option is to choose the one that is produced closest to the project site.
- Applying grass revetment often requires large amounts of imported clay. It is advised to base the decision of the transition height from hard to grass revetment on the distance between the source and the project site. When the project site is close to the source, the ECI for a grass revetment is relatively low. When large transport distances are required, the transport can increase the ECI such that it is not preferred to the hard revetment. For this case, a higher transition is recommended.

Thus, when designing a sea dike revetment probabilistically, aiming to reduce the ECI as much as possible, apply as little and the smallest possible loose rock grading, and replace the hydraulic asphalt concrete layer for placed elements.

6.1. Recommendations

This study applies to a specific section of a specific project and has a limited scope. The topic of sustainable sea dike design is encompassing more aspects, and designing an emission-free sea dike revetment is not possible yet. Therefore, further study should be done to reach the ultimate goal of a fully circular economy in 2050, as the Dutch government aims. The following recommendations and suggestions for further research are given.

- A large part of the total ECI of a dike reinforcement project is due to soil movement. Further research into optimising the shape of the dike concerning the total ECI is necessary to optimise sea dike design further.
- The number of sea dikes relative to other types of dikes in the Netherlands is relatively small. Further study into optimising river and regional dikes can potentially lead to a large reduction of emissions due to dike reinforcement projects. This could be combined with the previously mentioned recommendation.

- A sea dike revetment optimised for ECI only considers the emission aspect of sustainability. Other aspects regarding sustainability for which the dike can be optimized would be biodiversity or nitrogen deposition. These aspects are interesting because nitrogen deposition is limited by national law and is negatively impacting the surrounding nature. Biodiversity is decreasing; therefore, further research on how to design a dike such that it forms an attractive habitat for many species is an interesting topic for further research.
- Loose rock has the largest impact on ECI and is hard to replace by elements due to the more difficult circumstances of the installation. Loose rock originates from Norway and is hard to find elsewhere. Further study into alternative options to replace loose rock might reduce the ECI of sea dike revetment.
- The required rock size has the largest influence on the total ECI. Therefore, checking which grading leads to the lowest ECI possible is therefore important. An attempt has been made to include the maintenance of the loose rock revetment in the design. However, the results are not very accurate due to the lack of policy and, therefore, large uncertainty in maintenance. To decrease the ECI for the entire design lifetime, further study into the maintenance component of all the revetment types and the effect on the ECI is suggested.
- The model developed for this study specifically focuses on the Lauwersmeerdijk-Vierhuizen case. Further study into a model to design a sea dike revetment based on local parameters could lead to better designs for other projects.
- The ECI values used are mostly standard values from the 'Milieudatabase'. These values, however, are often estimates and not the real values. This might impact the outcome of the study significantly. When further study is done into how the products are manufactured, for example, more accurate ECI calculations can be performed.
- This study assumes a standard, deterministic filter layer. The filter layer is essential for the top layer stability. There are several options for filter constructions. Therefore, further study into filter layers' uncertainty and design options and their effect on the ECI is recommended.
- The equation developed by M. Klein Breteler is applied to determine the thickness for placed elements. Traditionally, the equation developed by Pilarczyk is used to determine the element thickness (Pilarczyk, 1995). A comparison between the two equations is interesting for further research.
- The probabilistic techniques studied to apply in the model are relatively traditional. Recently, more efficient methods that make use of surrogate models are being developed and have the potential to reduce computational time significantly. These models potentially allow for parametric design combined with probabilistic analysis without excessive calculation time. Also, non-continuous equations can be applied with those techniques. The application in hydraulic engineering is interesting for further study.
- This study applies to the traditional sea dike revetment design of sea dikes. Currently, a large study in the Netherlands called 'living dikes' is employed to study the effect of salt marshes in front of sea dikes. The idea is that the salt marsh grows with the rising sea level and reduces wave loading on the dike. This would result in an environmentally friendly solution. However, to apply this on a large scale, large salt marshes are to be constructed. As found by this thesis, the type, amount and origin of materials used are important to study before employing the solution. The solution should not have a negative net influence compared to traditional design.

Bibliography

- Arcadis (2022). Design report DO Lauwersmeerdijk, Landelijke dijk. Technical report, Arcadis, Amersfoort.
- Bak, I., Overmars, L., and van der Kruk, T. (2022). LCA achtergrondrapport voor nederlandse branchereferentiemengsels. Technical report, Ecochain technologies B.V., Amsterdam.
- Battjes, J. A. (1974). Surf similarity. Coastal Engineering Proceedings.
- Baudin, M., Lebrun, R., Iooss, B., and Popelin, A.-L. (2017). OpenTURNS: An Industrial Software for Uncertainty Quantification in Simulation. In Handbook of Uncertainty Quantification, pages 2001–2038.
- Bischiniotis, K. (2013). Cost optimal river dike design using probabilistic methods. Technical report.
- Botterhuis, T., Waterman, R., and Geerse, C. (2017). Gebruikershandleiding Waterstandsverloop. Technical report, HKV, Delft.
- Chbab, H. (2015). Waterstandsverlopen kust, Wettelijk Toetsinstrumentarium WTI-2017. Technical report, Deltares, Delft.
- Daamen, E. (2016). Designing a dike using a semi-probabilistic design method Bachelor Thesis. Technical report.
- Davidse, M. (2010). Asphalt nieuwe formule fitten door data punten. Technical report, KOAC NPC, Apeldoorn.
- de Looff, A. K., 't Hart, R., Montauban, K., and van de Ven, M. F. (2006). Golfklap a model to determine the impact of waves on dike structures with an asphaltic concrete layer. ICCE.
- Deltaexpertise (2015). Bestand: Breuksteen Philipsdam.jpg.
- Deltares (2015a). Handreiking dijkbekleding deel 2 - steenzettingen. Technical report.
- Deltares (2015b). Handreiking dijkbekleding deel 3 - asfalt. Technical report.
- Deltares (2015c). Handreiking dijkbekleding deel 4 - breuksteenbekledingen.
- Deltares (2015d). Handreiking dijkbekleding deel 5 - grasbekledingen. Technical report.
- Diermanse, F., Roscoe, K., Lopez De La Cruz, J., Steenbergen, H., and Vrouwenfelder, T. (2013). Hydra Ring Scientific Documentation. Technical report, Deltares, Delft.
- Dijksma, S. A. M. and Kamp, H. (2016). Nederland circulair in 2050. Technical report.
- Ditlevsen, O. and Madsen, H. O. (2007). Structural reliability methods. Wiley.
- Drok, W., Engering, N., Jutte, B., and Wolbers, M. (2021). Handreiking 'DuboCalc in dijkversterkingsprojecten'. Technical report.
- Duits, M. (2020). Hydra-NL Gebruikershandleiding versie 2.8. Technical report, HKV, Delft.
- Intergovernmental panel on climate change (IPCC) (2013). Climate Change 2013, The Physical Science Basis. Technical report.
- Jilmer Postma (2018). Opknappen van 47 kilometer Waddendijk in vijf jaar is een monsterklus.
- Jonkman, S. N., Steenbergen, R. D. J. M., Morales-Nápoles, O., Vrouwenfelder, A. C. W. M., and Vrijling, J. K. (2017). Probabilistic Design: Risk and Reliability Analysis in Civil Engineering. Technical report, Delft University of Technology, Delft.
- Kamphuis, J. W. (1991). Incipient wave breaking. Technical report.

- Kirchherr, J., Reike, D., and Hekkert, M. (2017). Conceptualizing the Circular Economy: An Analysis of 114 Definitions. SSRN Electronic Journal.
- Kiwa (2016). Beoordelingsrichtlijn Zetsteen van ongewapend beton voor de natte waterbouw. Technical report, Kiwa, Rijswijk.
- Klein Breteler, M. (2022a). Erosie van kleibekleding met gras op boventalud van Waddenzeedijken. Technical report.
- Klein Breteler, M. (2022b). Handleiding en documentatie GEBU-faalkanstool voor Waddenzeedijken - versie 22.1.1.
- Klein Breteler, M. and Mourik, G. C. (2014). Vereenvoudiging van Steentoets tot enkele eenvoudige formules-gekleemde rechthoekige blokken-zuilen-blokken op hun kant. Technical report, Deltares, Delft.
- Klerk, W. J. (2014). Definition of test set for deriving safety factors for failure of asphalt revetments under wave impact. Technical report, Deltares, Delft.
- Klerk, W. J. and Kanning, W. (2014). Calibration of Safety Factors for wave impact on Hydraulic Asphalt Concrete Revetments. Technical report, Deltares, Delft.
- Marelli, S., Schöbi, R., and Sudret, B. (2022). UQLab user manual structural reliability (rare event estimation). Technical report, Chair of Risk, Safety and Uncertainty Quantification, ETH Zurich, Switzerland.
- NEN (2015). NEN-EN 13383-1:2015 Ontw. en Waterbouwsteen - Deel 1: Specificatie. Technical report, NEN.
- Noppert Beton (2019). Verkalit voor de dijkverhoging Lauwersoog.
- Pilarczyk, K. W. (1995). Simplified Unification of Stability Formulae for Revetments ' under Current and Wave Attack. Technical report.
- Pilarczyk, K. W. and Klein Breteler, M. (1998). Alternative revetments. Technical report.
- Post, S. and van der Laar, R. (2021). Verkenningfase versterking IJsselmeerdijk Notitie mogelijke alternatieven. Technical report, Royal HaskoningDHV, Nijmegen.
- Purvis, B., Mao, Y., and Robonson, D. (2019). Three pillars of sustainability: in search of conceptual origins. on.
- Rackwitz, R. and Fiessler, B. (1978). Structural reliability under combined random load sequences. Technical report.
- Rijkswaterstaat (2017). Regeling veiligheid primaire waterkeringen 2017. Technical report.
- Ruthin Precast concrete Ltd (2023). Basalton technical refernces.
- Schiereck, G. and Verhagen, H. (2019). Introduction to Bed, bank and shore protection. Delft academic press / VSSD.
- Schipper, B., van Hövell, M., Verde, S., Roosendaal, J., Mentink, B., and Oranje, K. (2022). LCA Rapportage categorie 3 data Nationale Milieudatabase Hoofdstuk 52 Kust-en oeverwerken. Technical report.
- Senhorst, H. (2018). Vier quick wins grond en klei. Technical report.
- Stichting Nationale Milieudatabase (2022). Bepalingsmethode Milieuprestatie Bouwwerken. Technical report.
- TAW (1996). Technical Report: Clay for Dikes. Technical report.
- TAW (2002). Technisch Rapport Asphalt voor Waterkeren. Technical report.
- Terrafix (2007). Geotextiles for filtration, erosion control and scour protection.
- The OpenFOAM Foundation (2023). OpenFOAM.

- UNFCCC (2016). Overeenkomst van Parijs. Technical report.
- van den Bos, J. (2018). User Manual SwanOne User Manual V1.3. Technical report, TU Delft, Delft.
- van der Klauw, M., Lommers, M., and Schweitzer, G. (2018). Cursus DuboCalc.
- van der Meer, J. (1988a). Rock Slopes and Gravel Beaches under Wave Attack. Technical report.
- van der Meer, J. W. (1988b). Deterministic and Probabilistic Design of Breakwater Armor Layers. *Journal of Waterway, Port, Coastal and Ocean Engineering*, 114(1).
- Van Rossum, G. and Drake Jr, F. L. (2022). Python 11.
- Waterschap Noorderzijlvest (2023). Waterschap investeert miljoenen in droge voeten. Zeedijk Lauwersmeerdijk-Vierhuizergat en kering Zoutkamp wordt versterkt.
- Waterwet (2009). Waterwet.
- Zandbergen, J. (2021). MKI berekening Lauwersmeerdijk Op basis van voorlopig ontwerp. Technical report.

A

Parameter distributions

Table A.1: Decision parameter distributions

Variable	Symbol	Unit	Distribution	Expected value	Uncertainty	Start	Stop	Delta	Reference
Density concrete	ρ_c	kg/m^3	Normal	Variable	COV = 0.0103	2650	3000	50	Kiwa (2016)
Layer thickness (Basalton)	D	m	Normal	Variable	COV = 0.0304	0.2	0.6	0.05	Kiwa (2016)
Layer thickness (Verkalit)	D	m	Normal	Variable	COV = 0.0304	0.2	0.6	0.05	Kiwa (2016)
Layer thickness hydraulic asphalt concrete	d	m	LogNormal	Variable	COV = 0.1	0.1	0.4	0.05	Klerk (2014)
Nominal diameter rock	D_{n50}	m	Normal	Variable	COV = 0.03	0.31	1.44	Variable	van der Meer (1988b)
Damage number	S	-	Deterministic	Variable	-	2	17	1	van der Meer (1988b)

Table A.2: Control parameter distributions

Variable	Symbol	Unit	Distribution	Expected value	Uncertainty	Reference
Density Rock	ρ_s	kg/m^3	Normal	2650	$\sigma=79.5$	van der Meer (1988b)
Density water	ρ_w	kg/m^3	Normal	1025	$\sigma=30.75$	van der Meer (1988b)
Slope angle 1	α_1	-	Normal	0.18	COV = 0.05	van der Meer (1988b)
Slope angle 2	α_2	-	Normal	0.21	COV = 0.05	van der Meer (1988b)
Slope angle 3	α_3	kg/m^3	Normal	0.27	COV = 0.05	van der Meer (1988b)
Notional permeability	P	-	Normal	0.1	$\sigma=0.05$	van der Meer (1988b)
Uncertainty parameter a (plunging)	C_{pl}	-	Normal	6.2	$\sigma=0.4$	van der Meer (1988b)
Uncertainty parameter b (surging)	C_s	-	Normal	1	$\sigma=0.08$	van der Meer (1988b)
Density asphalt	ρ_a	kg/m^3	Normal	2325	$\sigma = 10$	Assumption
Stiffness subsoil	c	MPa/m	Lognormal	100	COV = 0.25	Klerk (2014)
Elasticity modulus asphalt	E	MPa	Normal	7000	$\sigma = 1400$	Klerk (2014)
Cracking strength	σ_b	MPa	Normal	6.3	COV = 0.2	Klerk (2014)
Slope depending impact factor	q	-	LogNormal	3.45	COV = 0.5	de Loeff et al. (2006)
Deterministic parameters						
Coefficient for length of loading	$c1$	-	Deterministic	0.15		Klein Breteler and Mourik (2014)
Coefficient for length of loading	$c2$	-	Deterministic	0.85		Klein Breteler and Mourik (2014)
Gravity	g	m/s^2	Deterministic	9.81		
Reduction factor due to relative position design water level to phreatic surface	R_w	-	Deterministic	1		TAW (2002)
Fatigue parameter	α	-	Deterministic	0.5		Davidse (2010)
Fatigue parameter	β	-	Deterministic	5.4		Davidse (2010)
Transverse contraction coefficient	ν	-	Deterministic	0.35		Davidse (2010)
Vertical distance between the lower bound asphalt to the outer water level	a	m	Deterministic	variable		
Vertical distance between the outer water level and phreatic surface	v	m	Deterministic	variable		
Parameters related to the filter						
Thickness filter 1	b_1	m	Deterministic	0.06		Arcadis (2022)
Permeability geotextile	k_2	m/s	Deterministic	0.00286		
Thickness geotextile	b_2	m	Deterministic	0.0053		Arcadis (2022)
Kinematic viscosity water	ν	m^2/s	Deterministic	$1.2 * 10^{-6}$		
Porosity granular material	n_f	-	Deterministic	0.35		Arcadis (2022)
15% fraction diameter filter Verkalit	$d_v, f_{15\%}$	m	Deterministic	0.004		Arcadis (2022)
15% fraction diameter filter Basalton	$d_b, f_{15\%}$	m	Deterministic	0.017		Arcadis (2022)

B

Workflow model

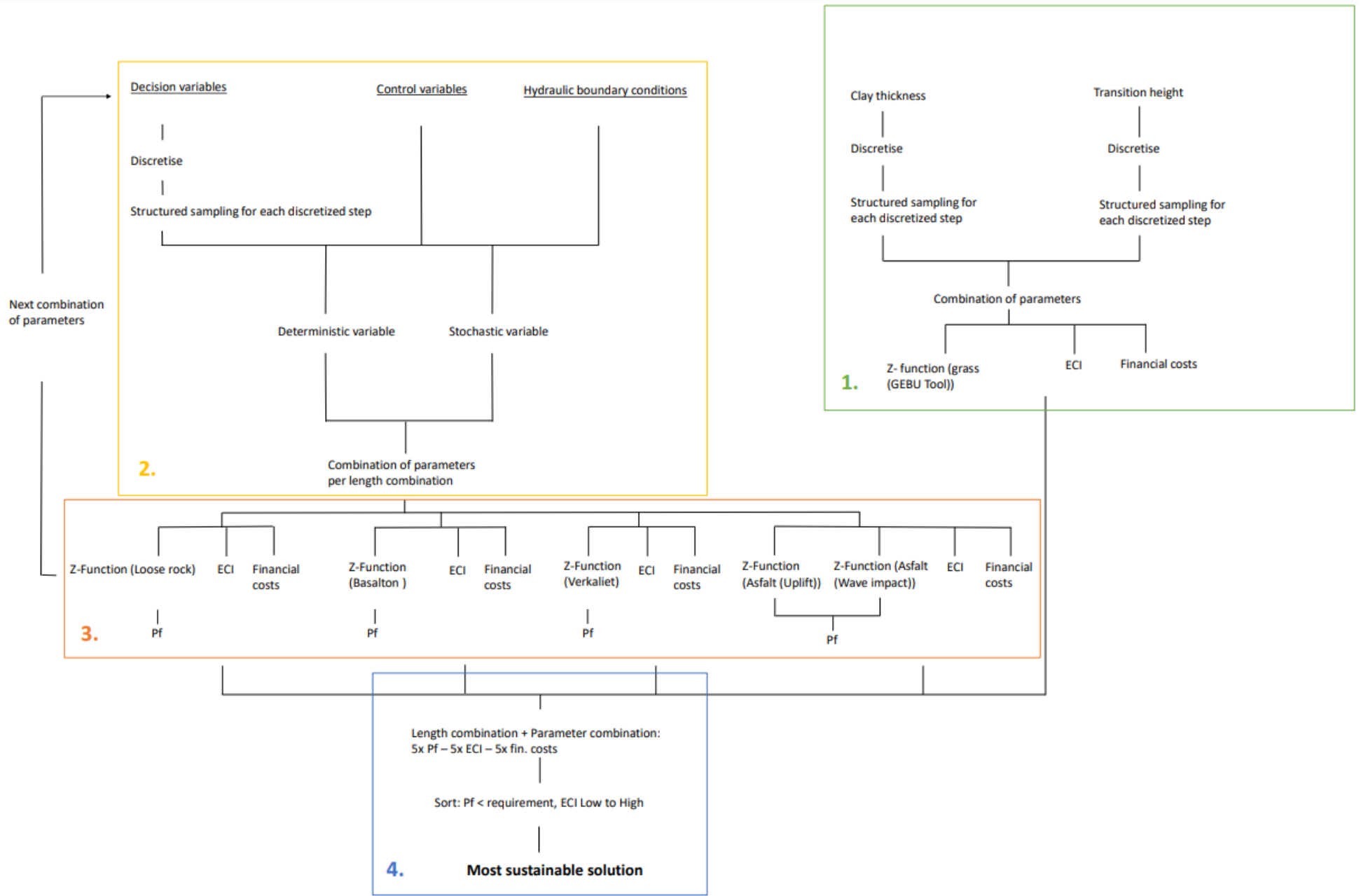


Figure B.1: Complete workflow of the model

C

Environmental cost indicator for all design options with varying transition heights

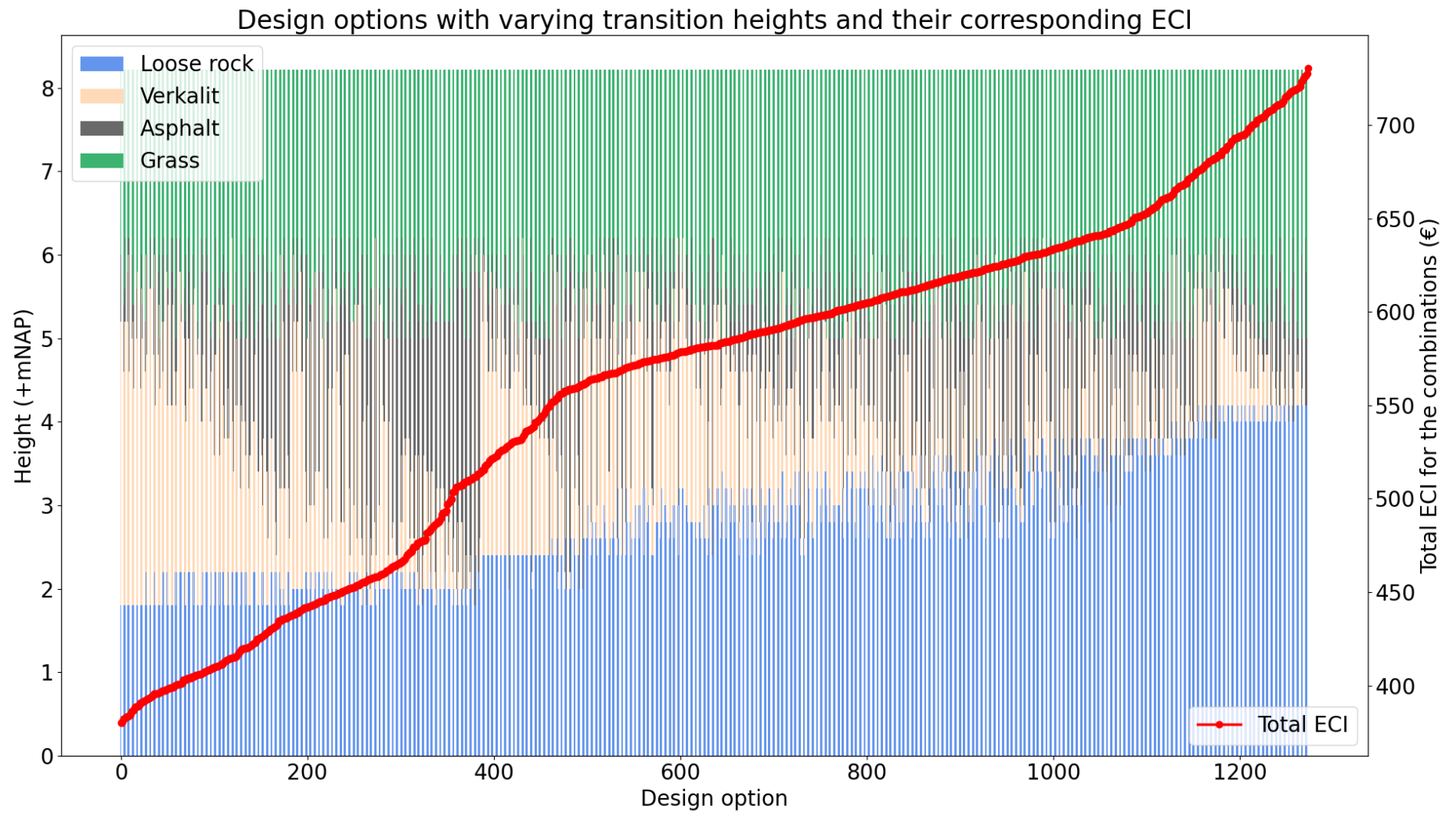


Figure C.1: Design with lowest ECI for loose rock, Verkalit, Hydraulic asphalt concrete and grass revetment. Designs are sorted by ECI, increasing to the right.

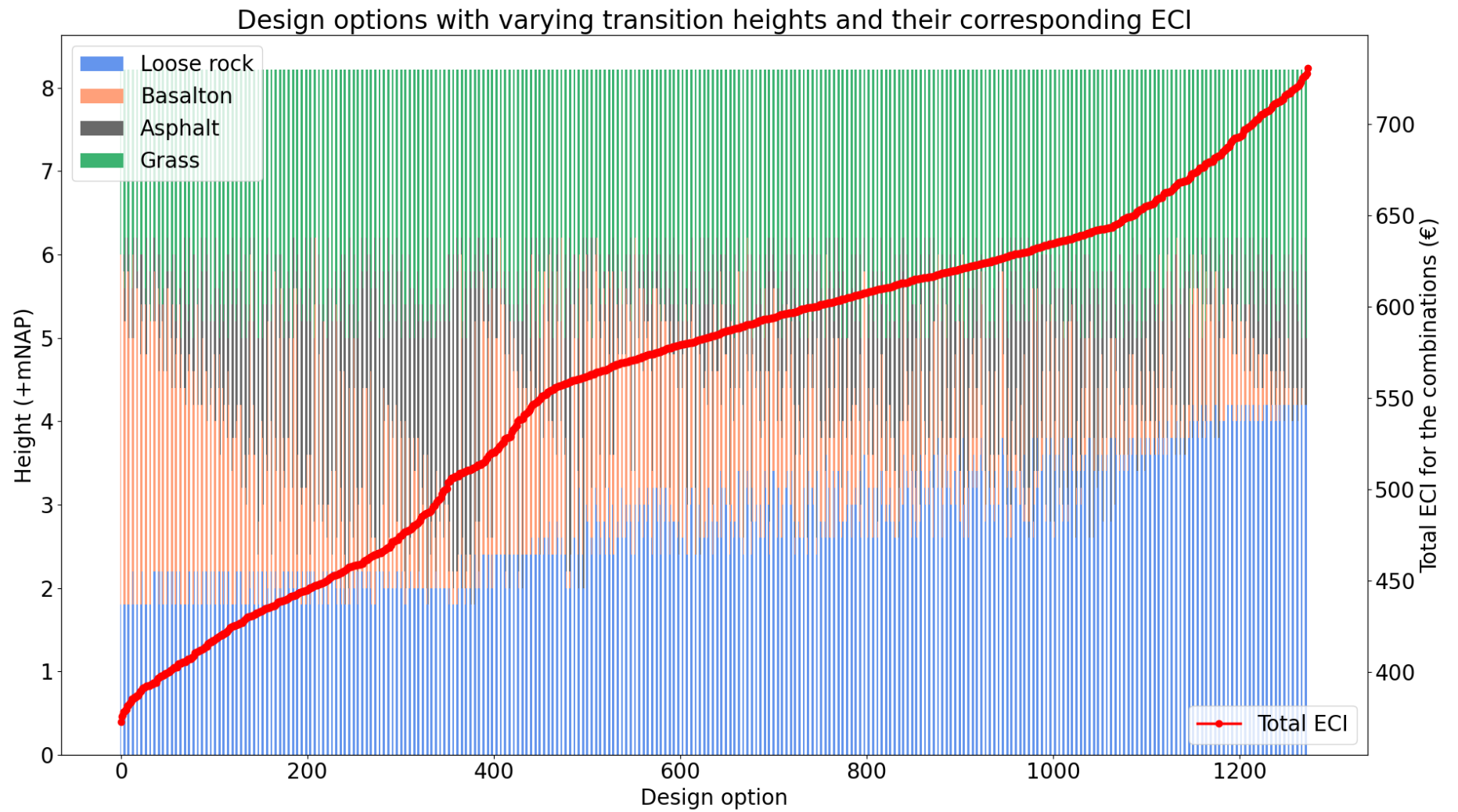


Figure C.2: Design with lowest ECI for loose rock, Basalton, Hydraulic asphalt concrete and grass revetment. Designs are sorted by ECI, increasing to the right.

D

Financial costs for all design options for
varying transition heights

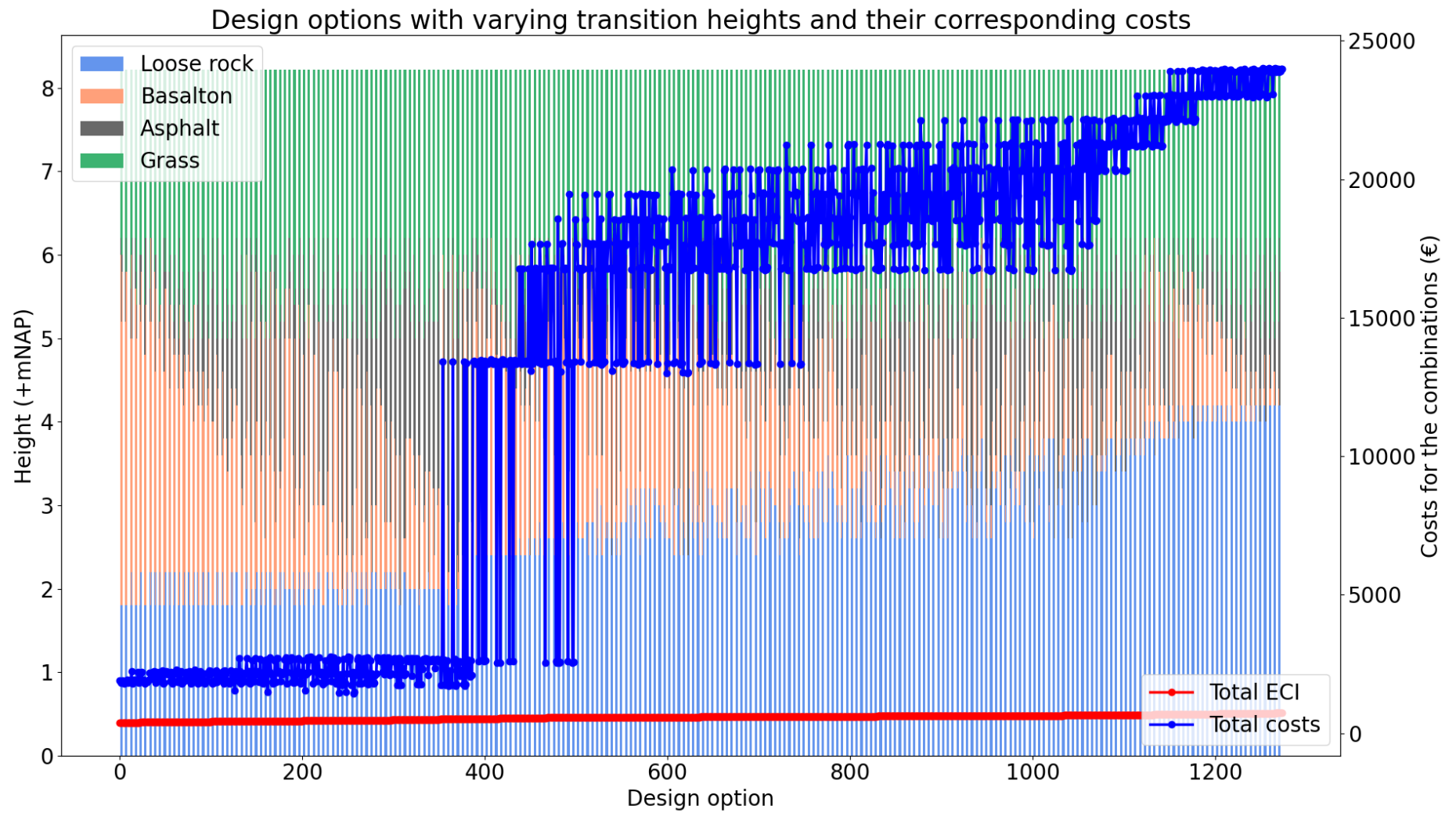


Figure D.1: Financial costs for design with loose rock, Basalton, Hydraulic asphalt concrete and grass revetment. Designs are sorted by ECI, increasing to the right.

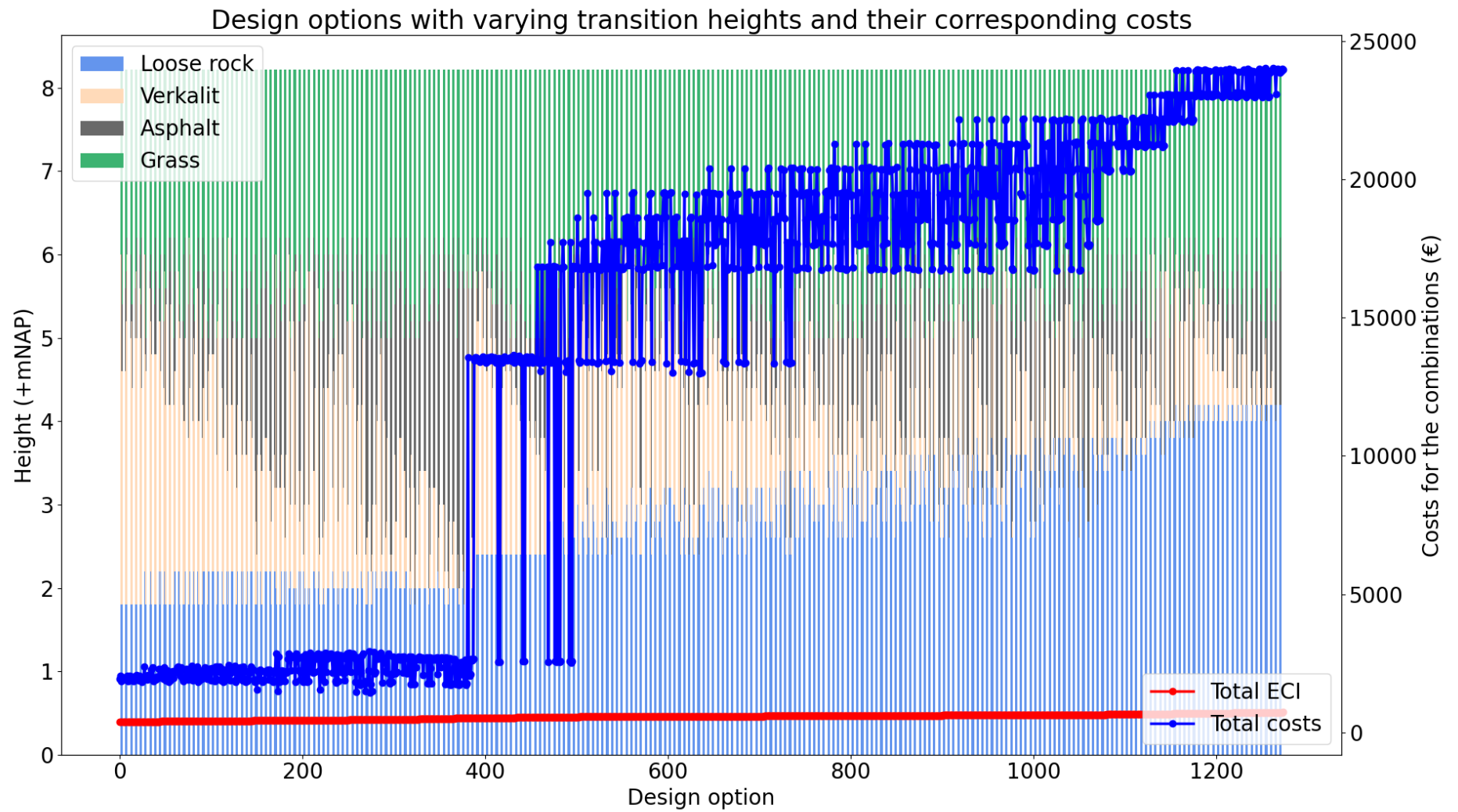


Figure D.2: Financial costs for design with loose rock, Verkalit, Hydraulic asphalt concrete and grass revetment. Designs are sorted by ECI, increasing to the right.

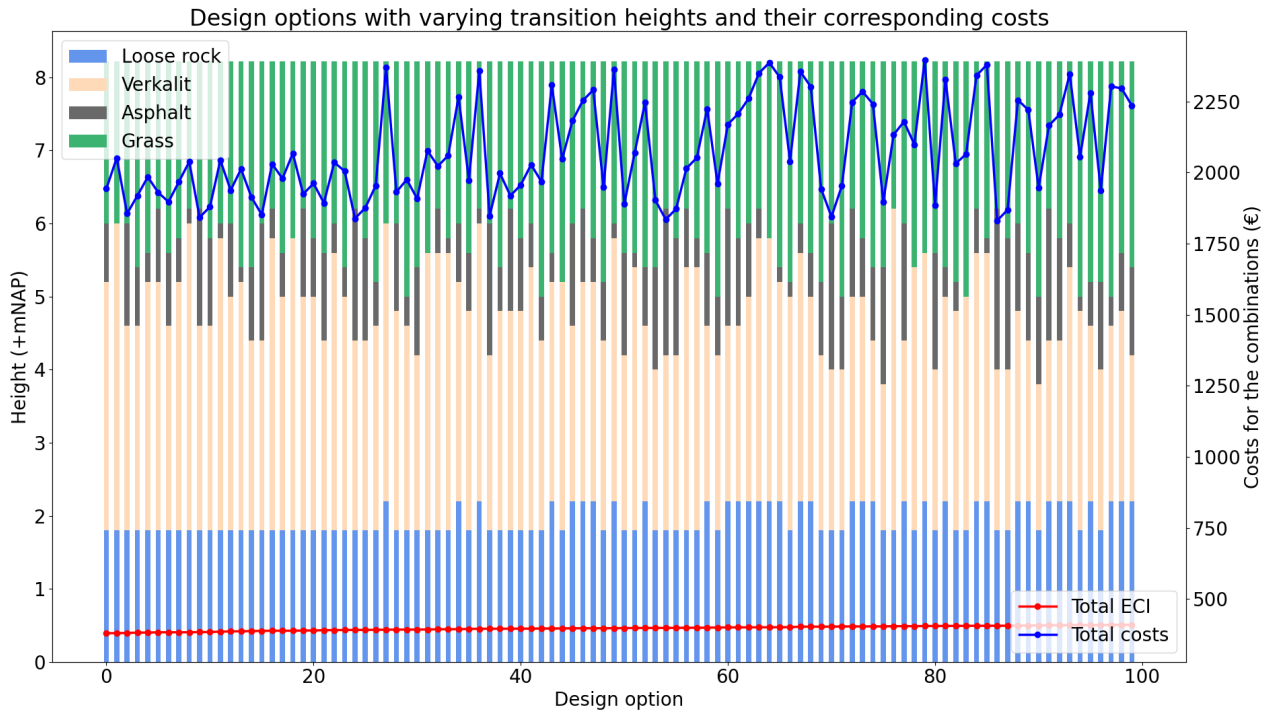


Figure D.3: Financial costs for 100 designs with lowest ECI with loose rock, Verkalit, Hydraulic asphalt concrete and grass revetment. Designs are sorted by ECI, increasing to the right.

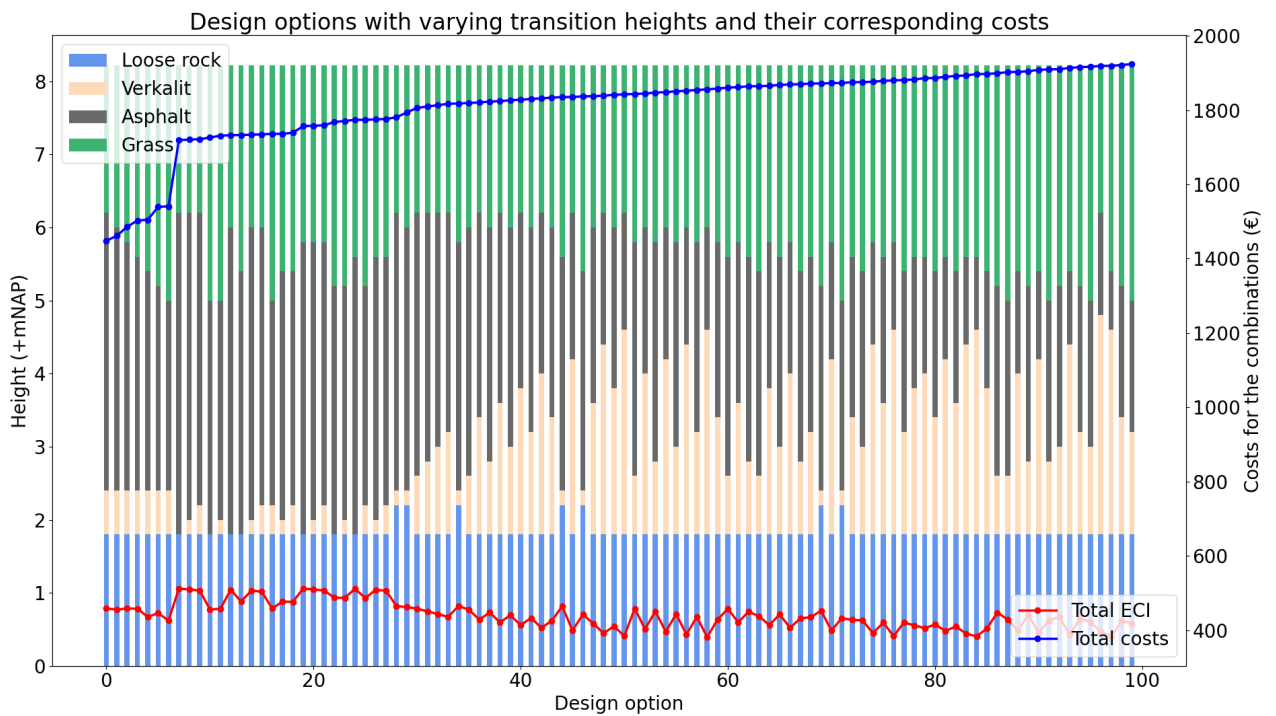


Figure D.4: Financially optimized design designs with loose rock, Verkalit, Hydraulic asphalt concrete and grass revetment. Designs are sorted by financial costs, increasing to the right.

E

Hydraulic boundary conditions

Table E.1: Hydraulic boundary conditions

Waterlevel (h) +mNAP	Significant wave height (H_s) [m]	Std. dev. H_s [m]	Peak period (T_p) [sec]	Std. dev. T_p [sec]	Storm duration (t) [sec]	Std. dev. t [sec]
1.6	0.92	0.17	3.46	0.38	20988	1049
1.8	0.93	0.18	3.50	0.38	21060	1053
2	0.90	0.17	3.09	0.34	21060	1053
2.2	0.96	0.18	3.53	0.39	21060	1053
2.4	0.95	0.18	3.50	0.39	20412	1021
2.6	1.04	0.20	3.79	0.42	20448	1022
2.8	1.04	0.20	3.78	0.42	20448	1022
3	1.02	0.19	3.66	0.40	19224	961
3.2	0.99	0.19	3.62	0.40	18000	900
3.4	1.08	0.21	3.89	0.43	17388	869
3.6	1.19	0.23	4.21	0.46	18036	902
3.8	1.26	0.24	4.32	0.47	18036	902
4	1.34	0.25	4.45	0.49	24048	1202
4.2	1.44	0.27	4.61	0.51	19800	990
4.4	1.52	0.29	4.74	0.52	20412	1021
4.6	1.61	0.31	4.87	0.54	20988	1049
4.8	1.70	0.32	5.00	0.55	23436	1172
5	1.79	0.34	5.13	0.56	22248	1112
5.2	1.89	0.36	5.28	0.58	22248	1112
5.4	1.98	0.38	5.41	0.60	22248	1112
5.6	2.08	0.40	5.55	0.61	22860	1143
5.8	2.17	0.41	5.69	0.63	22860	1143
6	2.26	0.43	5.80	0.64	21060	1053
6.2	2.36	0.45	5.97	0.66	16236	812

F

Input GEBU tool

GEBU Faalkans Tool voor Zeedijken

Bestand Info

Modus
Normaal

Berekening

Berekeningstype
 Toetsing
 Ontwerp

HLCD bestandslocatie
C:\Users\vandonsk5051\Do

Dijklocatie
WZ_1_6-5_dk_00037

Zichtjaar
2100

Graskwaliteit
Gesloten zode

Kernmateriaal
Zand

Grasbeschadigingen
Beschadigingen met diepte van 5 cm of meer en oppervlak van minimaal 15 x 15 cm²

Gemiddeld laagwater
-1.26 [m+NAP]

Gemiddeld hoogwater
1.05 [m+NAP]

Niveau overgang hard-gras
6.15 [m+NAP]

Minimum extra kleilaagdikte
0 [m]

Maximum extra kleilaagdikte
2 [m]

Stapgrootte kleilaagdikte
0.1 [m]

Geometrie

Voorlandhelling
0.02 [tan(α)]

Dijknormaal t.o.v. Noord
341 [graden]

X-coördinaat bij teen
0 [m]

Z-coördinaat bij teen
-0.4 [m+NAP]

Kleidikte bij teen
0.55 [m]

X Begin [m]	Z Begin [m+NAP]	Kleidikte Begin [m]	X Eind [m]	Z Eind [m+NAP]	Kleidikte Eind [m]	Helling [tan(α)]	Type
0	-0.4	0.55	5.6	1	1	0.25	Buitentalud
5.6	1	1	13.6	3	1	0.25	Buitentalud
13.6	3	1	23.6	5.5	1	0.25	Buitentalud
23.6	5.5	1.031	27.6	5.58	1	0.02	Berm/Kruin
27.6	5.58	0.949	28.86	6	1	0.33	Buitentalud
28.86	6	1	30.36	6.5	1	0.33	Buitentalud
30.36	6.5	1	36.96	8.7	1	0.33	Buitentalud

Start berekening

Figure F.1: Input screen GEBU tool